UNITED STATES DEPARTMENT OF THE INTERIOR

GEOLOGICAL SURVEY

Statistical Study of Seismicity Associated with Geothermal Reservoirs in California

by D. M. Hadley and D. S. Cavit

Sierra Geophysics, Inc.
150 N. Santa Anita Avenue
Arcadia, California 91006

Open-File Report 82-1068

1982

x x x x x x x x x x x x x x x x x x x x x x x x x x x x x x x x x x x x x x x x x x x x x x x

Project Information

This report was prepared under Contract No. 14-08-0001-16379 to Sierra Geophysics, Inc., from the U.S. Geological Survey's Geothermal Research Program, with Dr. D. M. Hadley as the Principal Investigator. The period of the contract was from August 1, 1979, to December 31, 1980. Objectives of the contract were to describe statistical methods to separate spatially, temporally, and magnitude-dependent portions of both the random and non-random components of the seismicity and to develop a general discriminant that combines several physical parameters for identifying the presence of a geothermal system.

TABLE OF CONTENTS

FIGURES

TABLES

1. SUMMARY

Although extensive and costly catalogs describing the occurrences of earthquakes have been compiled, attempts to correlate seismic characteristics with geothermal reservoirs have not been notably successful. One likely reason for this result is that the seismic data represent the superposition of several processes. Without careful separation of these components the seismic catalogs are not optimally useful. Recent studies of the temporal distribution of earthquakes show that seismicity can be described as a random process with a superimposed non-random component. Similarly, the spatial distribution or clustering of earthquakes changes from random to non-random as the magnitude threshold varies. Within this report we outline statistical methods to separate spatially, temporally, and magnitude-dependent portions of both the random and non-random components of the seismicity. The methodology employed compares the seismicity distributions with a generalized Poisson distribution. Temporally related events are identified by the distribution of the interoccurrence times.

The regions studied to date include the Imperial Valley, Coso, The Geysers, Lassen, and the San Jacinto fault. The spatial characteristics of the random and clustered components of the seismicity are diffuse and appear unsuitable for defining the areal extent of the reservoir. However, from the temporal characteristics of the seismicity associated with these regions we have constructed a general

discriminant that combines several physical parameters for identifying the presence of a geothermal system. This detection procedure sould be tested with additional data to evaluate its effectiveness.

2. INTRODUCTION

Over the last several years seismic arrays have been operated in very diverse geothermal environments. Perhaps predictably, the recorded earthquake activity has similarly shown great variability. Research in Iceland by Ward et al. (1969) and Ward and Bjornsson (1971) has shown that geothermal areas structurally related to a large number of faults and fissures are typified by high activity, whereas areas related to acidic intrusions or minor faulting contain only slight activity. These investigators have shown that the geothermal areas and the fissuring, faulting and seismicity are possible manifestations of transform faulting. This observation is similar to those made at The Geysers where earthquake mechanisms and locations show dextral strike-slip faulting and diffuse lineation along the trend of a major fault zone (Hamilton and Muffler, 1972; Majer and McEvilly, 1979). Within the Imperial Valley, the seismicity shows intense swarm activity superimposed on a background of distributed earthquakes. As in Iceland, many of these earthquakes are strike-slip and appear to be related to a series of en echelon or leaky transform faults (Hill et al., 1975; Johnson and Hadley, 1976; Fuis and Schnapp, 1977; Gilpin and Lee, 1978; Johnson, 1979). For areas such as the Imperial Valley and Iceland, Hill, 1977, has proposed a model that relates swarm activity with increasing fluid pressure in magma-filled dikes. Johnson, 1979, has generalized Hill's model to include fluctuations in fluid pore pressure that are

driven by a seismic deformation at greater depths. A different model relating swarm earthquakes and geothermal areas has evolved from observations of the seismicity associated with ridge crests and calderas. Sykes, 1970, notes that swarm sequences are frequently related to oceanic ridge crests. The correlation between rifting and swarms, if causally related, was offered as a means of detecting volcanic, hydrothermal or magmatic processes. Francis, 1974, proposed that mid-ocean ridge swarms were the result of the break-up and collapse of the central rift due to a drop in magma pressure in the inferred underlying chamber. As in Hill's model, the swarms result from changes in the pressure of magma-filled voids. The correlation between swarms and the probable heterogeneous distribution of material properties is very consistent with Mogi's, 1963, laboratory measurements.

Although many geothermal regions show nearly continuous or swarm sequences of activity, not all reservoirs are characterized by high rates of earthquake occurrences. For instance, within the Imperial Valley, earthquake clusters are not distinctly related to the Heber, Dunes and Glamis geothermal areas (Hill _et al._, 1975). This may be the result of slow migration and evolution of the active plate margins.

In geothermal areas, the temporal distribution of earthquakes ranges from slight to nearly continuous or swarm activity. The tectonic setting varies from transcurrent faulting to rifting. The wide range of both tectonics and

earthquake characteristics typically encountered in geothermal areas has limited the usefulness of earthquake catalogs generated in most seismic studies. Consistent correlations have not been obtainable between the hypocenters of earthquakes and other geological and geophysical data (such as heat flow, gravity, resistivity, magnetics, etc.). It is therefore not surprising that in a recent evaluation of the strategy for geothermal exploration (Goldstein, 1977), the effectiveness of earthquake studies was rated low. Although earthquake activity is considered a positive indicator in the exploration for geothermal resources, earthquake studies have not been particularly useful in the definition and development of a reservoir. This situation is perhaps paradoxical as many geothermal systems are intimately related to faults. This apparent paradox may, in part, be an artifact of the current techniques that utilize the seismic data. In the above-mentioned study of earthquakes in Iceland (Ward and Bjornsson, 1971) the investigators concluded that the temporal distribution of earthquakes was not random. The statistical analysis was not extended further in order to answer the question: At what interoccurrence times did the distribution strongly deviate from random and where were those non-random events located? The goal of this research project has been to answer a family of similar questions.

The Iceland results are very consistent with other systematic studies of the temporal distribution of seis-

micity that show occurrences can be described as a random process with a superimposed non-random component (Lomnitz and Hax, 1966; Vere-Jones and Davies, 1966; Shlien and Toksöz, 1970; McNally, 1976). Recent studies in central and southern California have shown that significant information can be extracted from the earthquake catalogs by examining separately the random and non-random aspects of the data (McNally, 1976). As with the temporal distribution, spatial distributions frequently show both random and non-random components. Within the following section we will outline the methodology to separate temporally related events from the random background seismicity. These statistical tests can be performed at several magnitude thresholds in order to evaluate the complete relationships among the occurrence times, locations and magnitudes of the random and non-random components of the earthquake catalogs.

3. DATA ANALYSIS AND THE IMPERIAL VALLEY

The detailed description of the data analysis techniques and the application of these methods to the Imperial Valley are combined together in this section. The following sections briefly describe the results of this analysis for The Coso, Geysers, Lassen and the San Jacinto fault zone. The San Jacinto region has been added to the study as a control for evaluating the results from known geothermal areas. Location of study areas shown in Figure 1.

GEOLOGIC SETTING

The Salton Trough is a fault controlled depression of Neogene-Quaternary age and is the landward extension of the Gulf of California (Elders et al., 1972). The margins are steeply faulted and the basin is filled with approximately 6 km of deltaic sediments deposited by the Colorado River (Biehler, 1964). The youngest sedimentary rocks in the Salton Trough are Holocene alluvium and lake sediments (Van de Kamp, 1973). These are followed in age by lacustrine and deltaic silts, sands, and gravels that range from late Miocene to Pleistocene (Freckman, 1978). The oldest sediments constitute the Anza Formation which is composed of Miocene coarse-grained, clastic, basin margin facies (Dronyk, 1977). Basement rocks consist of metasediments to granites of Mesozoic and older age which form a border to the younger trough along with some subsidiary Tertiary volcanics.

The basin is an area of active crustal extension and thinning. A series of northwest-trending right lateral en echelon faults constitutes the expression of transform faulting in the trough. Zones of spreading perpendicular to the transform faults are not observed. Instead, the transform faults connect via north-trending complex zones best characterized as leaky transforms (Elders and Biehler, 1975; Johnson and Hadley, 1976; Johnson, 1979).

Heat flow measurements have shown temperatures to be as high as 360°C at only 1500 to 2500 m depth (Helgeson, 1968). Salinities range up to 300,000 mg/l (Helgeson, 1968). These conditions result in ongoing greenschist metamorphism of the sediments (Elders, pers. comm.).

DETECTION THRESHOLDS

In order to carry out the statistical analysis of the historic seismicity, it is imperative to establish the magnitude thresholds for data completeness. Within most seismic arrays the station density and distribution periodically change. This results in an apparent change in the number of earthquakes occurring within the array. If the seismicity is to be compared with that in other regions and with that in the same region from year to year, it is necessary to establish the history of the magnitude thresholds. This has been accomplished by applying the standard frequency vs. magnitude relations (Log N = a-bM) on a year by year basis for the region shown in Figure 1. The point of deviation at the low magnitude level from the

frequency relation defines the magnitude threshold for uniform detection. Later analysis is directed towards only those portions of the catalog for which the data set is uniform.

For the Imperial Valley catalog (1973-1978 inclusive), we found that the year by year detection threshold for uniform detection varied from $M_L \geqq 2.0$ to 2.5. The following analysis has used a threshold of $M_L \geqq 2.5$. A frequency-magnitude plot for the entire period is shown in Figure 2. Note that the point for $M_L = 2.0$ (magnitude bin 1.75-2.25) falls significantly below the line predicted for uniform detection.

TEMPORAL DISTRIBUTION OF SEISMICITY

In order to examine the spatial distribution of seismicity as a function of magnitude it is first necessary to remove the time-dependent bias introduced by related earthquakes, which are hereafter called earthquake clusters. In this study, the earthquake distribution has been tested as a generalized Poisson distribution. That is, it is assumed that a series of centers of earthquake occurrences are randomly distributed. Centers may represent one or many events, i.e., we allow a finite probability for the occurrence of one or more events in the same time cell. The modified series thus contains points for the occurrence of each single event designated as independent and the first event of each cluster of related events. This generaliza-

tion of the series requires identification of the related events, or cluster.

Clustering can be simply identified from the inter-occurrence times between consecutive events. For a Poisson process in time, the time intervals between consecutive events are exponentially distributed. The probability of two consecutive events being separated by a time interval of length $t \pm dt/2$ is $F(t)dt$ where:

$$F(t) = \lambda e^{-\lambda t}$$

and λ is the mean rate of occurrence. The probability of two consecutive events being separated by a time interval less than or equal to a particular t_j is thus:

$$F(t_j) = \int_0^{t_j} \lambda e^{-\lambda t} dt = 1 - e^{-\lambda t_j} \cong \frac{j}{n+1}$$

where j is the position of the interval t_j in the set of n ordered (smallest to largest) time intervals. Deviations of the time intervals from an exponential distribution thus represent departures from a Poisson distribution and suggest an interdependence of earthquakes. A probability plot from the Imperial Valley data set is shown in Figure 3, where the set of j ordered time intervals is shown as a function of Log (1 - j/n+1). The small time intervals ($t < \sim 1$ day) are strongly deviant from the straight line expected for an exponential distribution. This departure from linearity

suggests a time interval that identifies related events or clusters within this group of earthquakes.

A range of trial cluster time intervals was derived from this probability plot. For each trial time, the modified series of independent events and the centers of related events were tested as a random distribution using a Chi-squared significance test and the Poisson dispersion coefficient (= variance/mean) as a function of increasing time interval. The dispersion coefficient was calculated by dividing the modified catalog into equally spaced time intervals or bins (e.g.: 2 day intervals). The variance and the mean number of events that occur within the particular binning were next calculated. If the distribution of the events in time is Poisson, then the variance equals the mean, and the dispersion coefficient is unity. This process was repeated for a range of time intervals. The dispersion coefficient plot for the raw or unclustered data set is shown in Figure 4. Clearly the unclustered catalog is not a Poisson distribution. Several declustering times were next selected from the probability plot, Figure 3. The catalog was declustered with these times. The dispersion coefficient plot for these modified catalogs is shown in Figure 5. From this analysis we conclude that at a magnitude threshold of $M_L \geq 2.5$ the declustering time of 1.5 - 2 days removes most of the related events.

Relationships between temporal and spatial clusters can be examined by plotting interoccurrence times vs. inter-

occurrence distances. For the raw unclustered catalog, it is obvious that swarms are spatially clustered. This is shown in Figure 6 by a tight grouping of points at short distances and short times. However, the removal of temporally related or clustered events qualitatively randomizes the interoccurrence distances, (Figure 7).

DISCUSSION IMPERIAL VALLEY

Independent or random events: Using the declustering time of 1.5 days, the catalog of events shown in Figure 1 has been separated into clustered events and random or independent events. The locations of the random events are shown in Figure 8. These events form a broad, diffuse zone along the Imperial fault and its northward extension. The earthquakes within the Salton Sea and Brawley geothermal areas are located in the western half of the designated resource area. The largest magnitude events are outside of the central portions of the reservoir (as defined by either gravity or heat-flow measurements). The slope of the frequency vs. magnitude distribution, for these independent events, is $b \sim 1.65$.

Clustered events: Using the declustering time of 1.5 days, all of the earthquake clusters have been separated from the catalog and are plotted in Figure 9. As discussed above, clustering in time is closely associated with spatial clustering. Figure 10 shows the distance between consecu-

tive events vs. occurrence time. The declustered series is plotted with an identical format in Figure 11. This figure provides additional confirmation that the declustering time adequately separates spatial and temporal swarms or clusters from the raw catalog. Unlike the continuous, diffuse seismicity that typifies the random events, the temporal clusters form discrete centers of activity (Figure 9). Although swarms or clusters do occur within the designated KGRA's,* intense swarms and large earthquakes have not occurred, to date, in the area of the highest heat flow. The slope of the frequency vs. magnitude distribution for the clustered events is b ~ 1.00. This b value is significantly lower than the value obtained for the declustered, random events. Laboratory studies on microfracturing of rock (Scholz, 1968) and macroscopic observations (Wyss, 1973) have shown that the b value is a strong function of the state of stress and is weakly dependent upon the material properties. Application of these results to the Imperial Valley suggests that the swarm or clustered events are responding to a higher than regional average stress environment.

---

* KGRA = Known Geothermal Resource Area

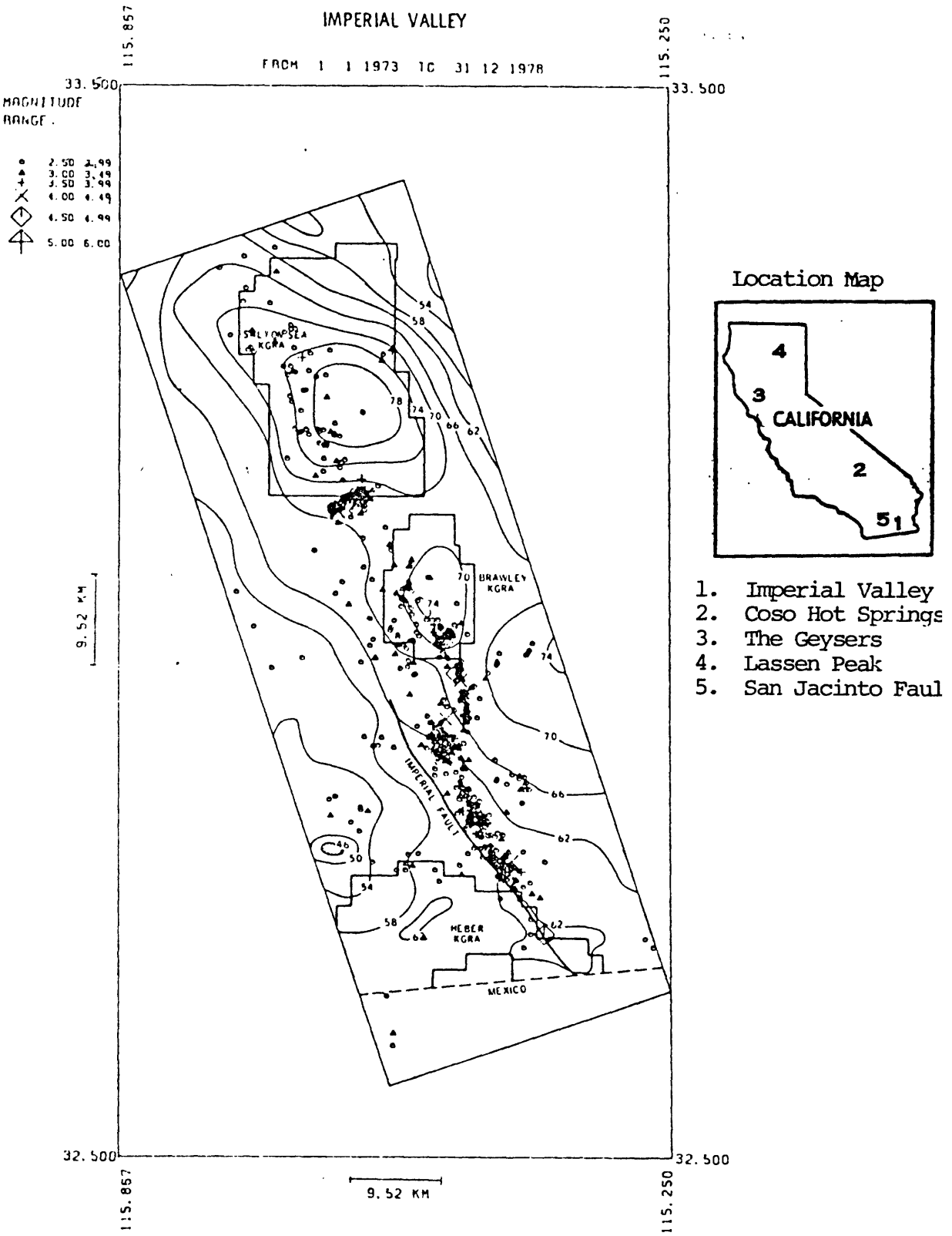

Figure 1. Earthquake locations within the Imperial Valley for the time period 1973 through 1978. The contours are Bouguer gravity isogals. Heavy lines outline Salton Sea, Brawley and Heber KGRA.

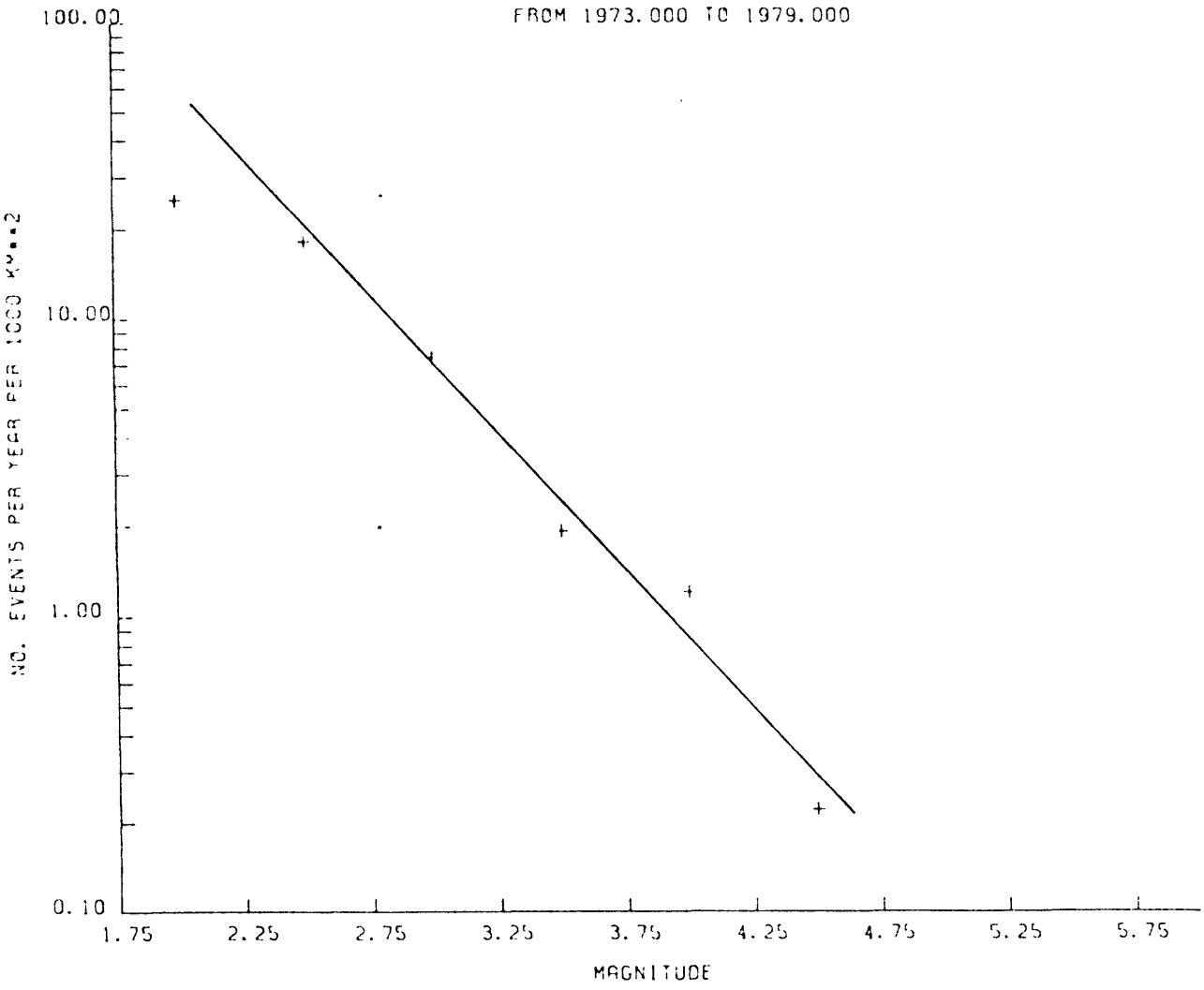

Figure 2. Frequency vs. magnitude for the Imperial Valley earthquakes shown on Fig. 1. The point of deviation at the low magnitude level from the Gutenberg and Richter, 1949, frequency relationship defines the magnitude threshold for uniform detection.

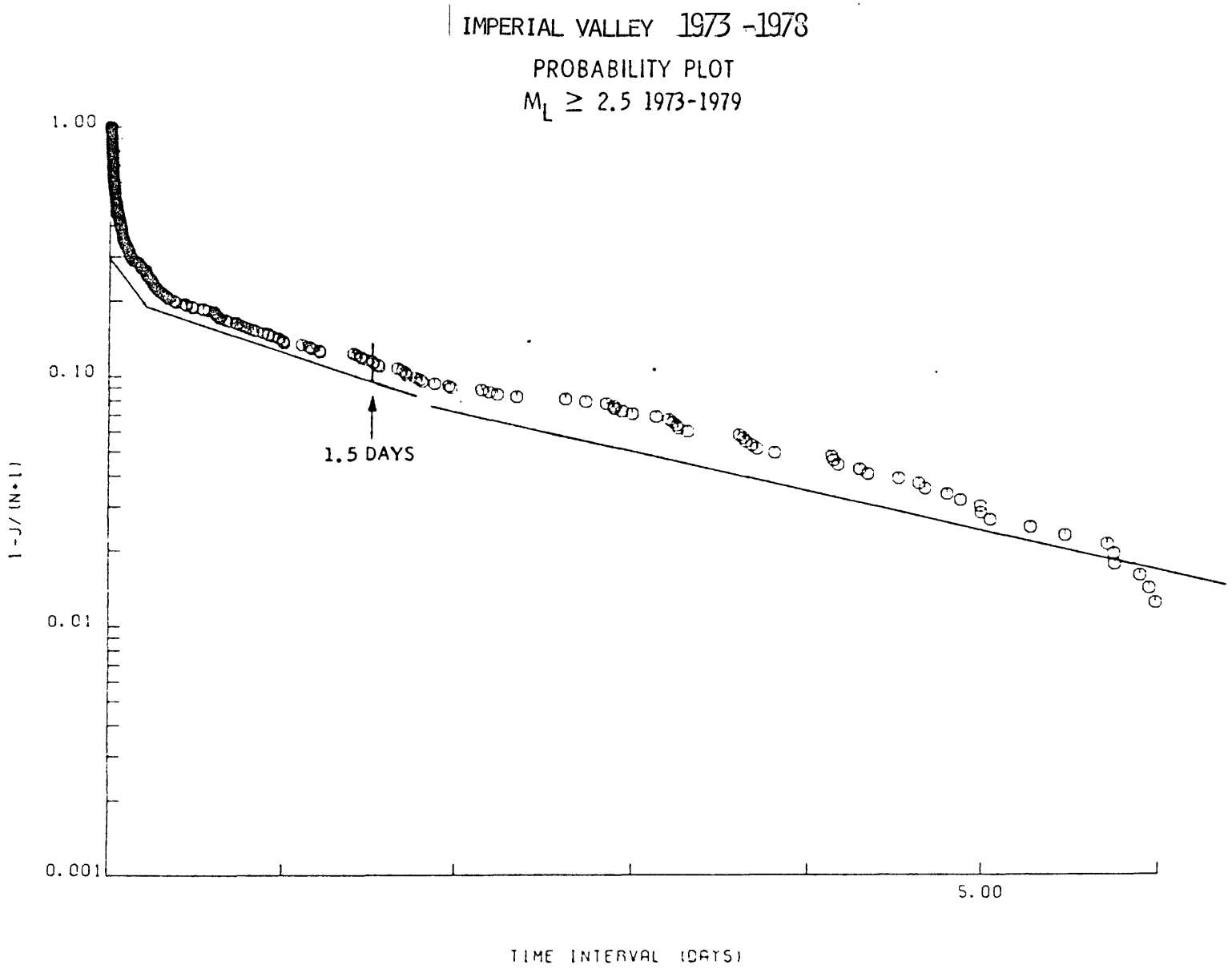

Figure 3. Probability Plot. For a Poisson distribution the time intervals between earthquakes should be exponentially distributed. Hence on a log probability plot the intervals should form an approximately straight line. The strong deviation at small time intervals demonstrates the non-random relationship for events separated by ~ 1.5 or fewer days.

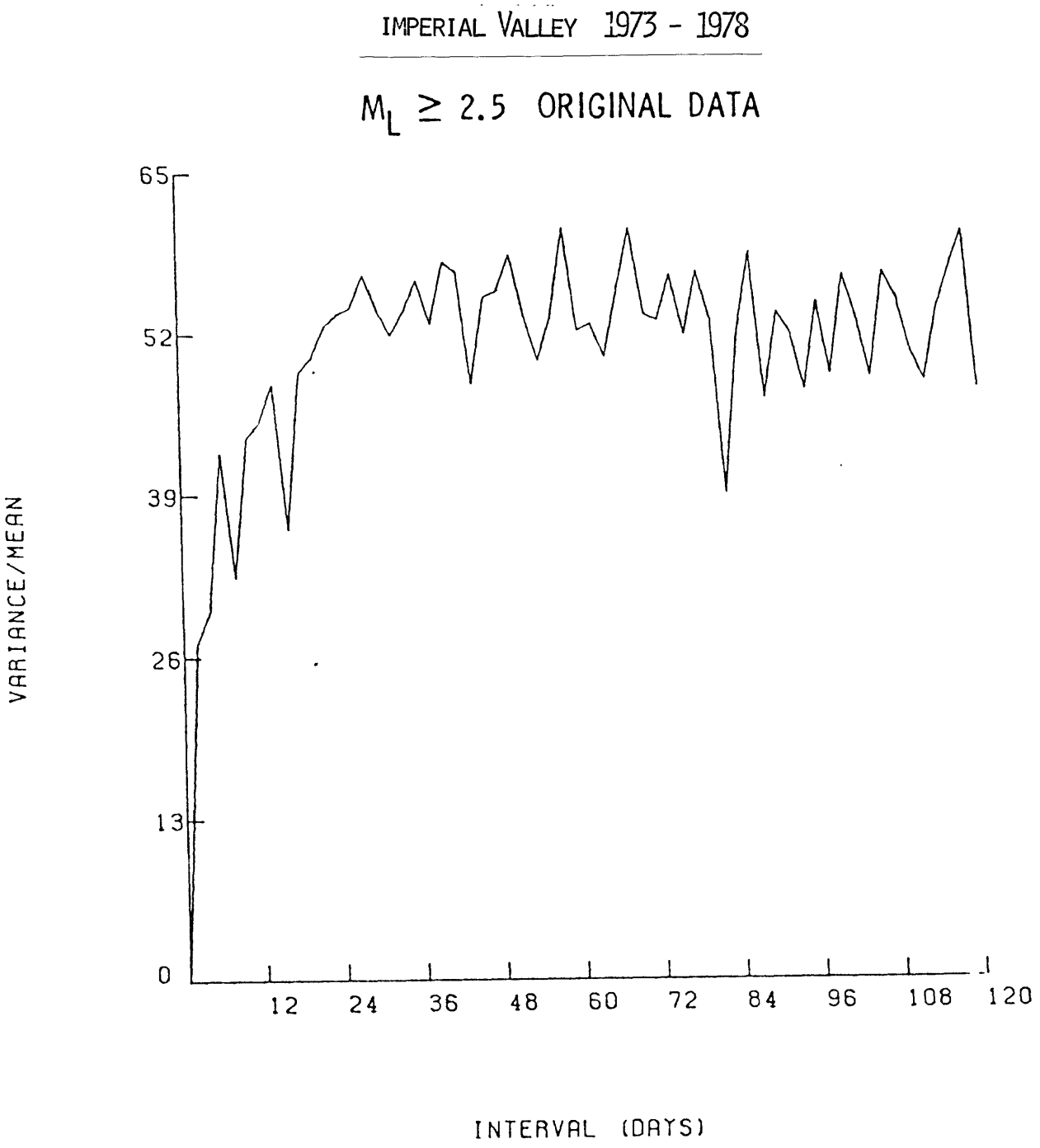

Figure 4. Dispersion Coefficients. This plot is constructed by repeatedly dividing the catalog into time intervals and calculating the mean and the variance of the number of earthquakes per time interval. For a Poisson distribution the variance/mean = 1. The raw data clearly shows deviations from a random sequence.

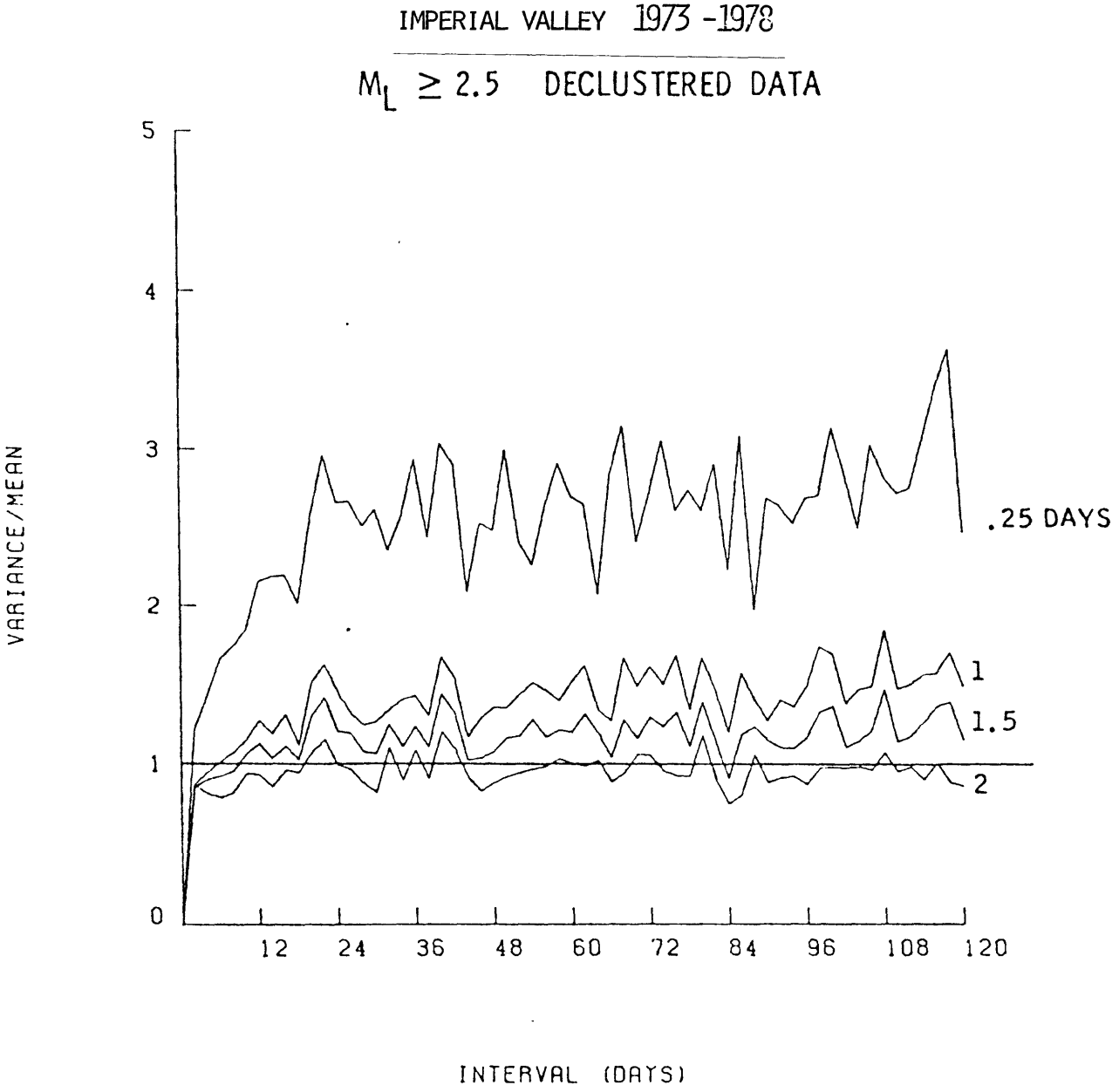

Figure 5. Dispersion Coefficient for four declustering times. The catalog is declustered by deleting all events that follow a previous event within a time interval less than the declustering time. If the declustered catalog approximates a Poisson distribution, then the variance/mean for all intervals is ~ 1.

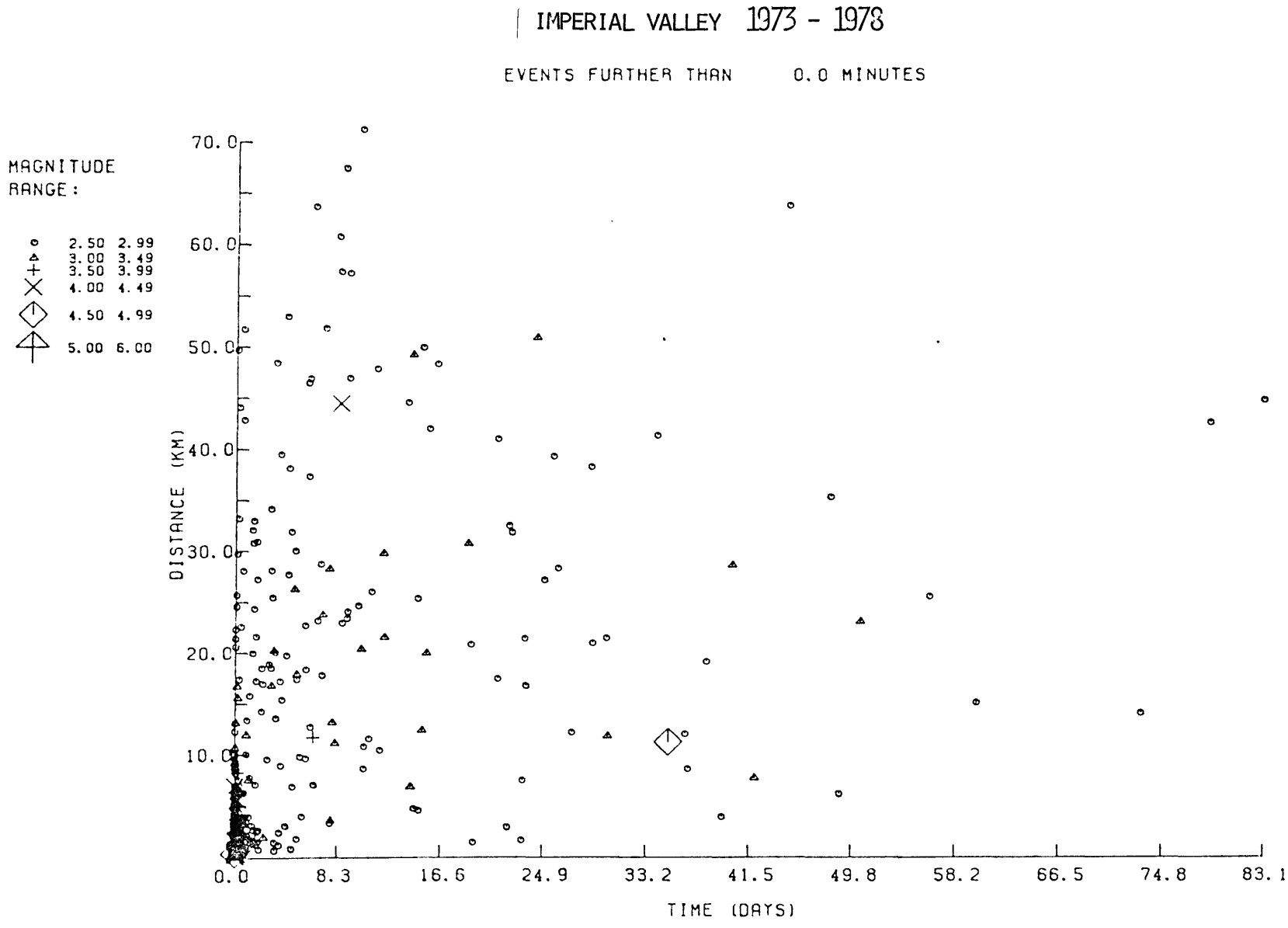

Figure 6. Interoccurrence time vs. interoccurrence distance for the raw catalog. The strong clustering of events at short times and distances show the interdependence of temporal and spatial clusters of events.

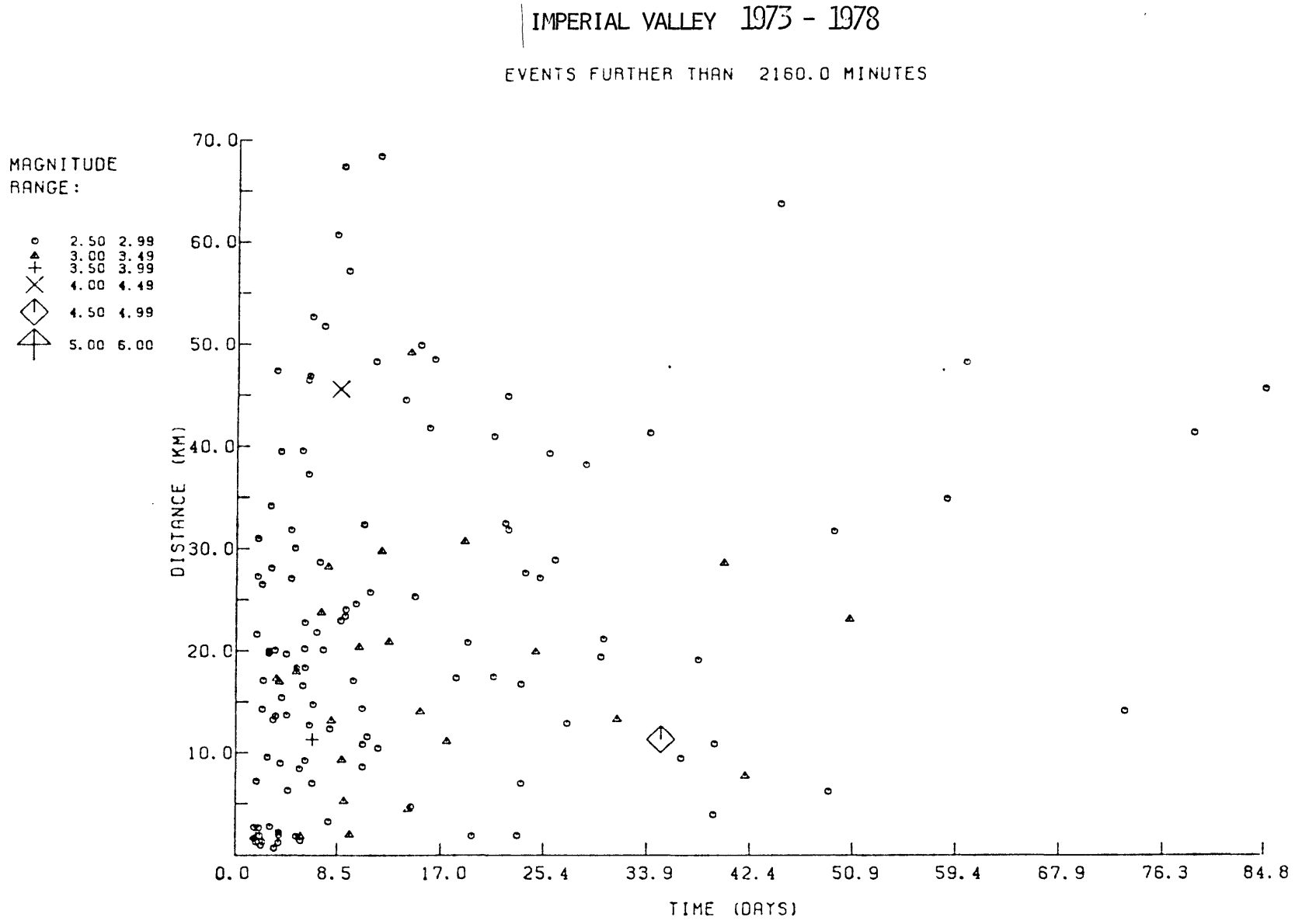

Figure 7. Interoccurrence time vs. interoccurrence distance for the declustered catalog.

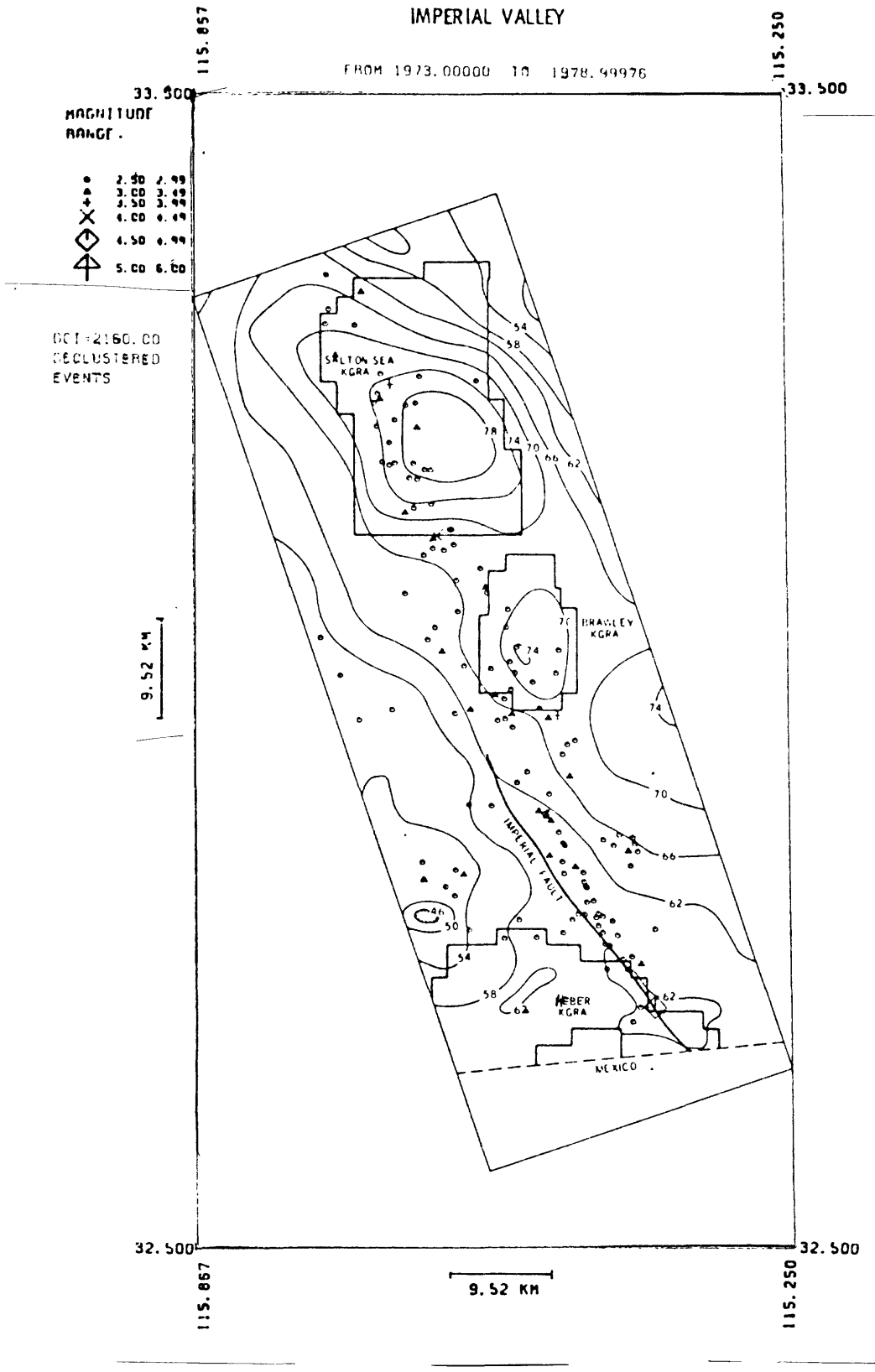

Figure 8. Epicentral locations of the independent or declustered earthquakes, $M_L \geq 2.5$.

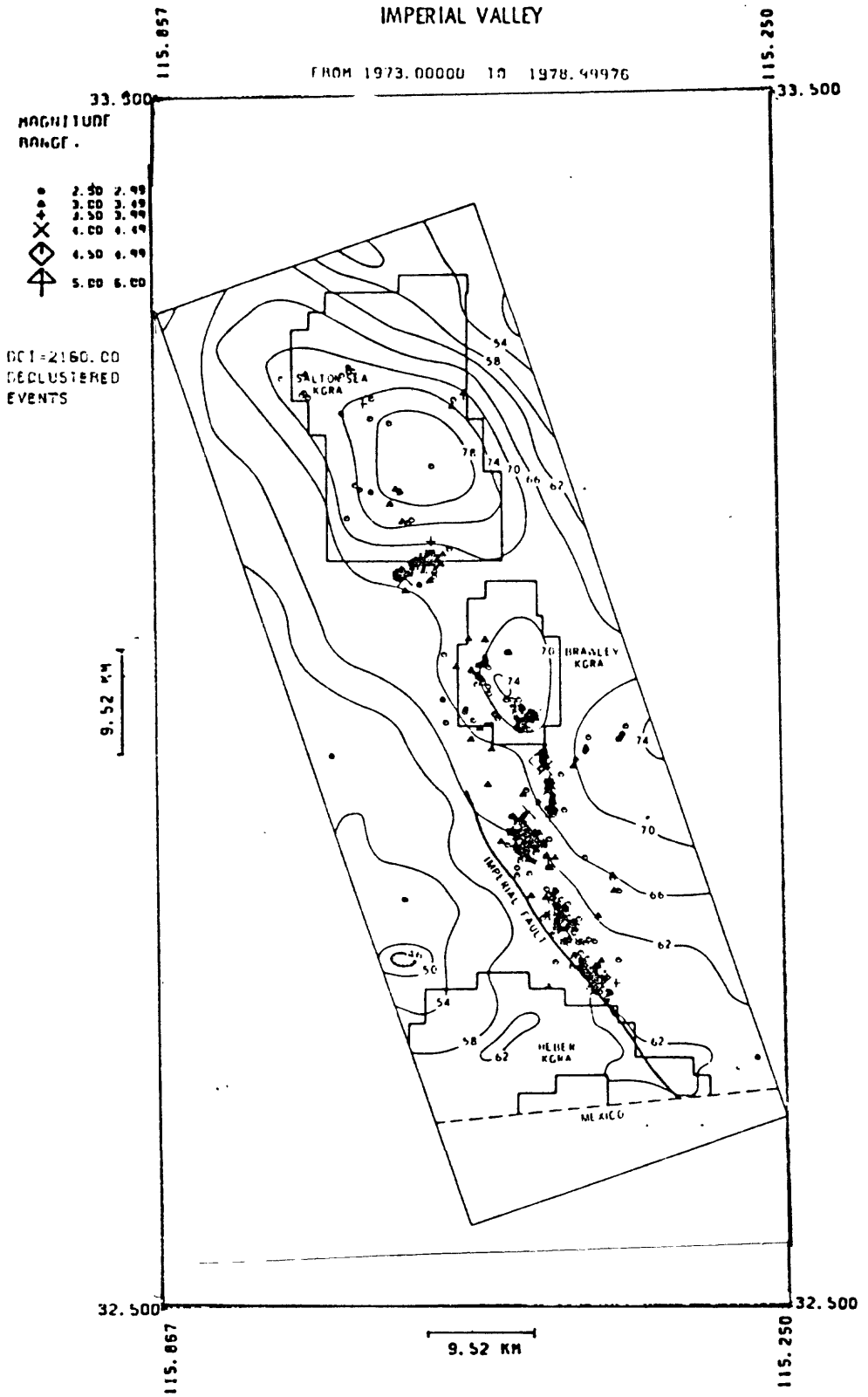

Figure 9. Epicentral locations of the clustered earthquakes, $M_L \geq 2.5$.

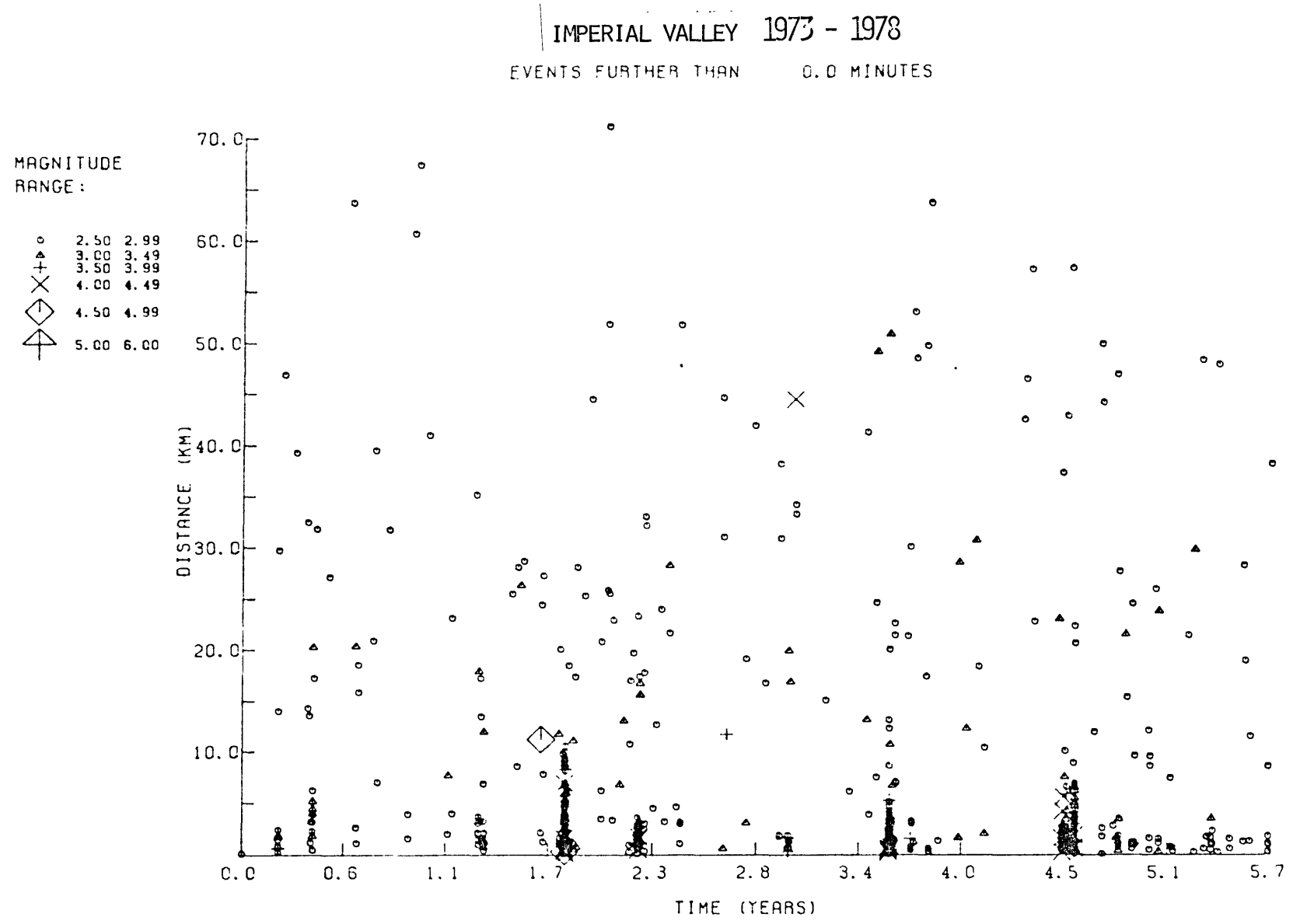

Figure 10. Interoccurrence distance vs. occurrence time. Zero time corresponds to June 1973.

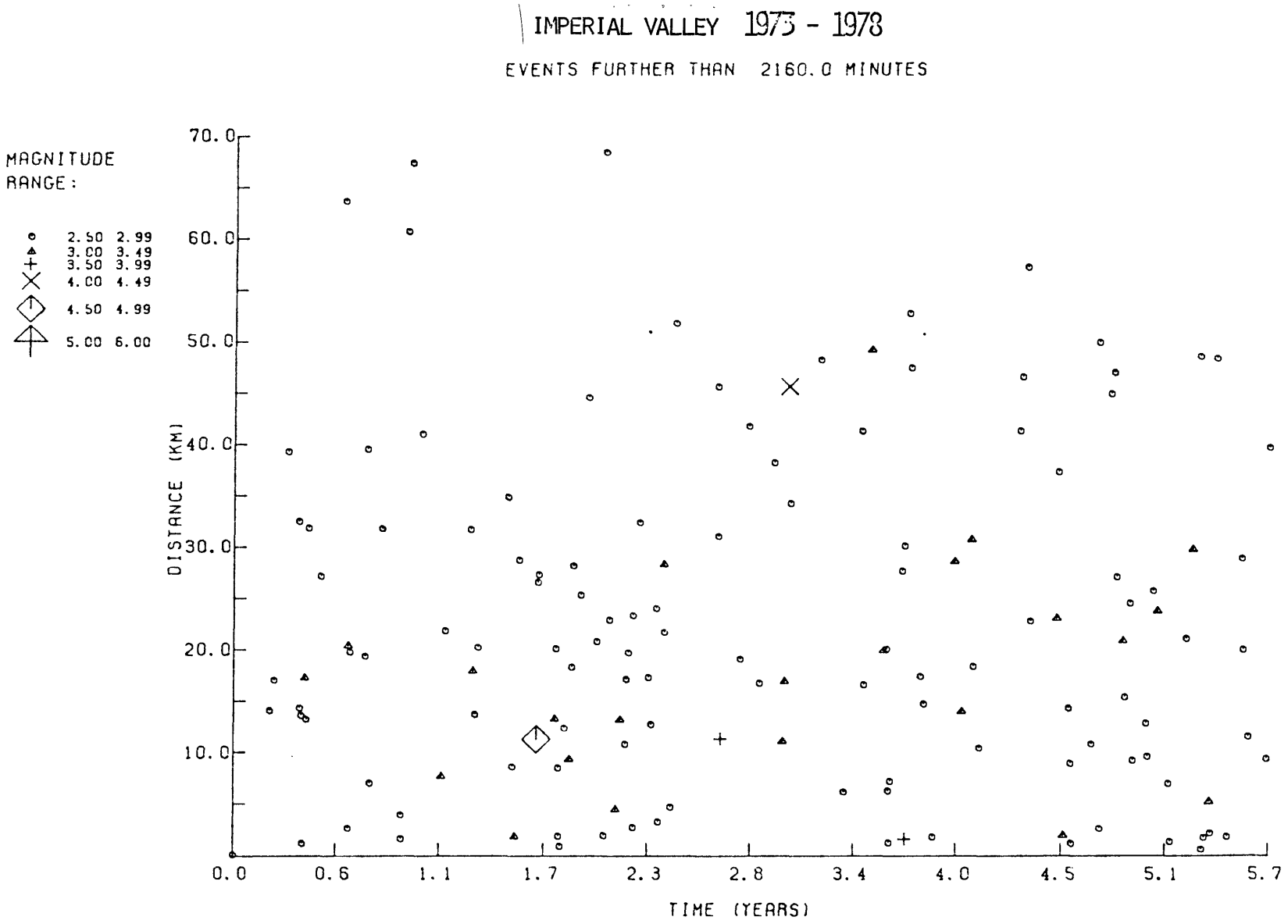

Figure 11. Declustered interoccurrence distance vs. occurrence time. Zero time corresponds to June 1973.

4. COSO GEOTHERMAL AREA

INTRODUCTION

The Coso geothermal area is a young volcanic field with active geothermal surface expressions. The area is located along the Eastern Sierra-Nevada front and is on the China Lake Naval Weapons Center. A sixteen-station seismograph network 40 km north-south by 30 km east-west was operated in the region by the U.S. Geological Survey from September 1975 until October of 1977 when the array was altered and stations were removed (Walter and Weaver, 1980). The network consisted of short period vertical seismometers with an average station spacing of five km. The U.S. Geological Survey assigned magnitudes by the coda-length technique, and events were located with a revised version of HYP071 (Lee and Lahr, 1975). A study of the resulting catalog shows that the threshold for uniform detection is $M_L \geq 1.25$. Nearly 1,500 events with magnitudes greater than this threshold were detected and included in this study.

GEOLOGIC SETTING

The Coso geothermal field is located along the southwest edge of the Basin and Range Province. The area is covered by basaltic and rhyolitic volcanics dating from 4.0 to .04 million years old (Duffield et al., 1980). The basement consists of a pre-Cenozoic volcanic granitic and metamorphic complex that is overlain by late Cenozoic vol-

canic rocks and by small basins of shallow Quaternary alluvial deposits. The area is characterized by rhyolite domes that occur along a north-trending structural high and are 1.1 to .04 million years old (Combs, 1980).

The faulting in the Coso region is extensive and quite complex. Two types of faulting dominate the region: vertical faults trending north to northwest, and a group of arcuate faults. Based on the recent volcanism and faulting, the primary heat source for the Coso area is thought to consist of a crustal magma body (Smith and Shaw, 1975). This is in good agreement with the observed heat flow which reaches a maximum of ~15 HFU (heat flow units) in the central part of the rhyolitic domes (Combs, 1980).

DATA ANALYSIS

Figure 12 shows the epicentral locations of the events used in this study. This catalog covers the period June 1975 to August 1977 (discussed by Walter and Weaver, 1980). Figure 13 shows the frequency vs. magnitude plot for this catalog. The deviation from the expected linearity at approximately $M_L \geqq 1.25$ defines the threshold for uniform detection. The following paragraphs describe the analysis carried out for three magnitude thresholds: 1.25, 1.5, and 2.0.

At each of these thresholds, significant temporal clustering was found. The catalog was converted into a time series and the probability plots of the ordered time in-

tervals for each threshold were next computed. Figure 14 shows the probability plot for the $M_L > 2.0$ threshold. From these probability plots trial declustering times were chosen for analysis with the Poisson dispersion test (variance/mean). Figures 15 and 16 show examples of the raw and declustered plots of the dispersion coefficients for the magnitude threshold $M_L \geq 2.0$. From this analysis the declustering time intervals that render the catalog most random for each threshold are : $M_L \geq 1.50$ - 810 min; $M_L \geq 1.25$ - 900 min; and $M_L \geq 2.0$ - 2160 min.

For the magnitude thresholds studies for Coso we have found that the dispersion coefficient curves have only a slight positive trend. This suggests that the catalog contains few long term mainshock-aftershock sequences.

The spatial and temporal clustering of earthquakes is also illustrated by plotting the distance between consecutive events as a function of time (Figure 17). The effectiveness of declustering the catalog on the basis of interoccurrence times is shown in the declustered plot of interoccurrence distance versus time (Figure 18). Epicenter maps showing the random (Figure 19) and clusters (Figure 20) components of the seismicity have also been prepared. In the Imperial Valley, these subcatalogs showed a localized, narrow zone of clustered events and a diffuse broad zone of random earthquakes. In the area of highest heat flow, the number clustered or random events that were rarely associated with the reservoirs was very low. For Coso, the

area of highest heat flow is associated with both clustered and random events. On the sole basis of the spatial distributions of either the random or the clustered events, we cannot identify the reservoir location. The only significant observation from the spatial study is that the reservoir region is void of the larger (M_L > 3.0) events.

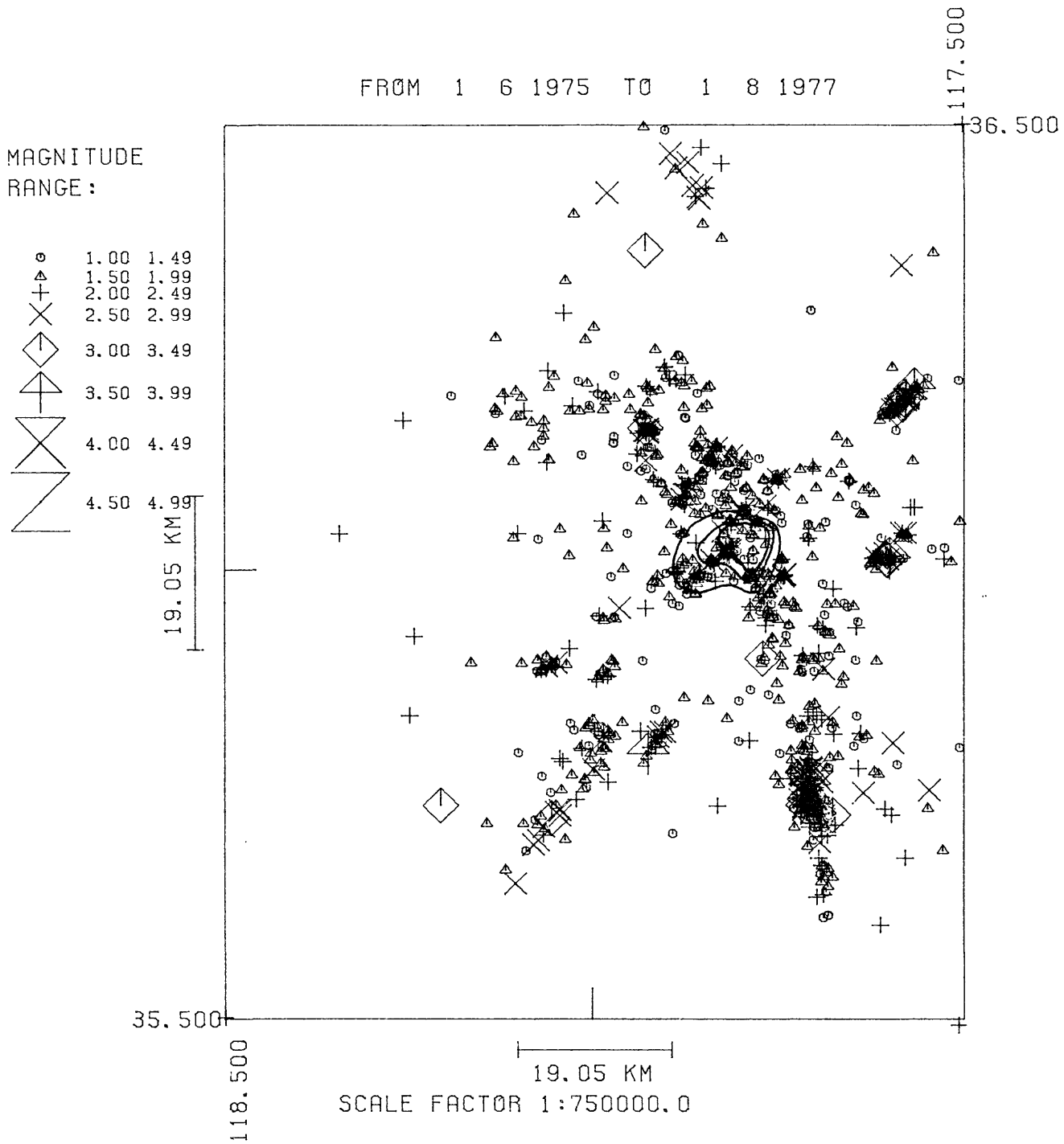

Figure 12. Earthquake locations within the Coso Region for the period June 1975 to August 1977. The heat flow contour values are 3, 5 and 10 HFU (Combs, 1980).

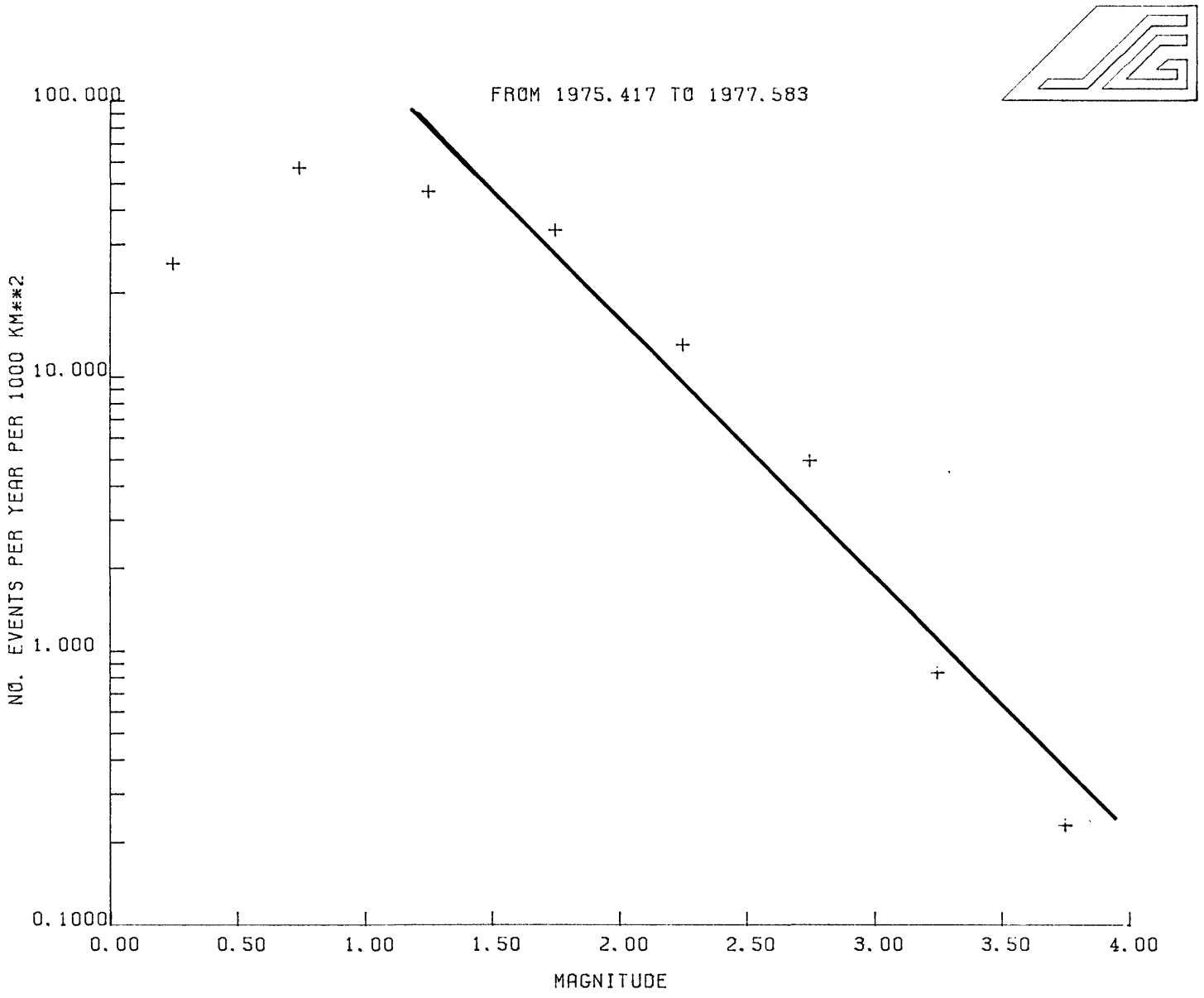

Figure 13. Frequency versus magnitude for the Coso earthquakes shown in Figure 12. The magnitude threshold for uniform detection is approximately $M_L \geq 1.25$.

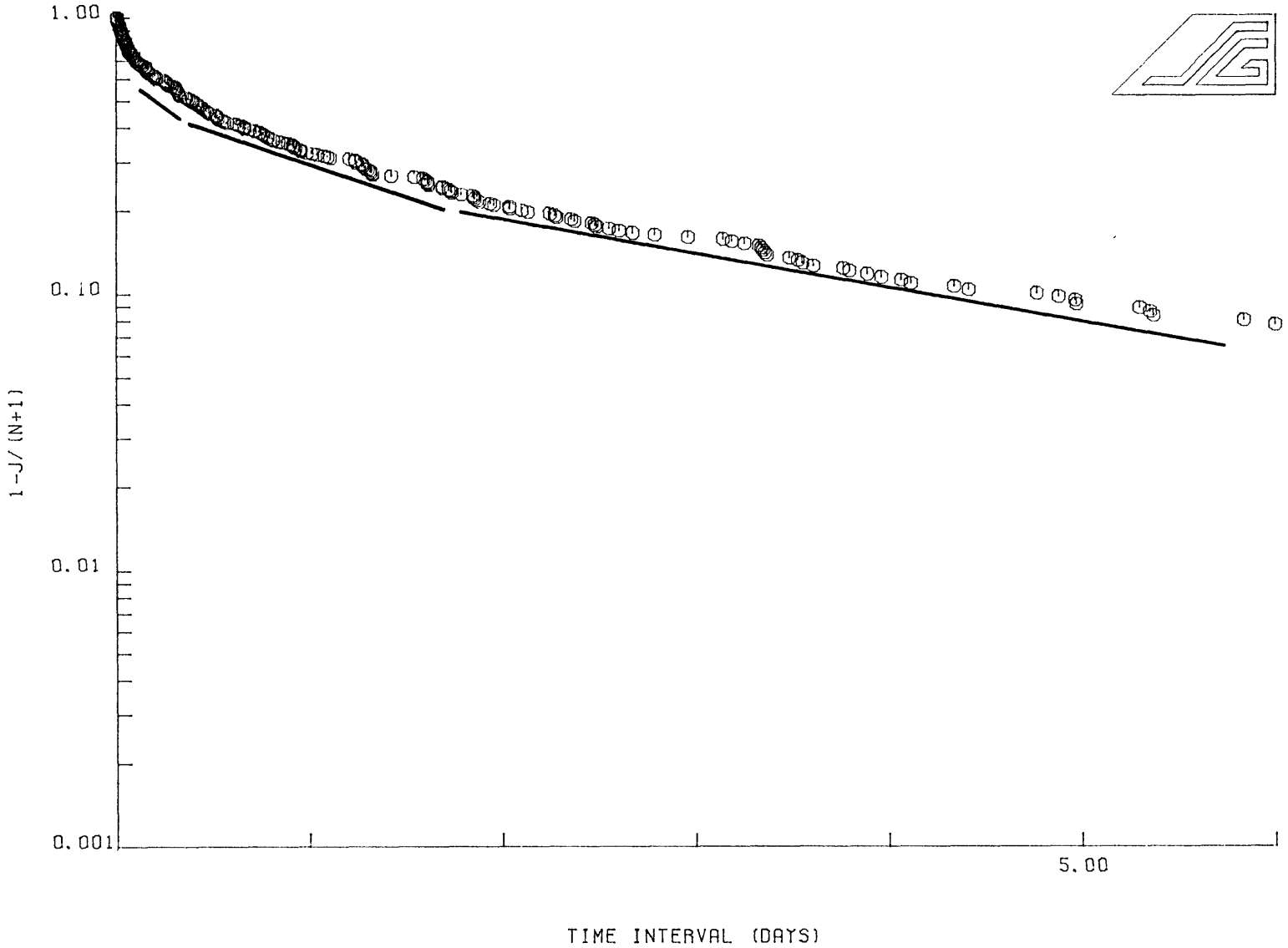

Figure 14. Probability plot for the Coso data, $M_L \geq 2.0$. The deviation of the points from a straight line demonstrates the non-random character of short interoccurrence time intervals.

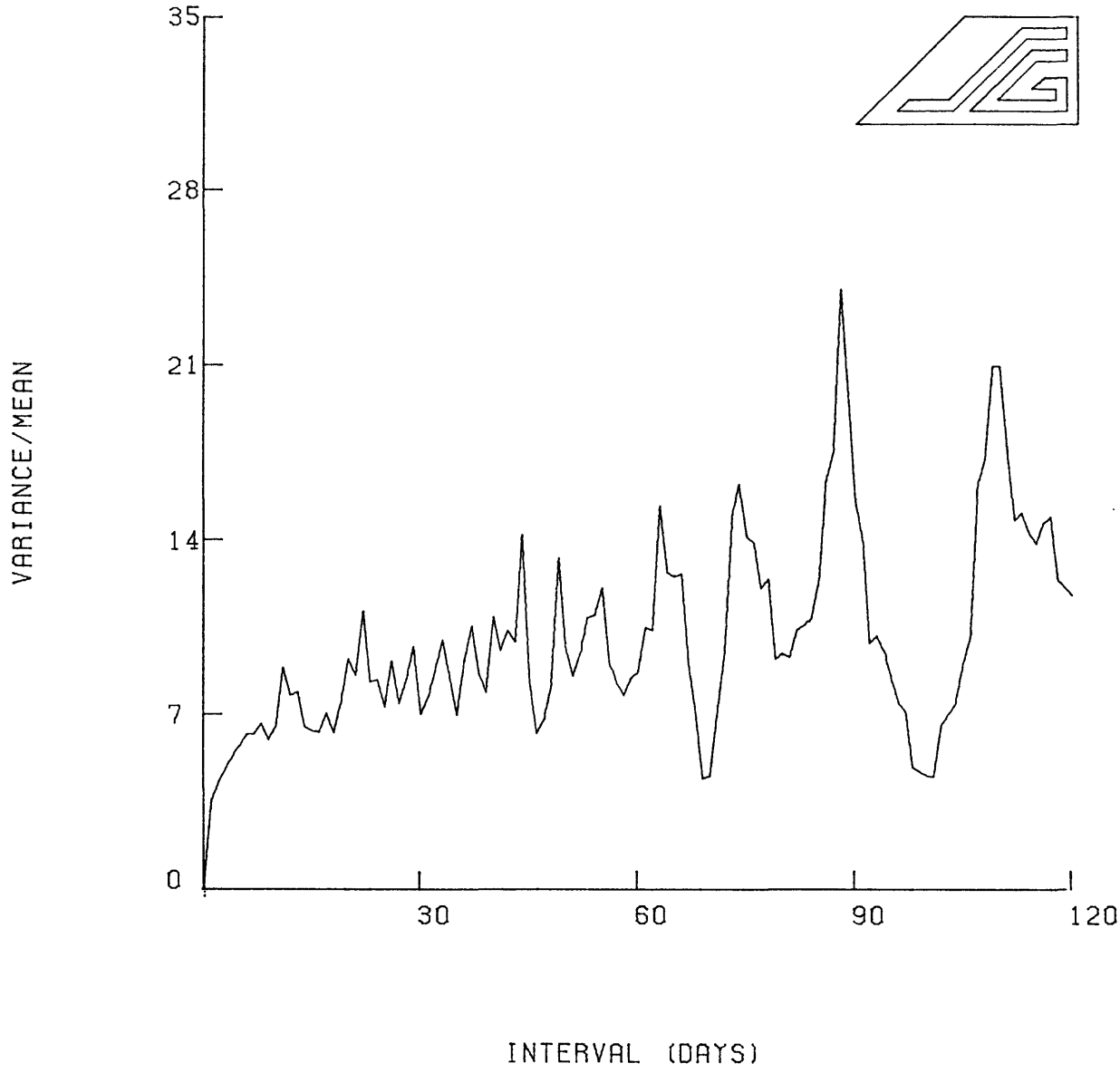

Figure 15. Dispersion coefficients for raw Coso catalog, $M_L \geq 2.0$

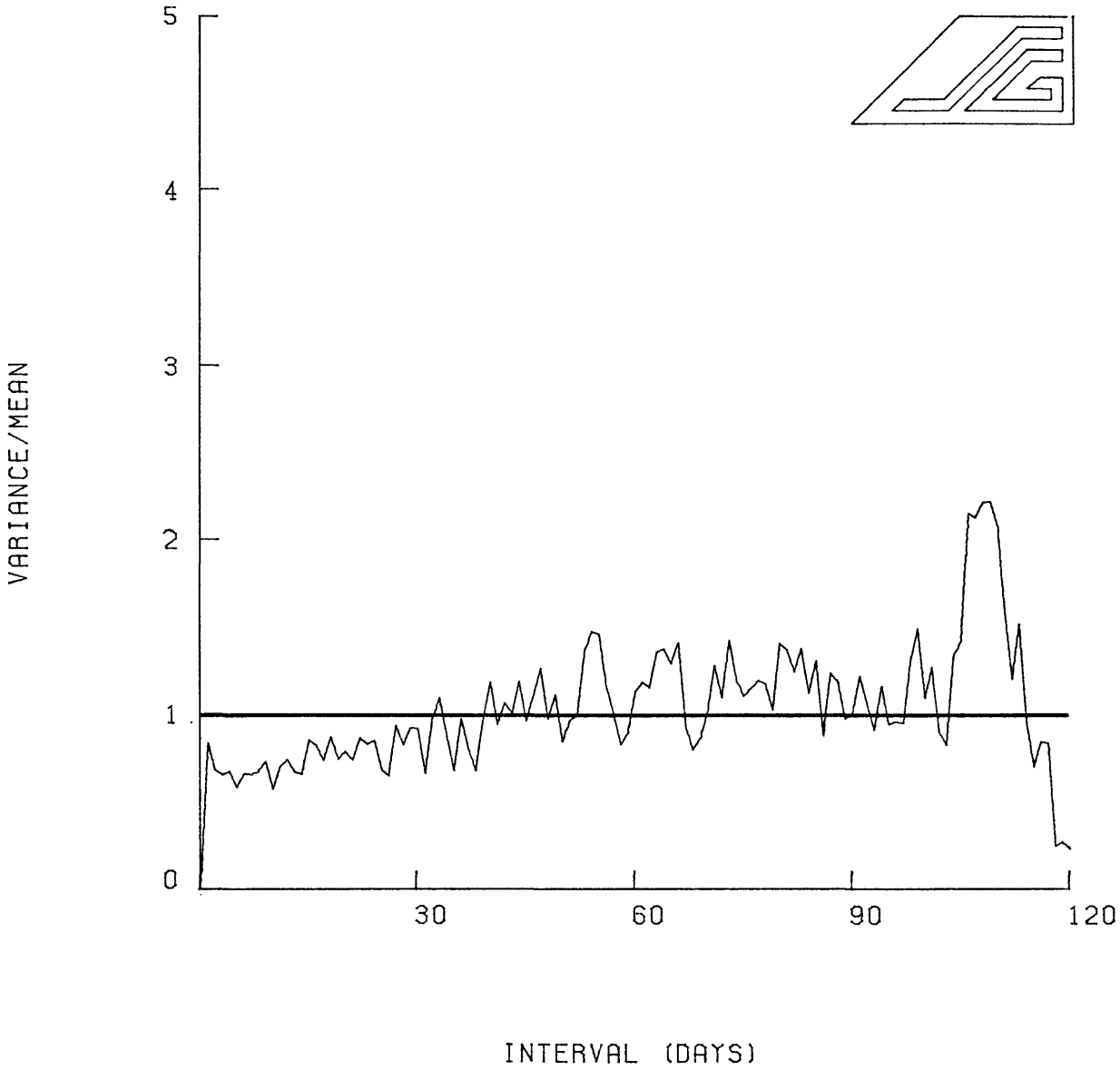

Figure 16. Dispersion coefficients for the declustered Coso catalog, $M_L \geq 2.0$. The best declustering time was 2160 min (1.5 days).

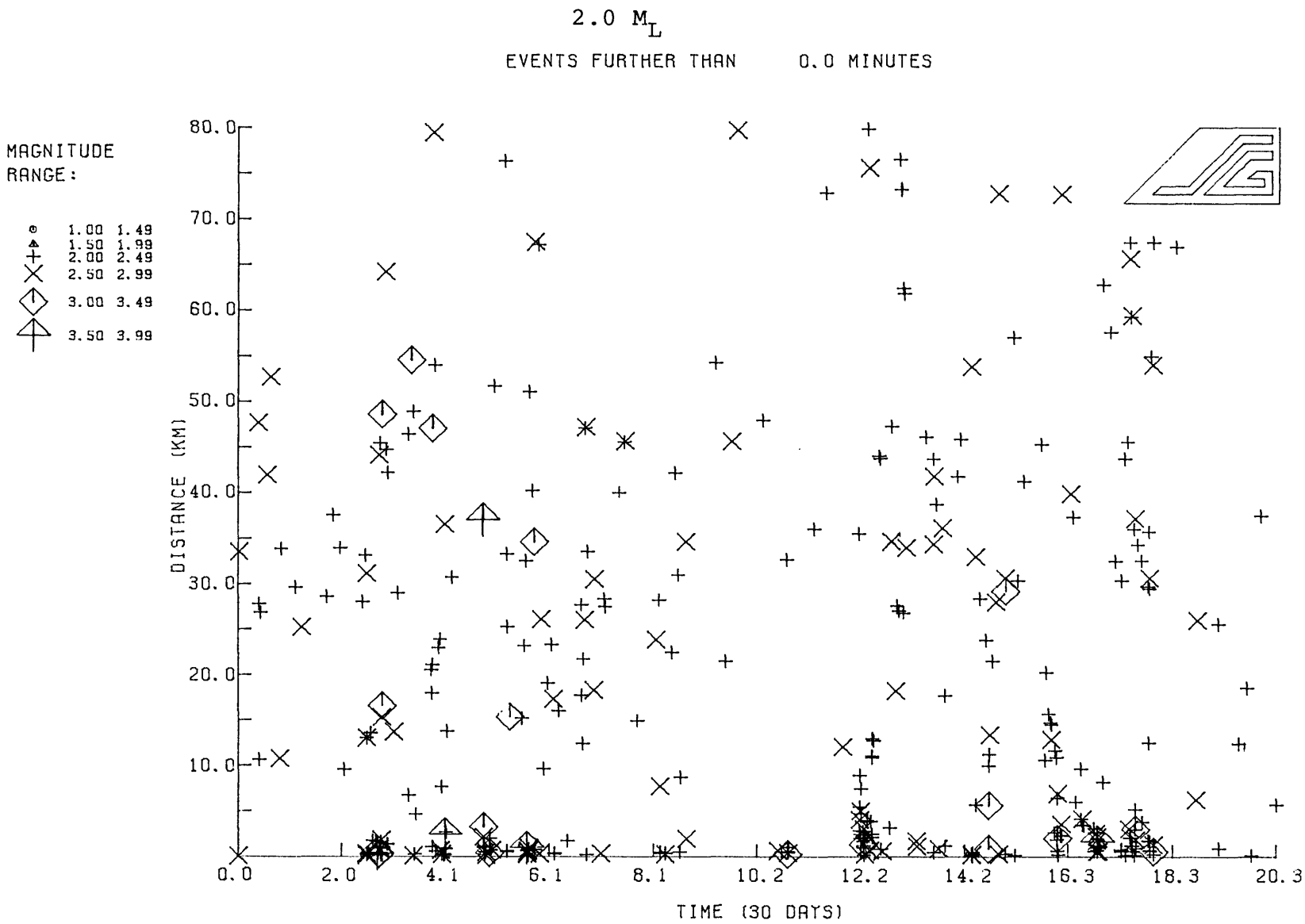

Figure 17. Interoccurrence distance vs. occurrence time for the raw Coso catalog, $M_L \geq 2.0$, zero time corresponds to June 1975.

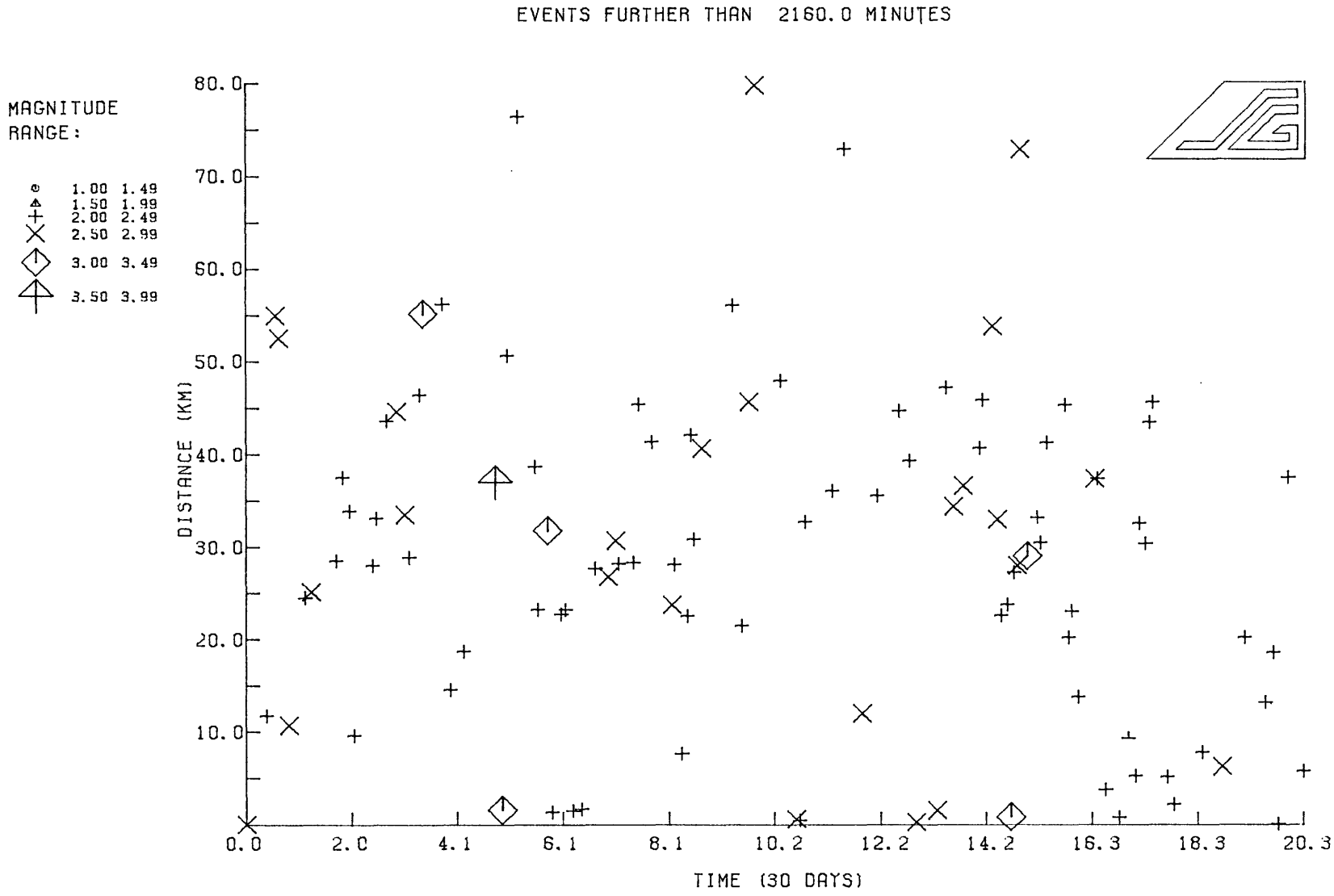

Figure 18. Interoccurrence distance vs. occurrence time for the declustered Coso catalog, $M_L \geq 2.0$.

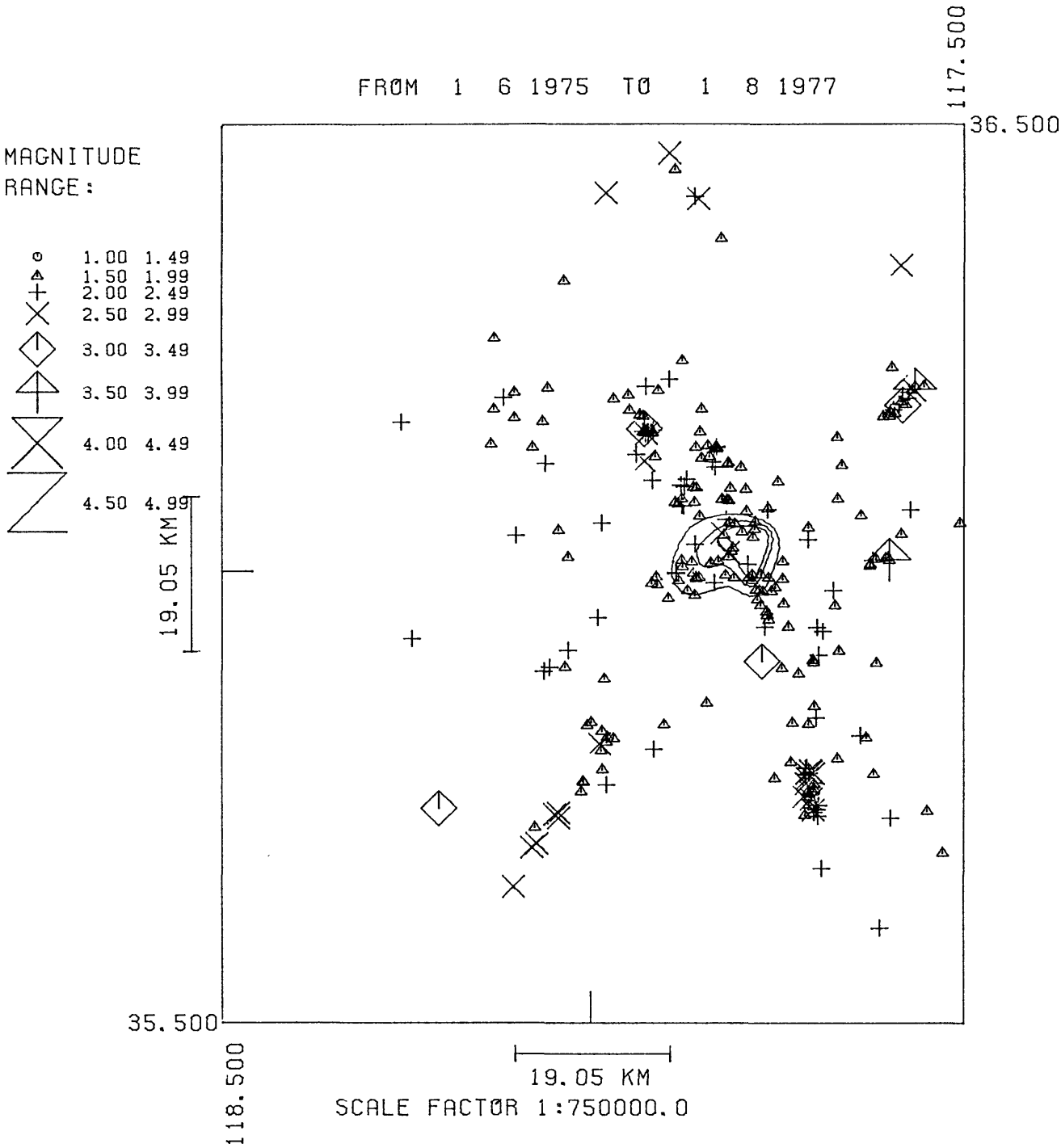

Figure 19. Epicentral locations of the temporally random, independent events from the Coso catalog $M_L \geq 1.5$. Note that the removal of temporal clusters from the catalog has not eliminated spatial clustering.

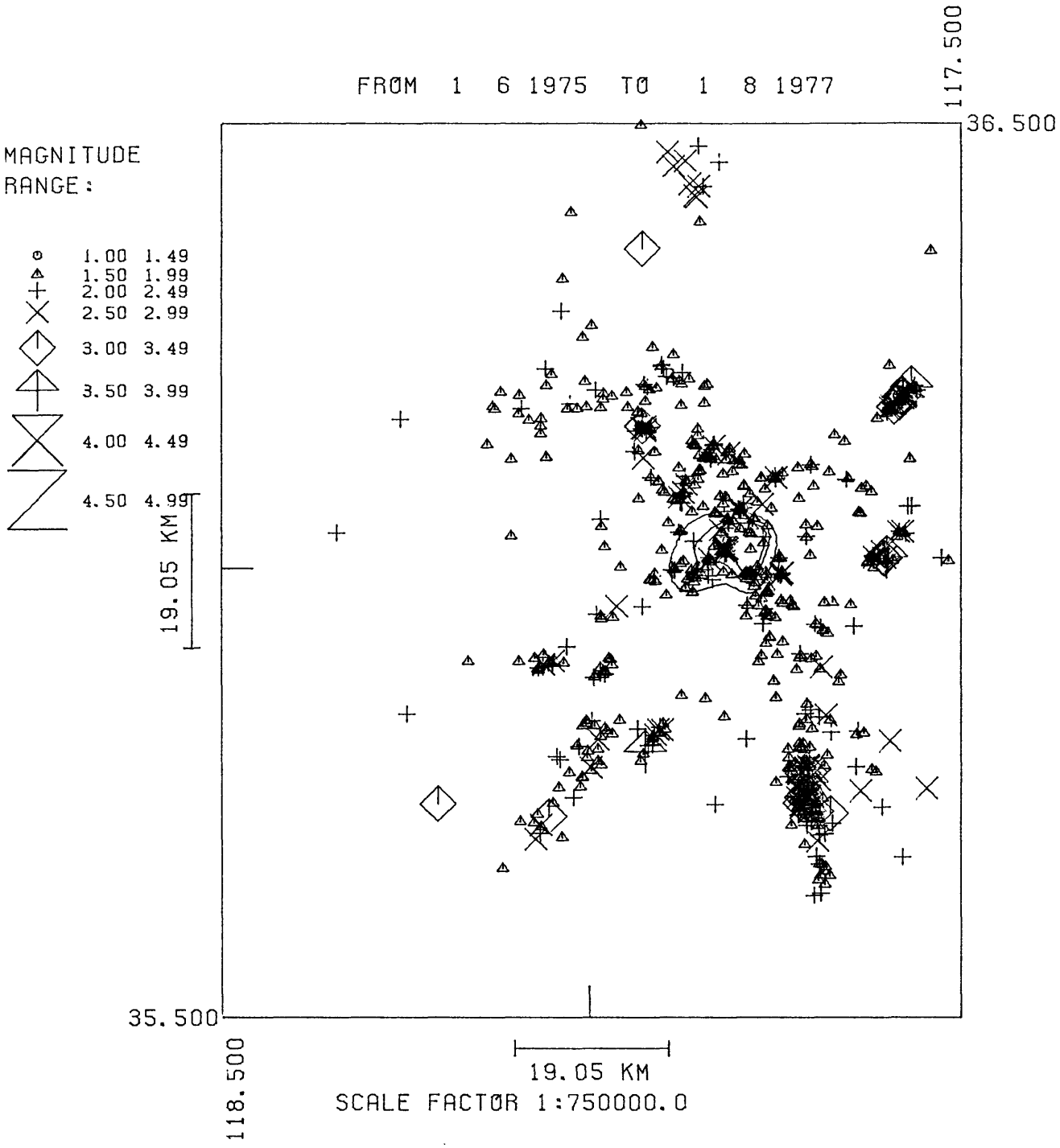

Figure 20. Epicentral locations of the clustered events from the Coso catalog $M_l \geq 1.5$.

5. THE GEYSERS GEOTHERMAL AREA

INTRODUCTION

The geothermal electric power produced from the Geysers reservoir is the largest in the world with 663 megawatts of generating capacity in place and 320 additional megawatts soon to be in operation (Brook et al., 1979). Although the areal extent of the reservoir is unknown, various estimates range from 60 to 120 square kilometers and the production depth extends to approximately 3 km. Most of the steam production comes from depths of 2 to 2.5 kilometers. Pressures range from 30 to 40 bars and temperatures are near 240°C (Weres, et al. 1977).

The earthquake data used in the present study came from stations operated by the U.S. Geological Survey (Ludwin and Bufe, 1980). The data spans the period January 1973 to August 1979. Analysis of yearly frequency versus magnitude plots shows that the catalog is complete at a magnitude threshold of $M_L \geq 1.25$. Approximately 1000 events were within this threshold and were used in the following analysis. The epicenter map for this threshold is shown in Figure 21. The star-shaped symbols indicate the location of geothermal production wells.

GEOLOGIC SETTING

Mesozoic Franciscan rocks and units from the Great Valley sequence, combined with the younger Clear Lake volcanics underlie the region (McLaughlin, 1977). The

Franciscan consists of graywacke and minor shale with serpentinite in the highly sheared and faulted regions. The Great Valley section consists of a clastic sequence of marine sedimentary rocks. The Clear Lake volcanics are composed primarily of dacite and andesite, ranging in age from two million to approximately 10,000 years (Hearn et al., 1976). This formation forms the most prominent landforms in the area. The Great Valley sequence has been only mildly altered while the Franciscan assemblage represents a metamorphic regime associated with subduction.

The fault pattern is oriented northwest-southeast with both strike-slip and thrust faulting. Keeping with the overall pattern of the San Andreas system, strike-slip faulting is the dominant mode of strain release. Because of the relatively low permeability of the unfractured rock (Garrison, 1972), zones of steam production are characteristically associated with shear zones in the lower Franciscan formation. Along a zone of older regional faults, the Great Valley sequence has been thrust over the Franciscan assemblage, contributing to the overall complexity of the structure.

DATA ANALYSIS

The magnitude threshold of 1.25 for uniform detection was determined by plotting, on a yearly basis, frequency versus magnitude. The plot for the entire period is shown in Figure 22. Over 1,000 earthquakes in the available

catalog have magnitudes greater than 1.25. These earthquakes were used in the following statistical analysis.

A first estimate of the best declustering times was derived from the probability plot of the ordered set of J time intervals, log (1-j/n+1). The resultant plot for $M_L \geq 1.25$, Figure 23, shows a nearly linear distribution of time intervals. This sharply contrasts to those areas with strong earthquake clustering such as the Imperial Valley. This plot indicates that the catalog is nearly a Poisson distribution in its raw form. At magnitude thresholds of $M_L \geq 1.5$ and $M_L \geq 2.0$, the catalog is even more random. This impression is further confirmed by the Poisson dispersion analysis of the raw catalog, Figure 24. Note that the variance/mean ratio for the raw catalog is much closer to unity than the ratios for either the Imperial Valley or Coso catalogs. Using a range of small trial declustering times, Poisson dispersion coefficient plots were analyzed to identify any weak temporal clustering. Figure 25 shows the plot of the dispersion coefficients versus increasing time interval for several declustering times. This curve shows a steep slope which, in comparison with the slope of the curve for Coso, has few deviations from linearity. The positive linear slope of the Geysers dispersion coefficient is probably the result of small aftershocks and weak long-term clustering that is superimposed on the continuum of random events. Coso has considerably less positive bias. This linearity is also not due to major reservoir differences since Lassen, which is

thought to have similar reservoir characteristics, does not show the same trends. At higher magnitude thresholds the slope of the Poisson dispersion coefficient for the Geysers data decreased. This is possibly the result of eliminating aftershocks from the data set. This effect was noted previously by McNally, 1976, in studies of Central California earthquakes.

The deviations from linearity or "spiky" nature of the data, or lack thereof, give clues to the nature of the clustering. The effects of cyclic sequences of events that are of long duration with numerous events can never be completely removed from the dispersion coefficient calculations. Small oscillations or deviations indicate little of this long-term clustering. Figure 25 shows clearly how the use of different declustering times on this time series does little to affect the already near Poisson distribution or the linear trend. We may therefore conclude that The Geysers exhibits little or no short-term (1-30 day) clustering of earthquakes in the currently defined reservoir area. This is further demonstrated by examining the inter-occurrence distance versus time relation for the raw catalog (Figure 26). Note that short vertical clusters (temporally and spatially close), such as found in Figure 17 for Coso and Figure 10 for Imperial Valley, are not observed in the data shown in figure 26.

The spatial distribution of earthquakes in The Geysers reservoir is quite clustered when compared with the temporal

distribution. This clustering appears to occur around currently operating injection wells near the power plants. Figure 21 shows this distribution quite clearly along with the locations of the injection wells, plotted as star-shaped symbols. Figures 27 and 28 show the epicenter maps for the random and clustered subcatalogs respectively.

Based on the temporal and spatial distribution of earthquakes at The Geysers and the comparison of these characteristics with other geothermal reservoirs, it appears that the seismicity of this region is quite unusual. These data suggest that the power generation activities at The Geysers and the attendant removal and reinjection of fluids have altered the normal seismicity in the production zone.

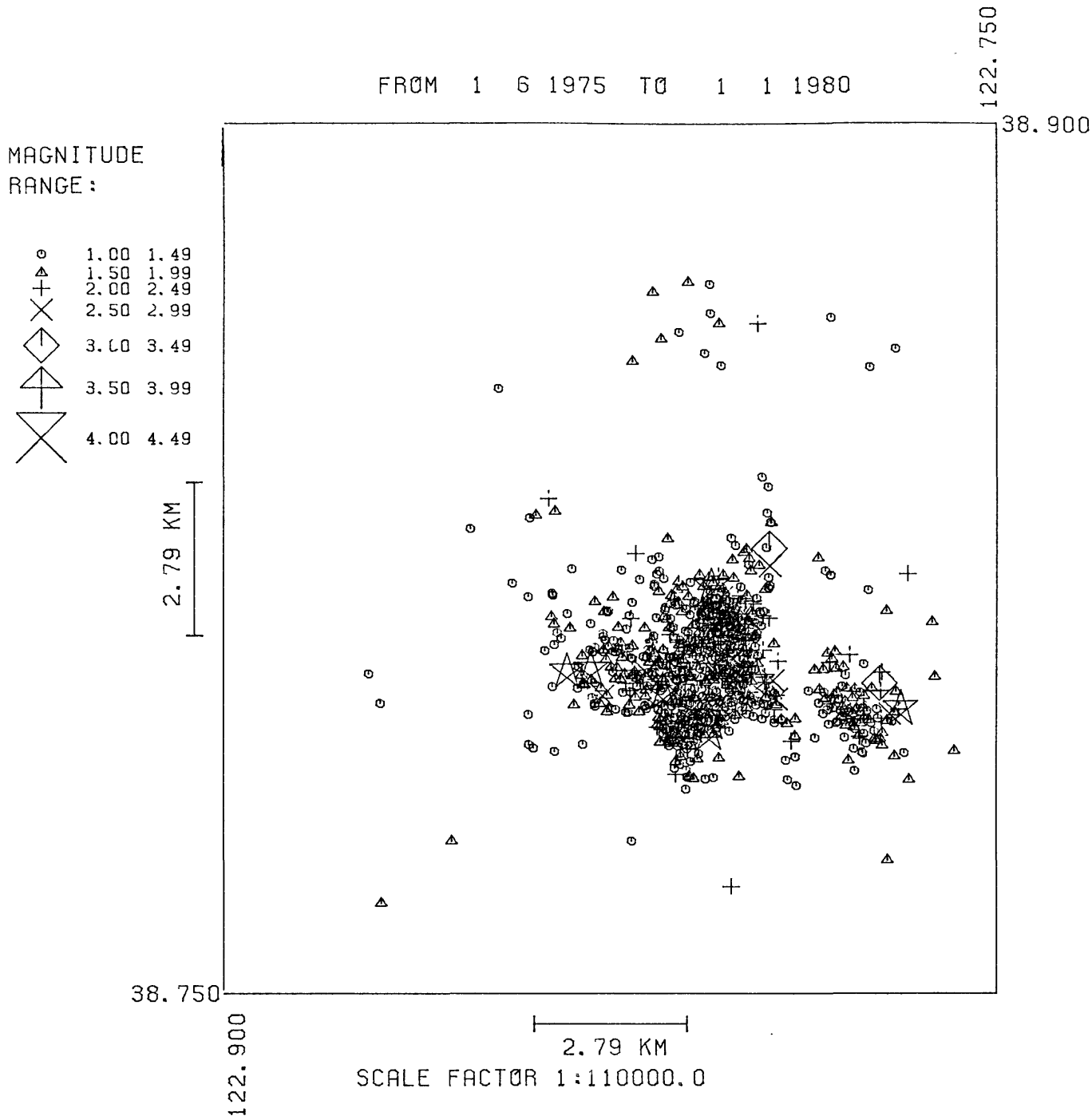

Figure 21. Earthquake locations within The Geysers Region, $M_L \geq 1.25$. The analyzed portion of the catalog spans the period June 1975 through August 1979. The star-shaped symbols indicate the location of production wells.

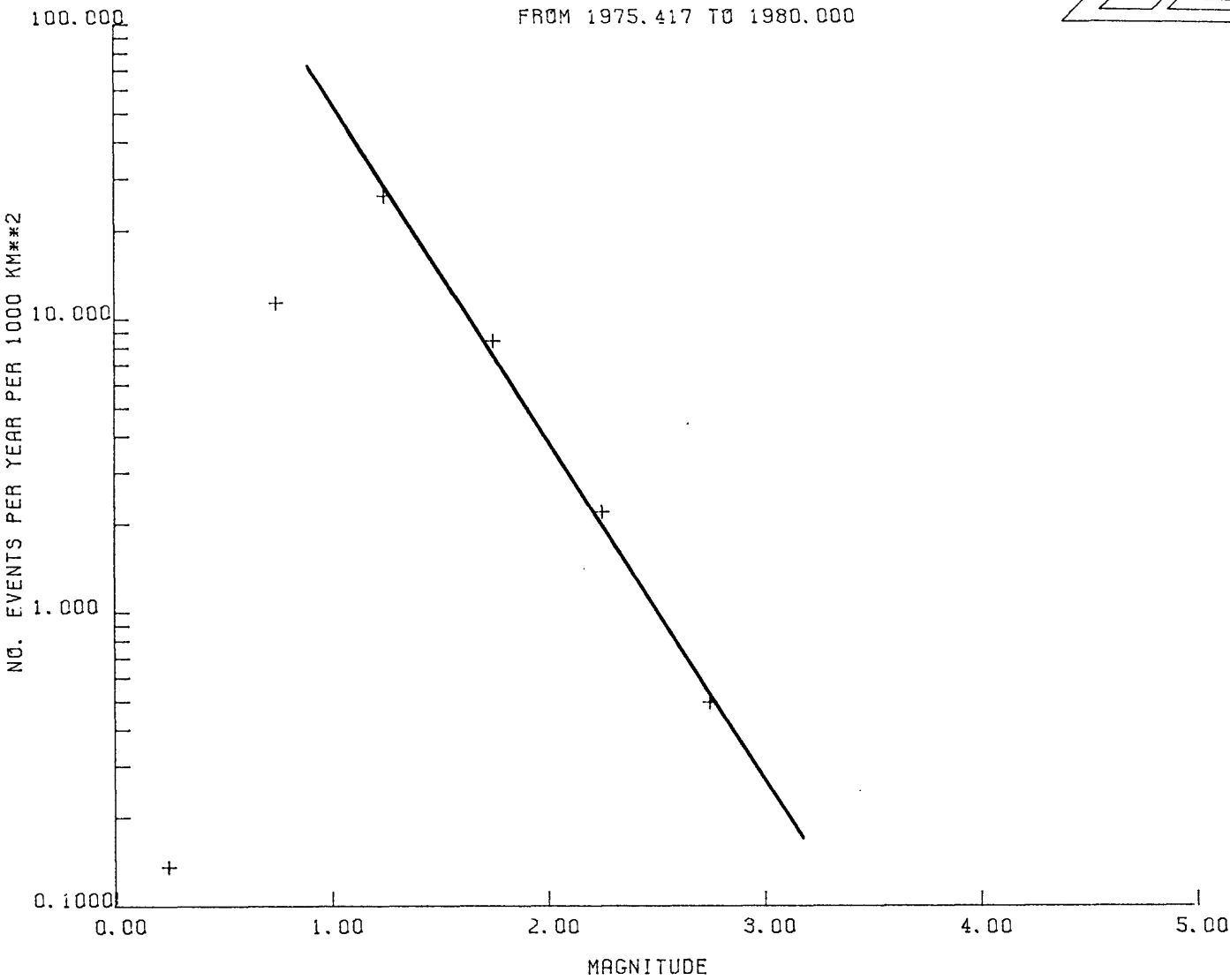

Figure 22. Frequency versus magnitude for The Geysers catalog. The magnitude threshold for uniform detection is approximately $M_L \geq 1.25$.

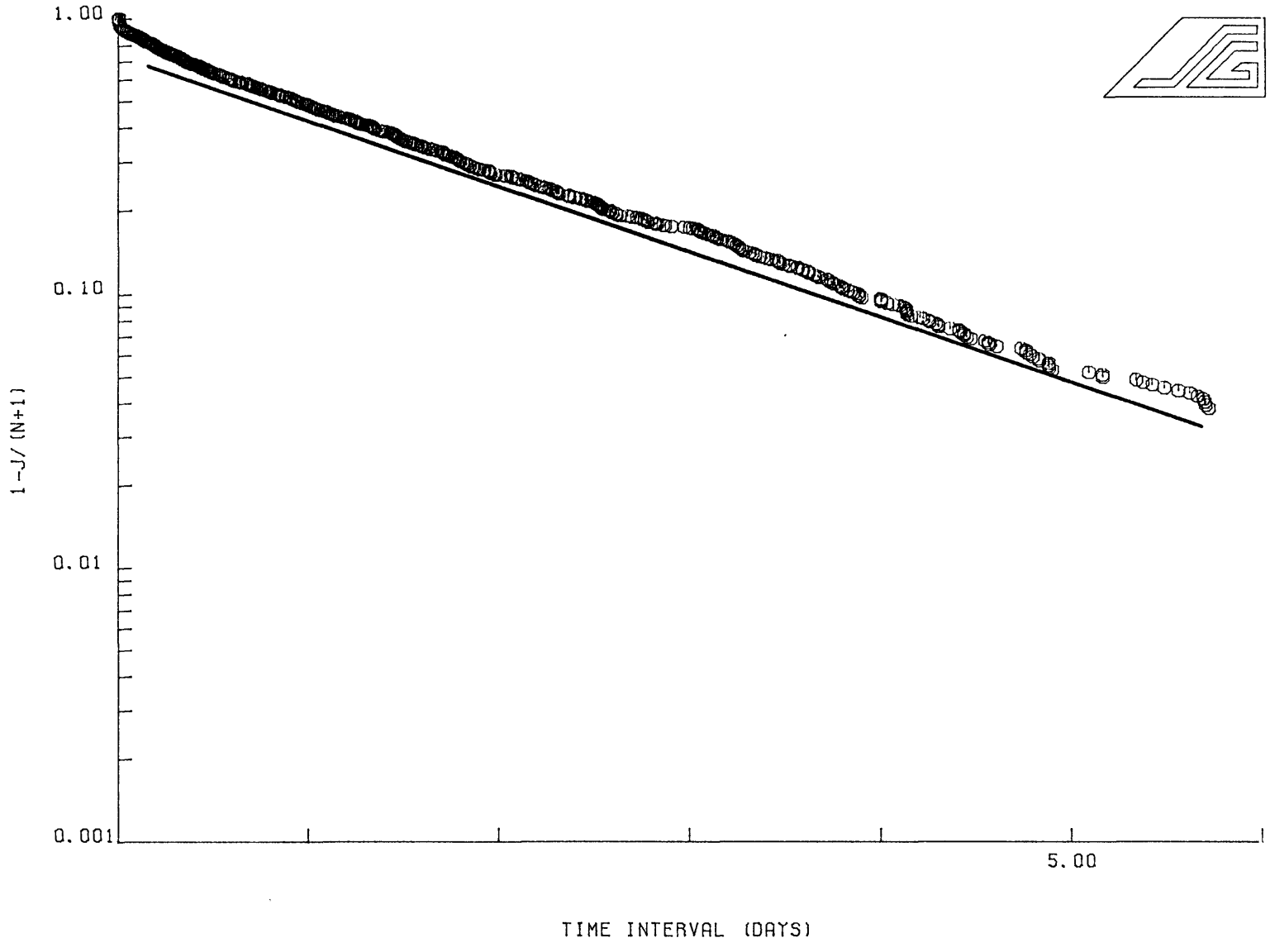

Figure 23. Probability plot for The Geysers data, $M_L \geq 1.25$. This plot shows that The Geysers seismicity is nearly random in time. This is in marked contrast with the results for the other geothermal systems studied.

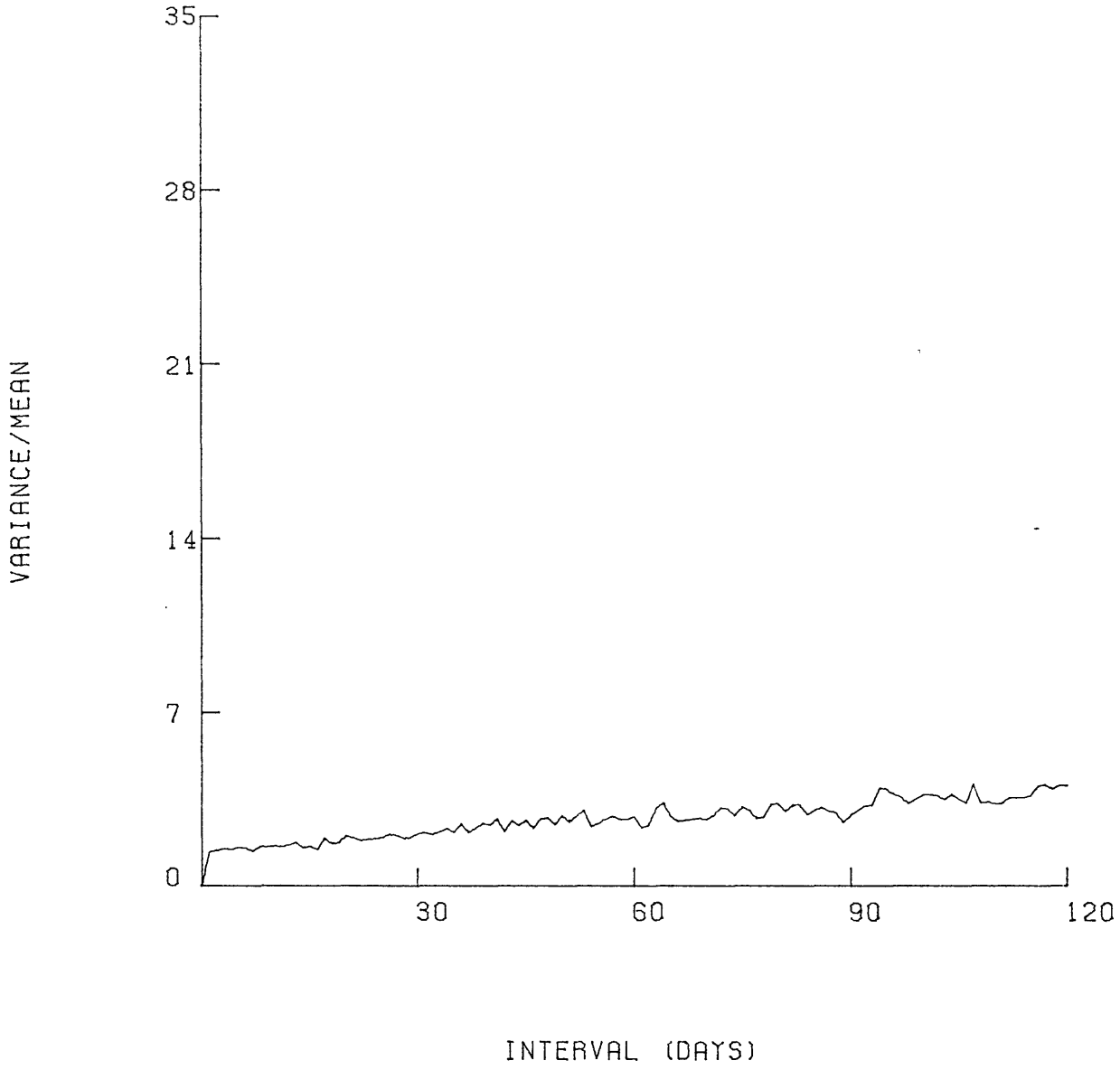

Figure 24. Dispersion coefficients for raw The Geysers catalog, $M_L \geq 1.25$.

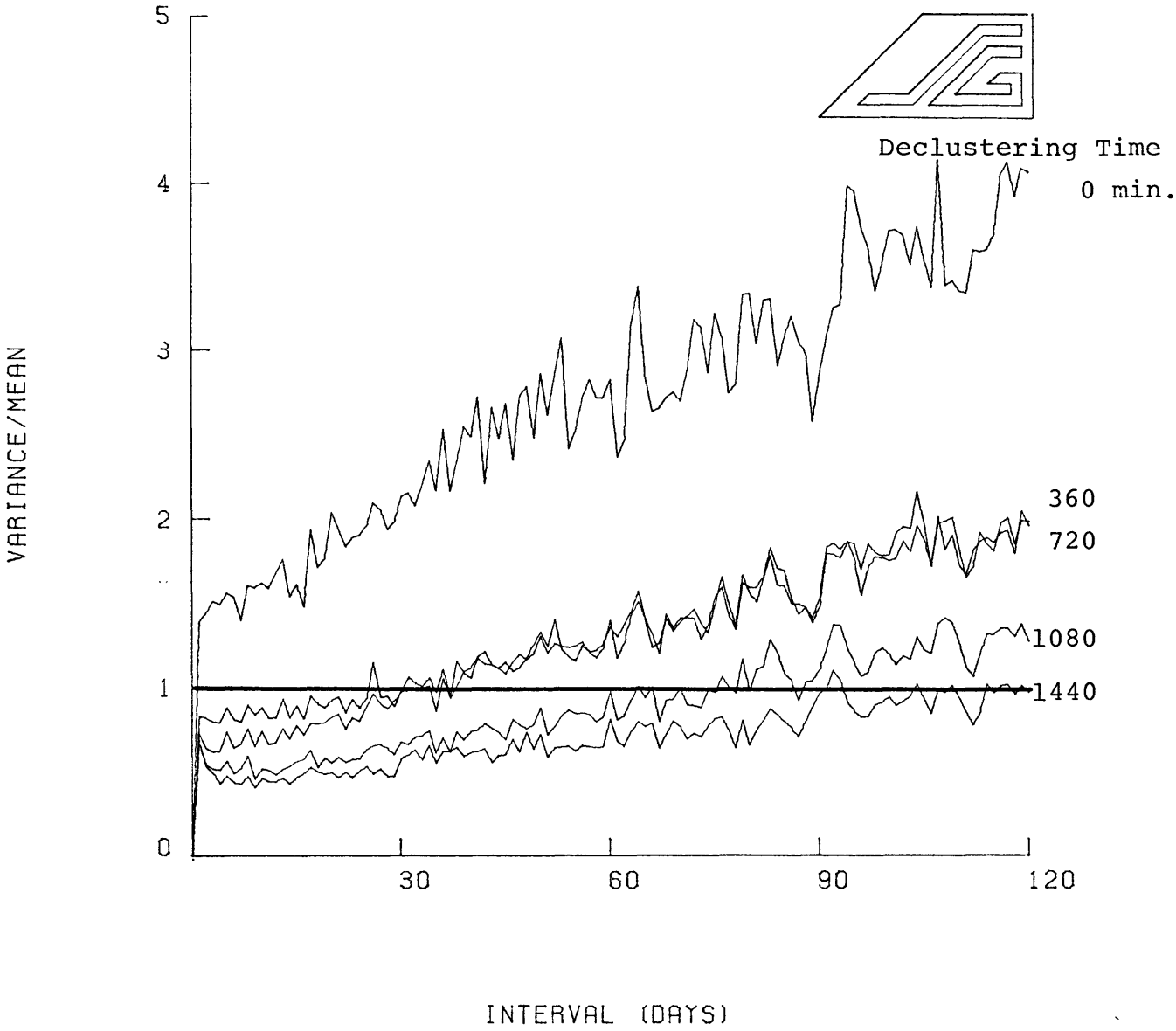

Figure 25. Dispersion coefficients for The Geysers catalog, $M_L \geq 1.25$, for several declustering times.

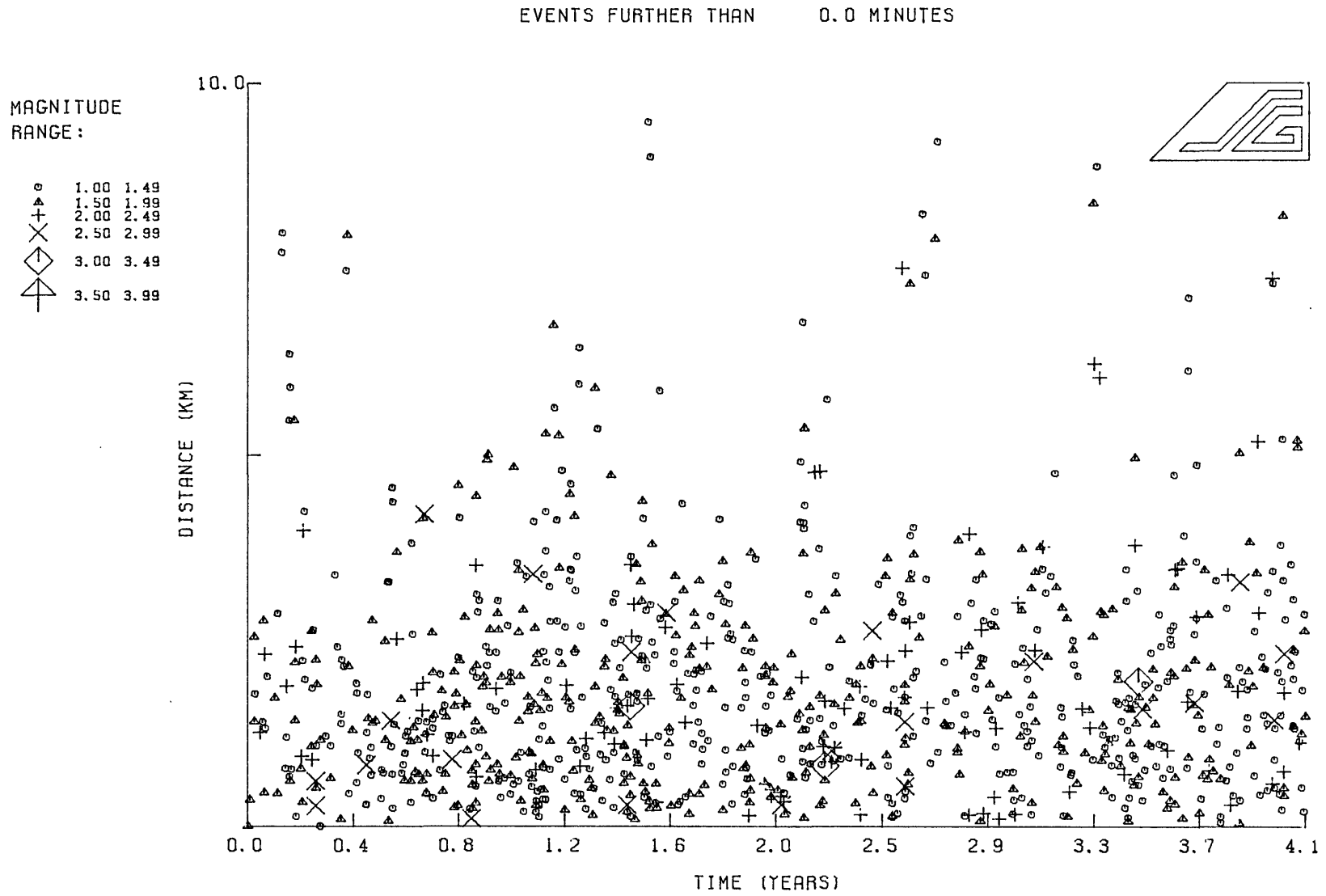

Figure 26. Interoccurrence distance versus time for raw The Geysers catalog, $M_L \geq 1.25$.

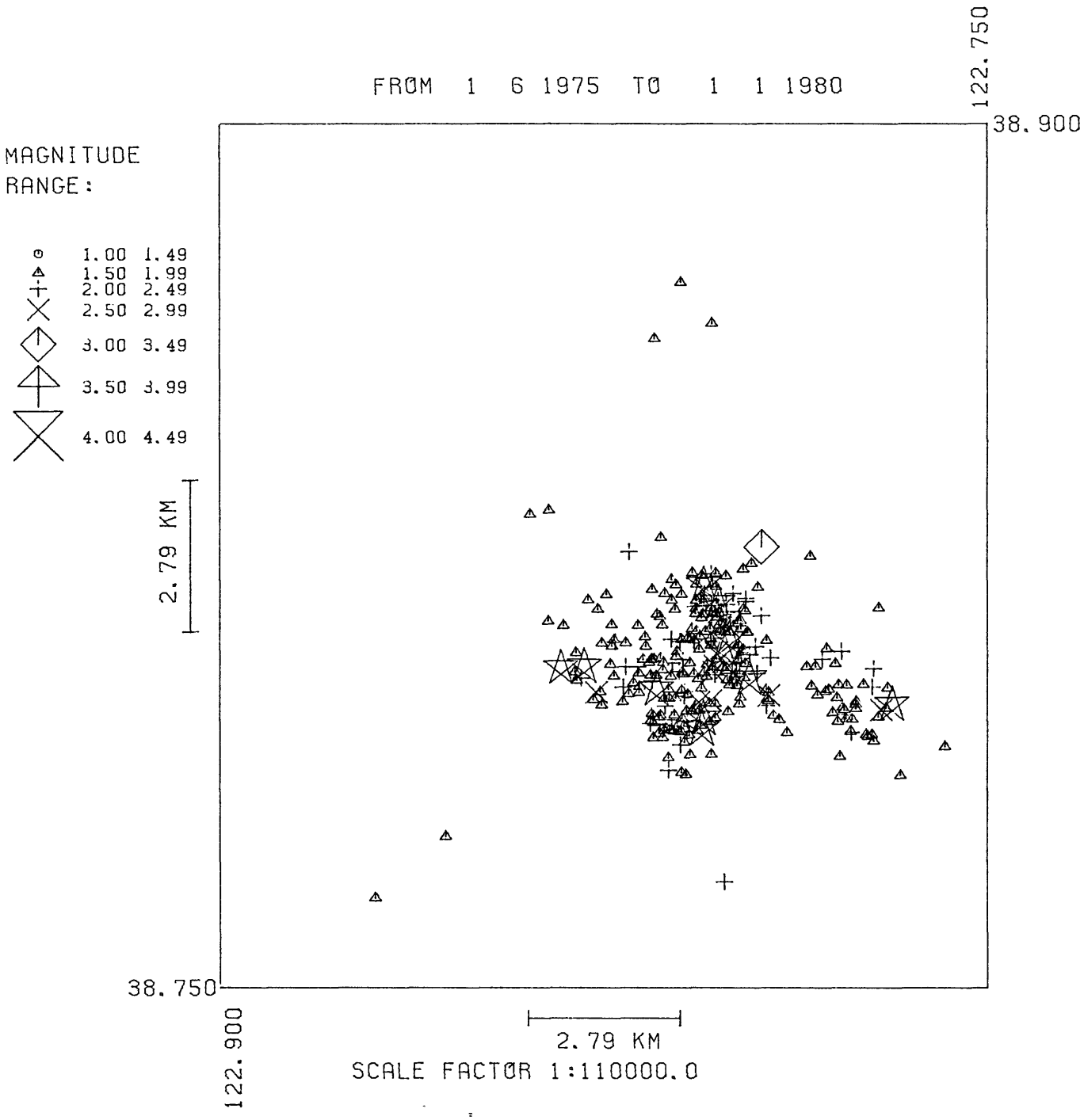

Figure 27. Epicentral locations for the random independent events from The Geysers catalog $M_L \geq 1.5$. The star-shaped symbols indicate the location of production wells.

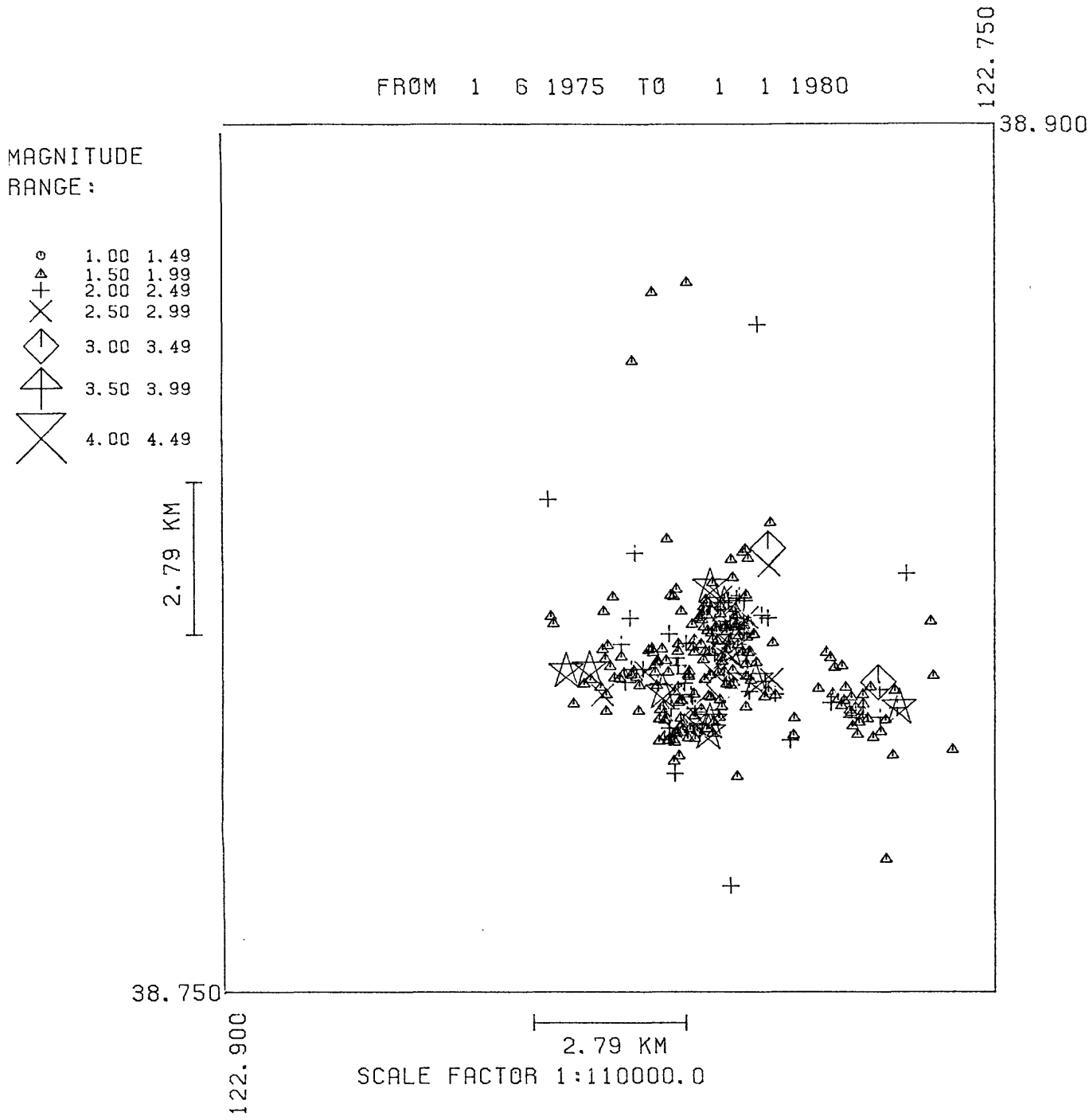

Figure 28. Epicentral locations for the temporally clustered events from The Geysers catalog, $M_L \geq 1.5$. The star-shaped symbols indicate the location of production wells.

6. LASSEN GEOTHERMAL AREA

INTRODUCTION

The anomalous characteristics of the seismicity at The Geysers, in comparison with Coso or the Imperial Valley, could be the result of either production or the peculiarities of a vapor dominated reservoir. Brook et al. (1979) have classified Lassen as a vapor-dominated geothermal resource. For this reason Lassen was added to this study as a control for evaluating The Geysers. Very recently we have learned that a single well was drilled at Lassen. This well found mostly chloride brines under an andesitic cap rock. Although the results from a single well should not be used to typify the entire reservoir, it does weaken the value of the data set as a control for comparison with The Geysers.

The Lassen region has been monitored by six seismographic stations operated by the U.S. Geological Survey since October 1977. The data set used in this study was discussed by Klein (1979) and represents approximately 14 months of continuous recording. At the threshold for uniform detection of $M_L \geq 1.25$, the resulting catalog contains 197 events, Figure 29.

GEOLOGIC SETTING

The Lassen geothermal area is centered around the southern most of the active Cascade volcanoes and is located at the juncture of the Cascade, the Sierra Nevada, and

the Basin and Range provinces. Late Pliocene andesite covers most of the region. Very young basalt and dacite cinder cones and flows are common (Macdonald, 1966). Lassen Peak (11,000 feet) last erupted in 1915 and is still considered an active volcano. Several fumaroles and hot springs exist in the region with near-surface temperatures as high as 117.5°C (Macdonald, 1966).

DATA ANALYSIS

The frequency of occurrence vs. magnitude data are plotted in Figure 30. Because of the short time interval of the data set and the small number of events, these data do not form a simple linear trend. The data suggest that the recurrence intervals for events larger than $M_L \geq 3.5$ are comparable to or greater than the length of the catalog. Taking this into consideration, a reasonable threshold for uniform detection is approximately $M_L \geq 1.25$.

Following the procedure from previous sections, the occurrence times were converted into a time series. A probability plot of the ordered interoccurrence times is shown in Figure 31. Note the strong deviation from linearity at short time intervals. From this plot a range of trial declustering times was chosen for further study with the Poisson dispersion tests. Figure 32 shows the plot of the variance over the mean for the raw or underclustered data. The declustering time of 1440 minutes was found to render the catalog most random, Figure 33. The "spiky"

nature of this curve is similar to the character of the dispersion coefficient plots for Coso and the Imperial Valley, Figures 16 and 5, and is in contrast with the Geysers and San Jacinto results. Because of the short length of the catalog it was not possible to investigate the character of the seismicity at larger thresholds.

The spatial and temporal aspects of the raw catalog are shown in the plot of interoccurrence distance vs. time, Figure 34. Vertical clusters of events on this plot indicate clustering in both space and time. Also noteworthy is the almost continuous activity in the area with most large events being widely separated from previous smaller events. The declustered data are shown in Figure 35. Epicenter plots of the clustered and random subsets of the catalog are shown in Figures 36 and 37. These plots indicate that some spatial clustering of earthquakes is present but it is not as well defined as the distributions found in other geothermal fields. This may be due to the short recording span or the actual nature of the seismicity.

In summary, the Lassen catalog has been examined as a possible control for estimating pre-production seismicity in a steam-dominated reservoir. The significance of these results is limited by the short duration of the catalog. However, the derived declustering time interval and the spatial and temporal clustering are very comparable to those of other undisturbed geothermal areas studied in this project and are in contrast with those of The Geysers.

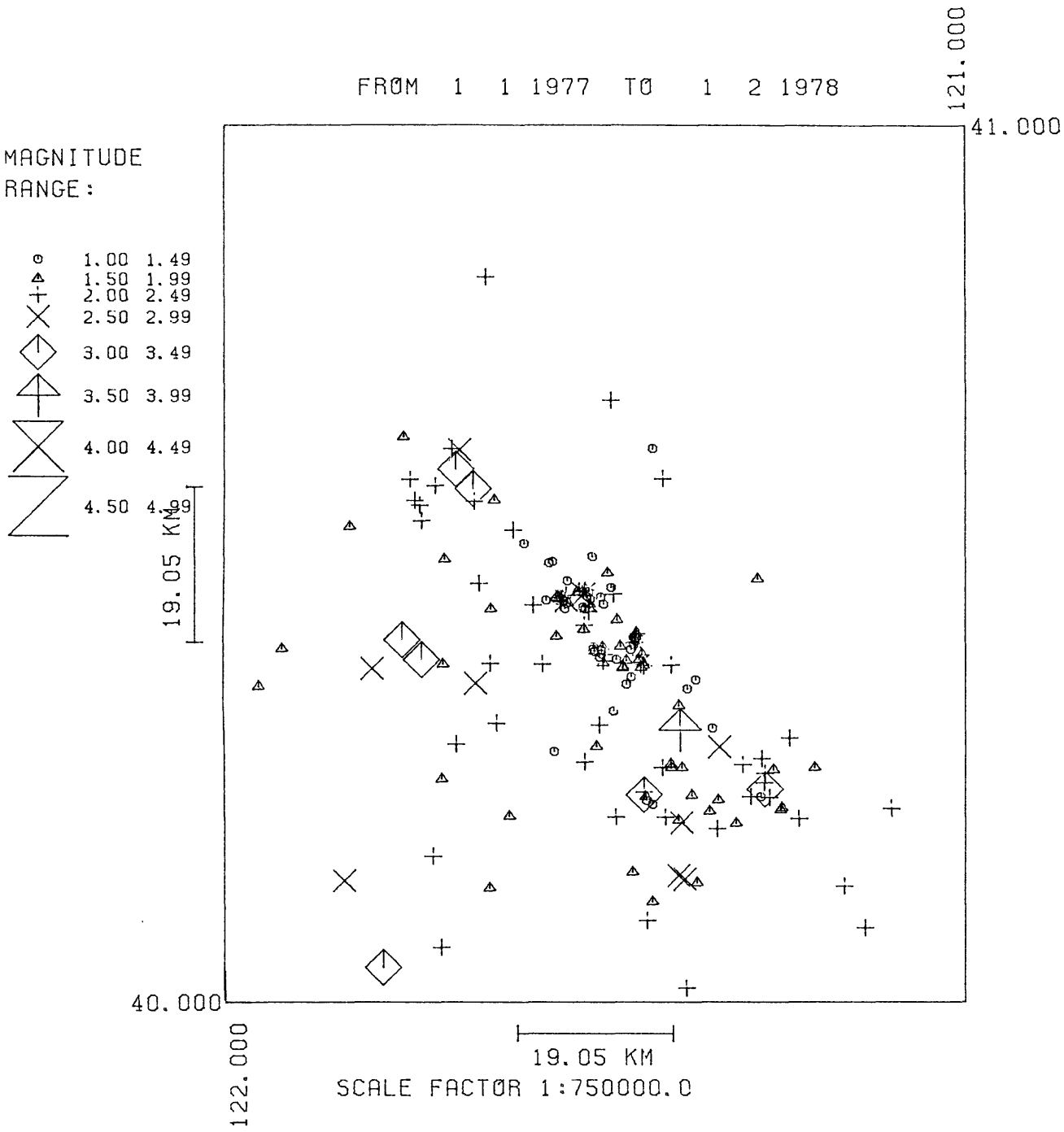

Figure 29. Epicenter map for the Lassen region for the period January 1977 to February 1978, $M_L \geq 1.25$.

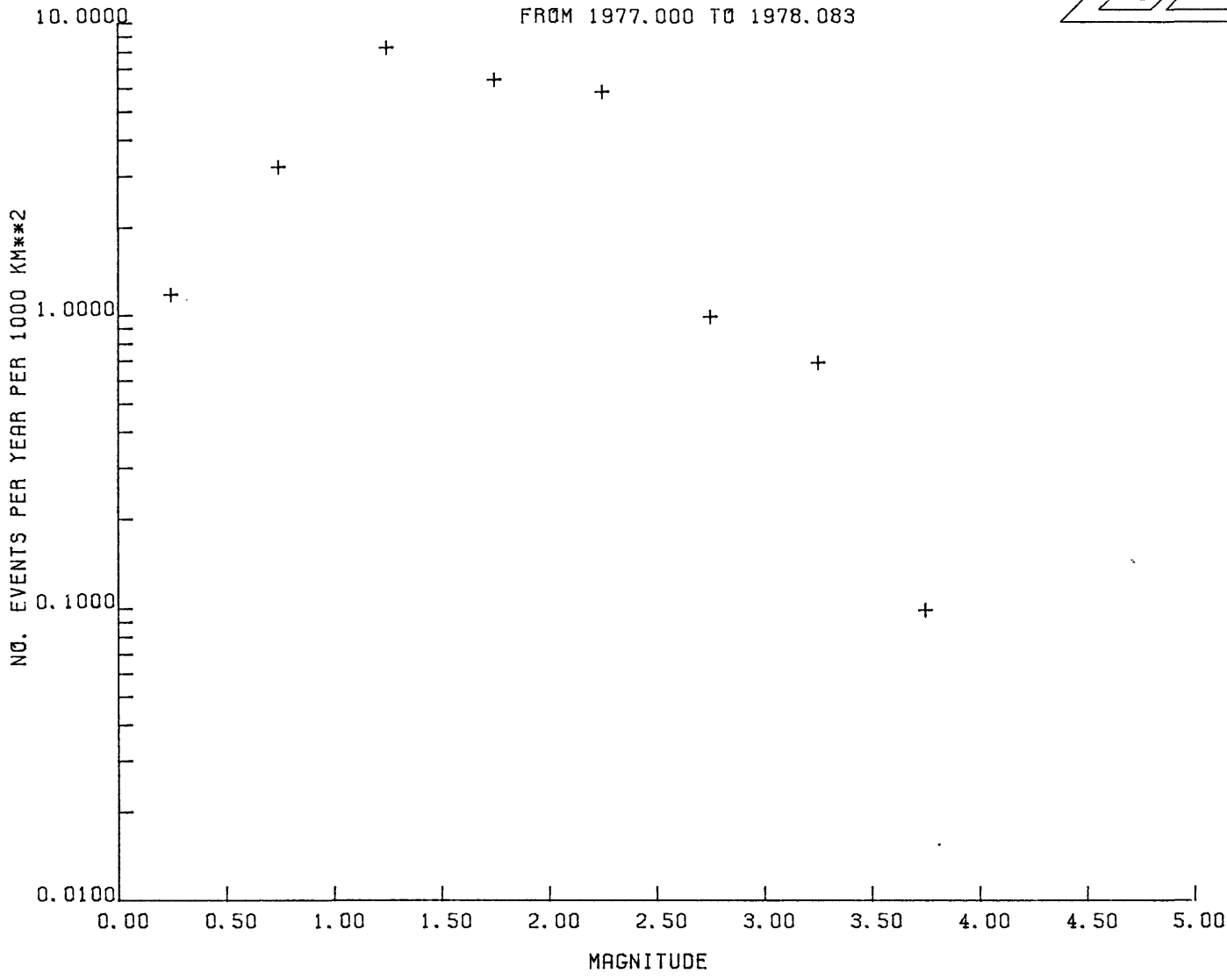

Figure 30. Frequency versus magnitude for the Lassen catalog.

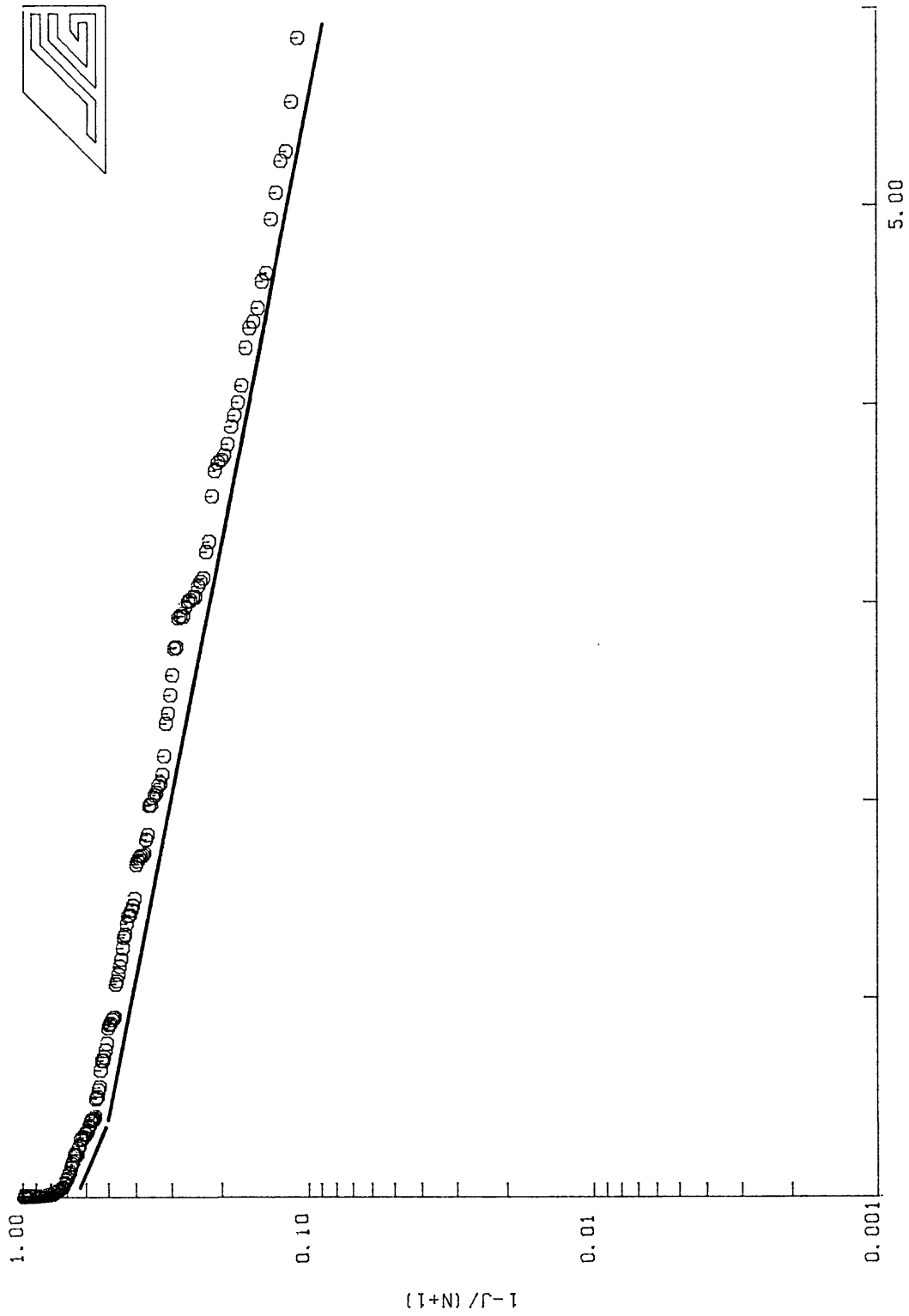

Figure 31. Probability plot for the Lassen catalog, $M_L \geq 1.25$.

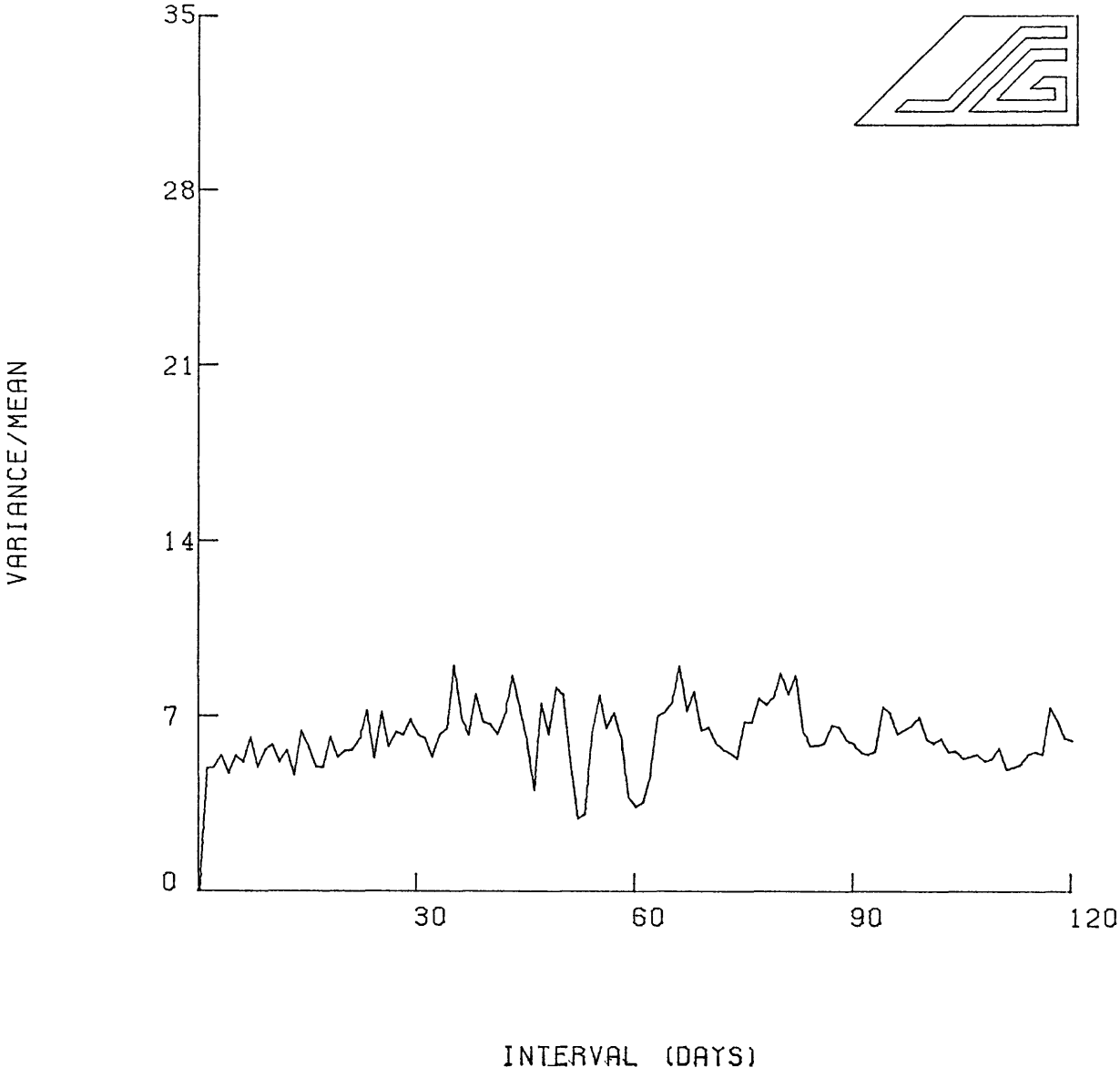

Figure 32. Dispersion coefficients for the raw Lassen catalog, $M_L \geq 1.25$.

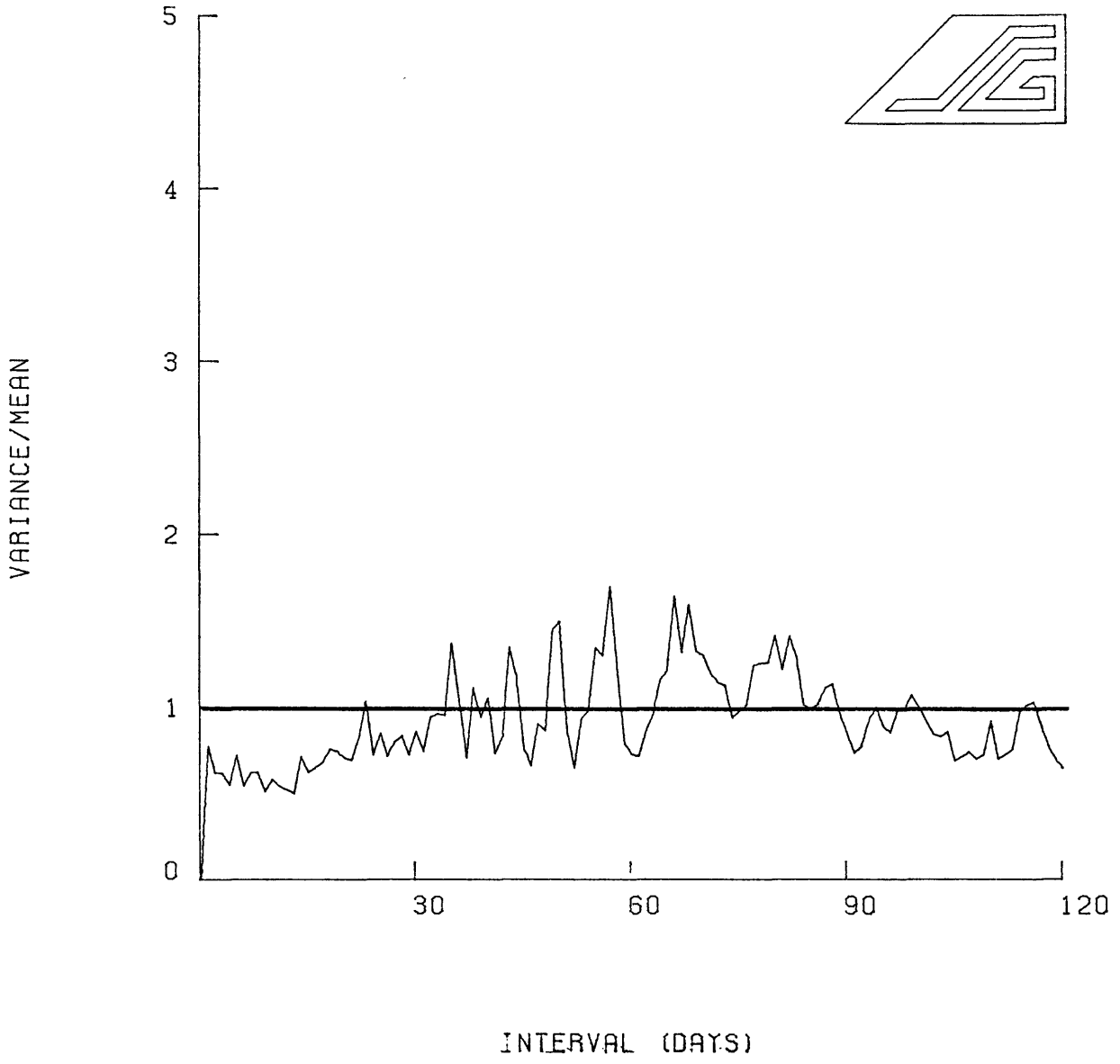

Figure 33. Dispersion coefficients for the Lassen catalog, $M_L \geq 1.25$, for the declustering time of 1440 min. (1 day).

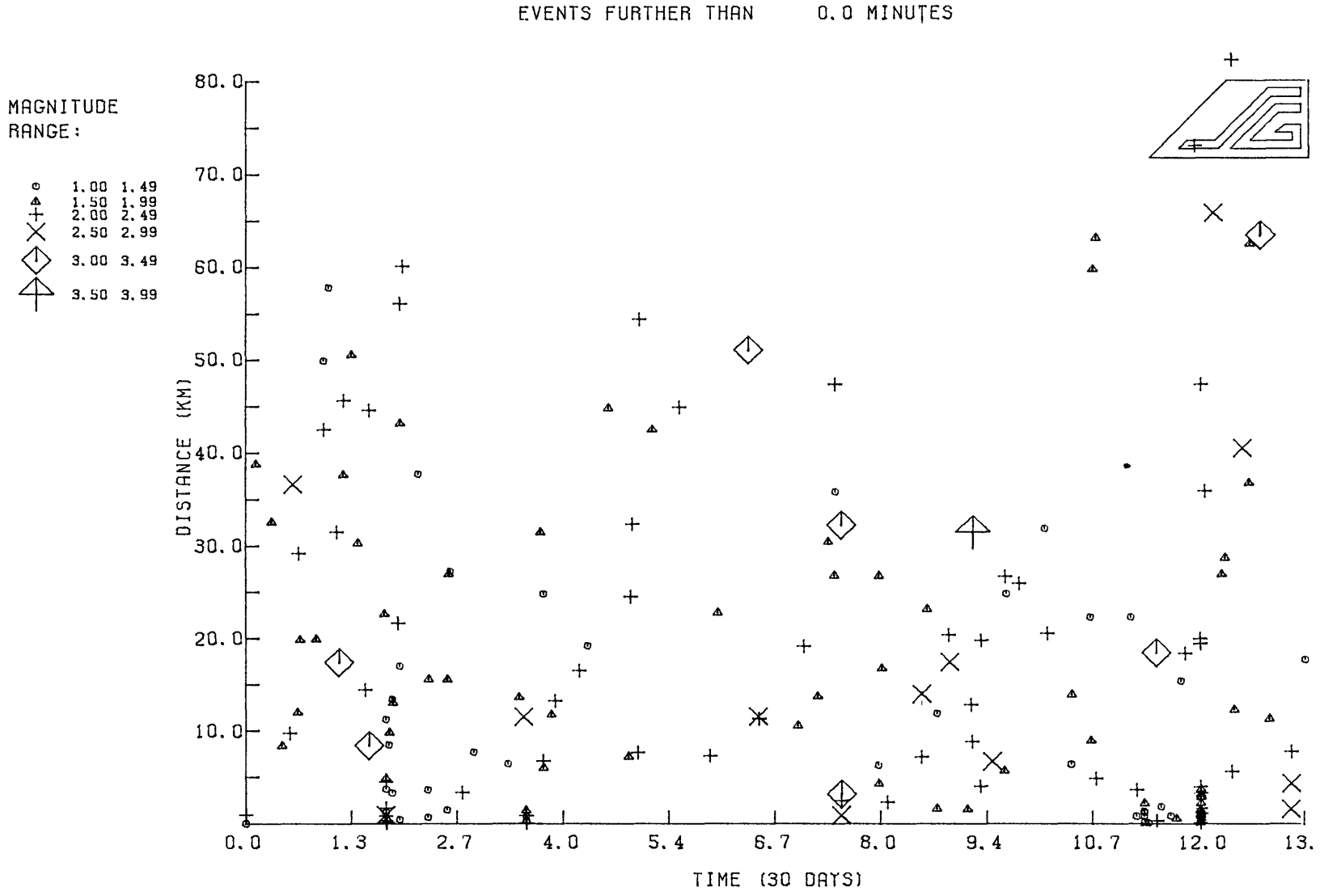

Figure 34. Interoccurrence distance versus time for the raw Lassen catalog, $M_L \geq 1.25$.

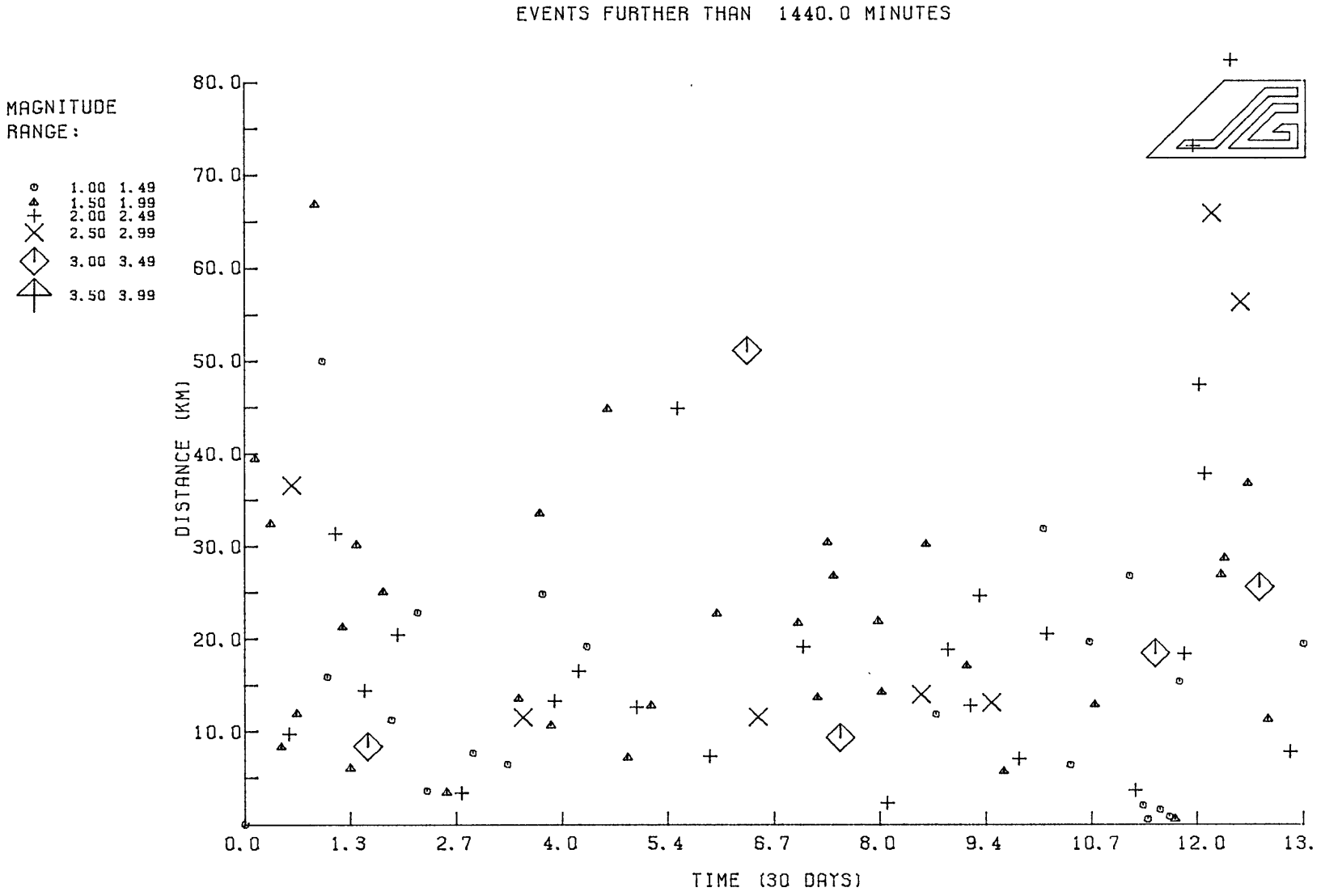

Figure 35. Interoccurrence distance versus time for the declustered Lassen catalog, $M_L \geq 1.25$.

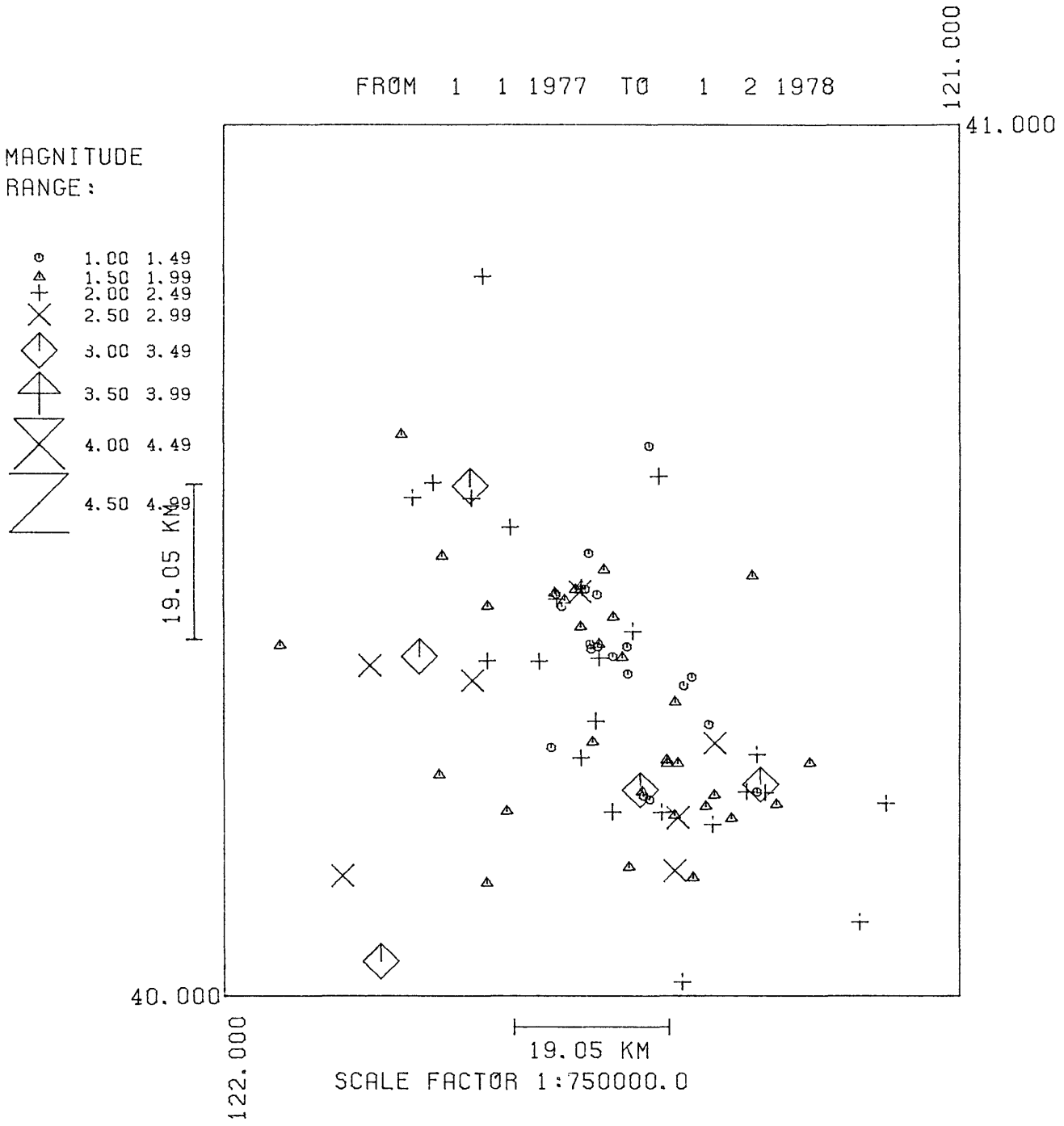

Figure 36. Epicentral locations for the random, independent events from the Lassen catalog, $M_L \geq 1.25$.

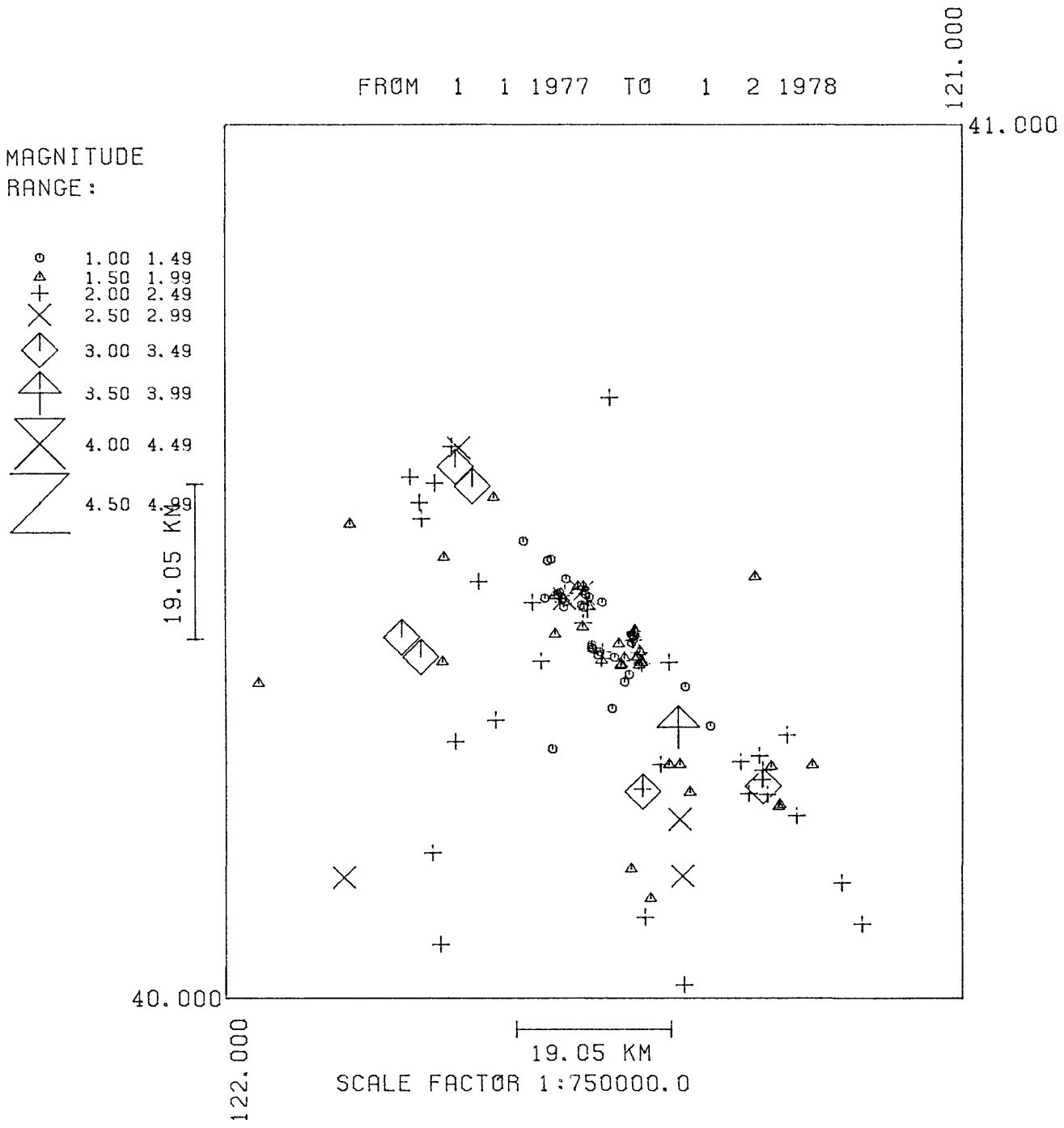

Figure 37. Epicentral locations for the temporally clustered events from the Lassen catalog, $M_L \geq 1.25$.

7. SAN JACINTO FAULT

As a test to determine if the seismic characteristics examined in this report are unique to geothermal areas, an essentially non-geothermal region was chosen for comparison. In terms of both macro- and micro-seismic activity, the San Jacinto fault system is the most active feature in Southern California. The locations of the earthquakes in the region studied, $M_L \geq 2.0$, are shown in Figure 38. This data set spans the period 1970 to 1980. The frequency, magnitude plot, Figure 39, indicates that $M_L \geq 2.0$ is the lower threshold for uniform detection. At this magnitude threshold the catalog contained 1146 events.

Using the threshold $M_L \geq 2.0$, a standard probability plot was generated, Figure 40. This plot does not show a strong deviation at short time intervals which indicates a lack of close temporal clustering. Trial declustering times of 1440, 2880, 3600 and 7200 min were selected from this plot and tested with the Poisson dispersion analysis. Figure 41 shows the curve for the undeclustered data. The curve is highly skewed with a positive trend and does not show the spiky character seen in the curves for geothermal areas. Figure 42 shows the dispersion plot for the best declustering time of 3600 min. The significant differences between this declustered plot and similar plots for the geothermal area is the skewed linearity and lack of sharp oscillations.

Interoccurrence distance vs. time for the raw catalog is shown in Figure 43. This figure shows a lack of tight clustering of events at short interoccurrence distances. This is not to say that events do not occur close together in space but rather there exists a more uniform distribution of interoccurrence distances than found in the geothermal areas. The declustered interoccurrence plot is shown in Figure 44. This figure shows the random distribution of the declustered data. Figures 45 and 46 show the epicenter maps of the random and the clustered events, respectively.

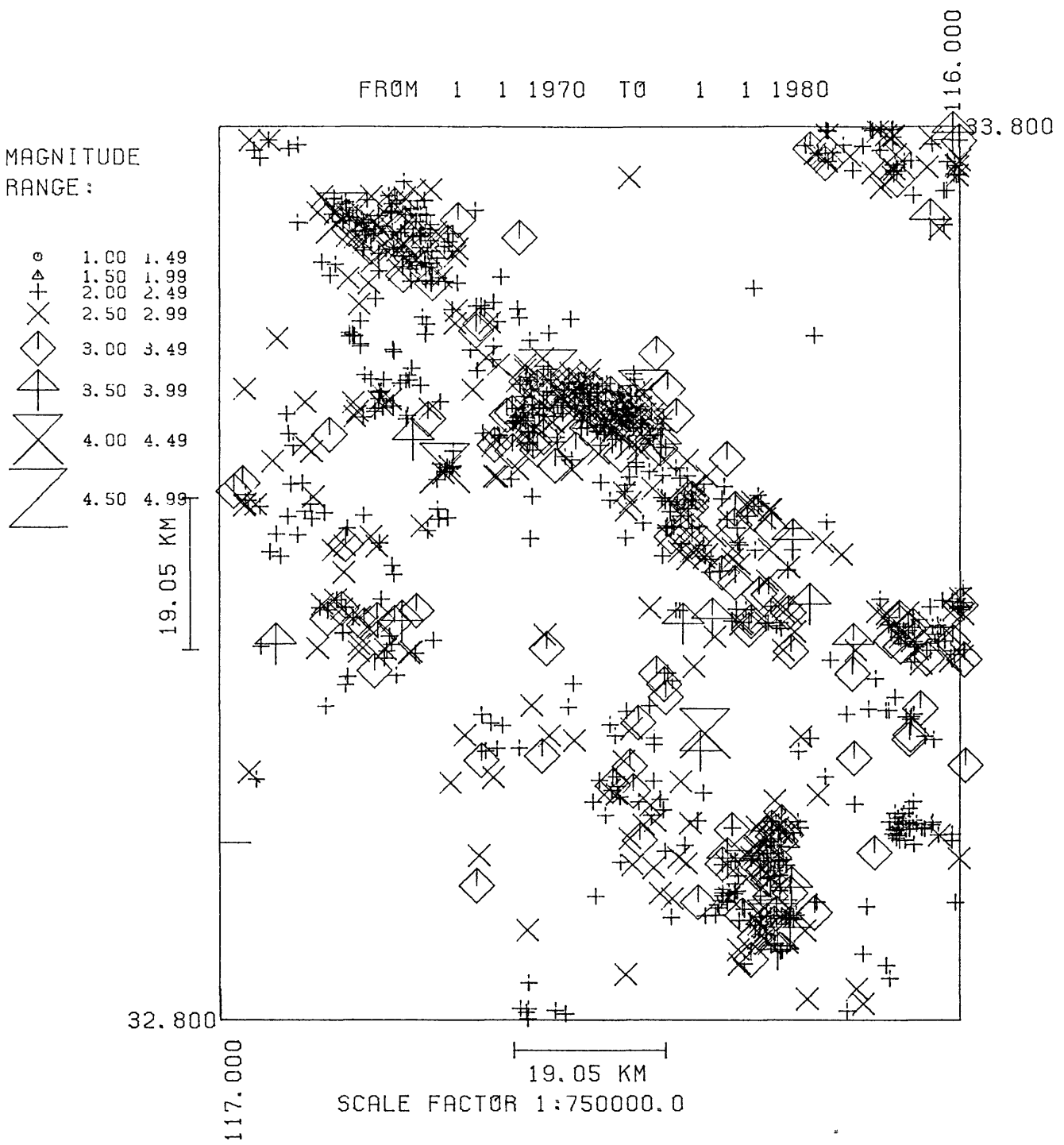

Figure 38. Epicenter map for the San Jacinto fault zone for the period January 1970 to January 1980, $M_L \geq 2.0$.

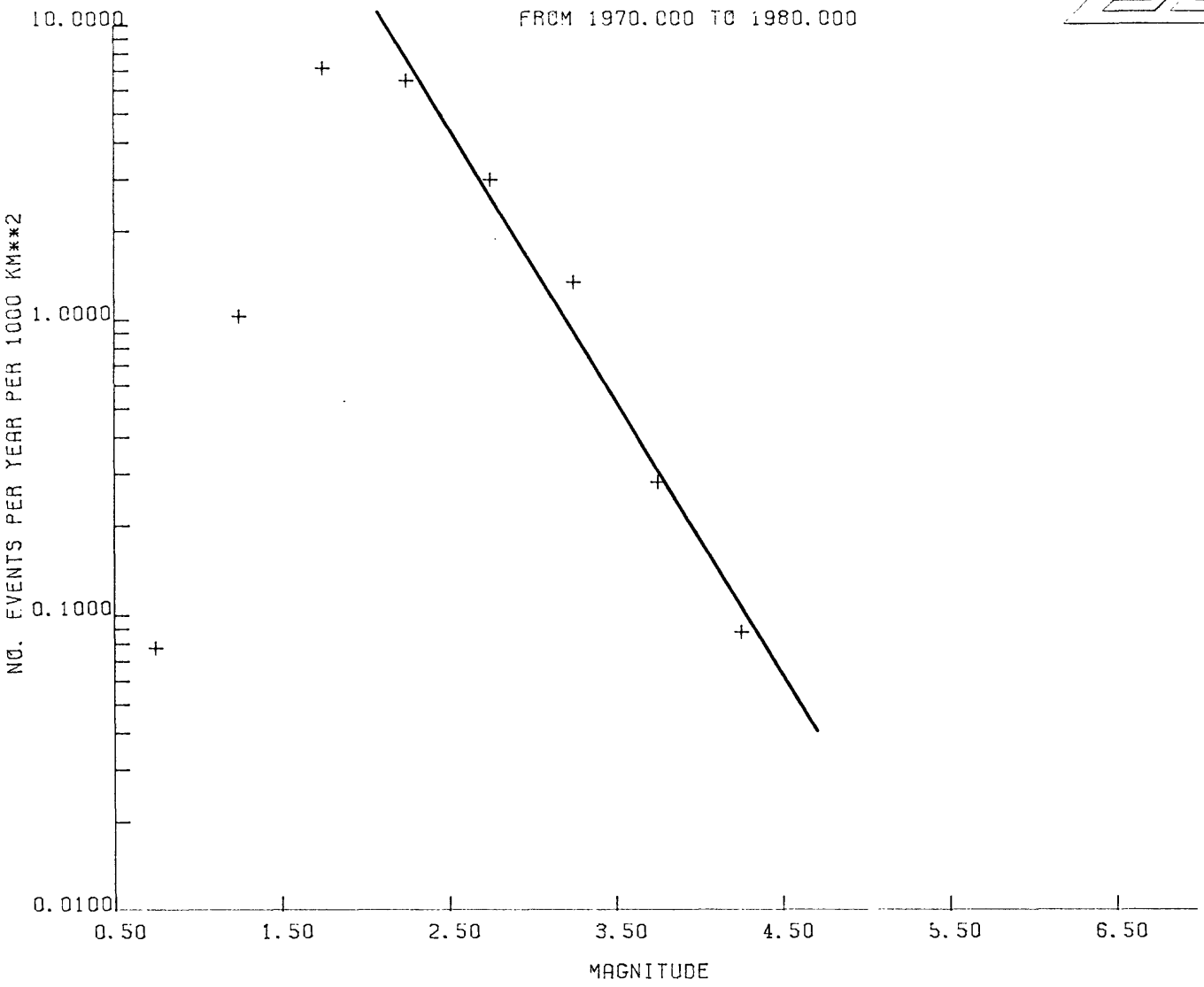

Figure 39. Frequency versus magnitude for the San Jacinto fault zone.

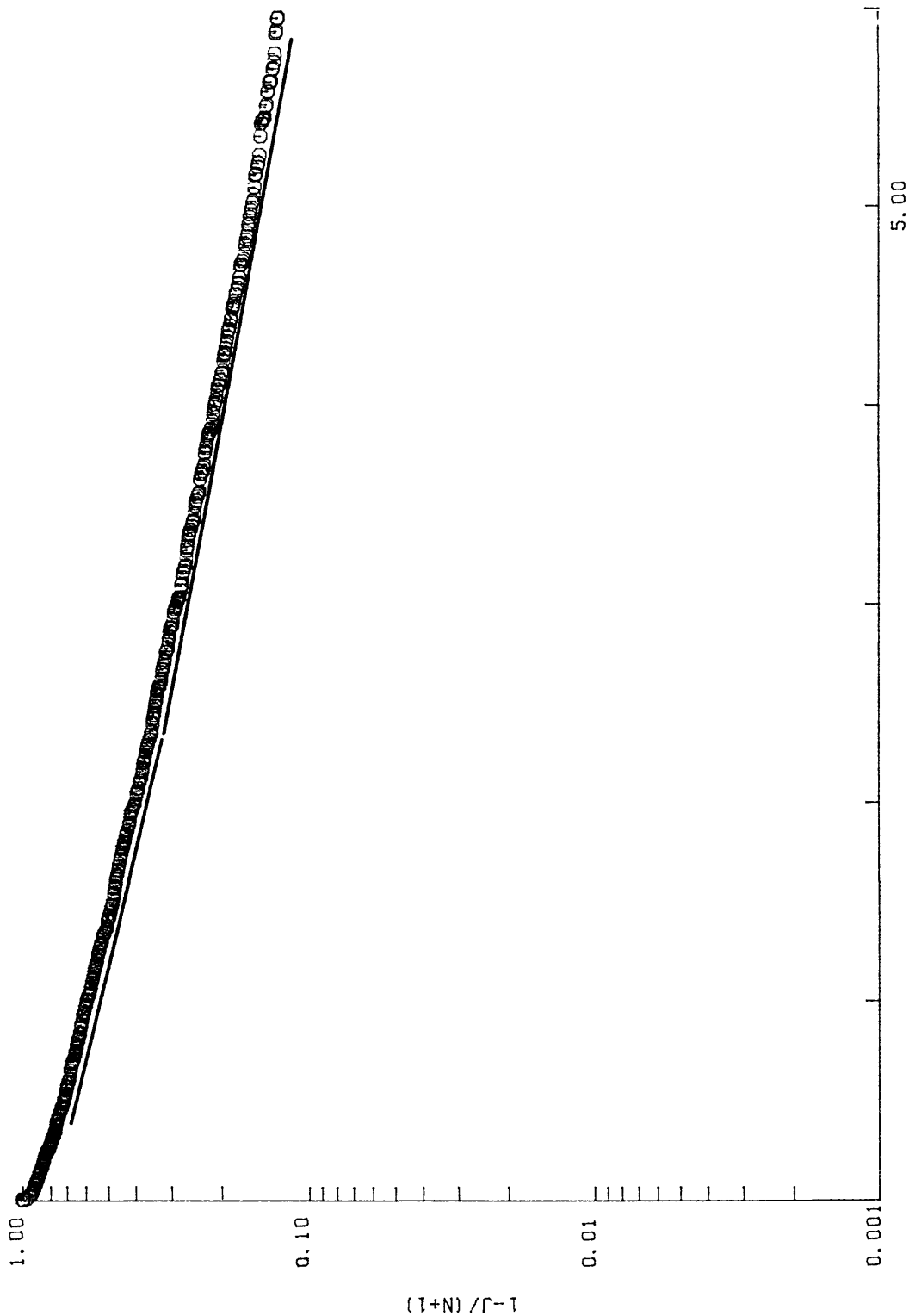

Figure 40. Probability plot for the San Jacinto catalog, $M_L \geq 2.0$.

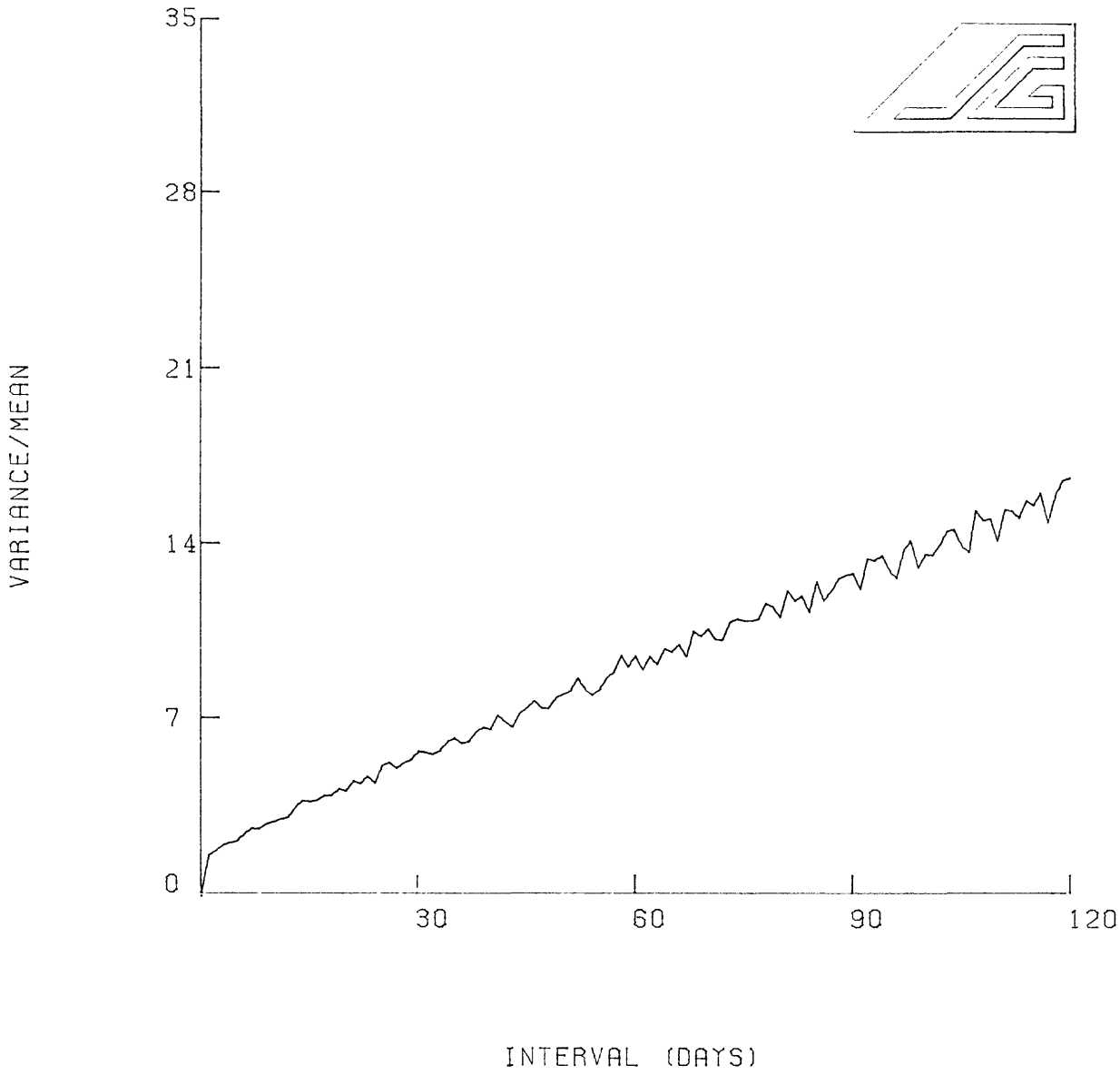

Figure 41. Dispersion coefficients for the raw San Jacinto catalog, $M_L \geq 2.0$.

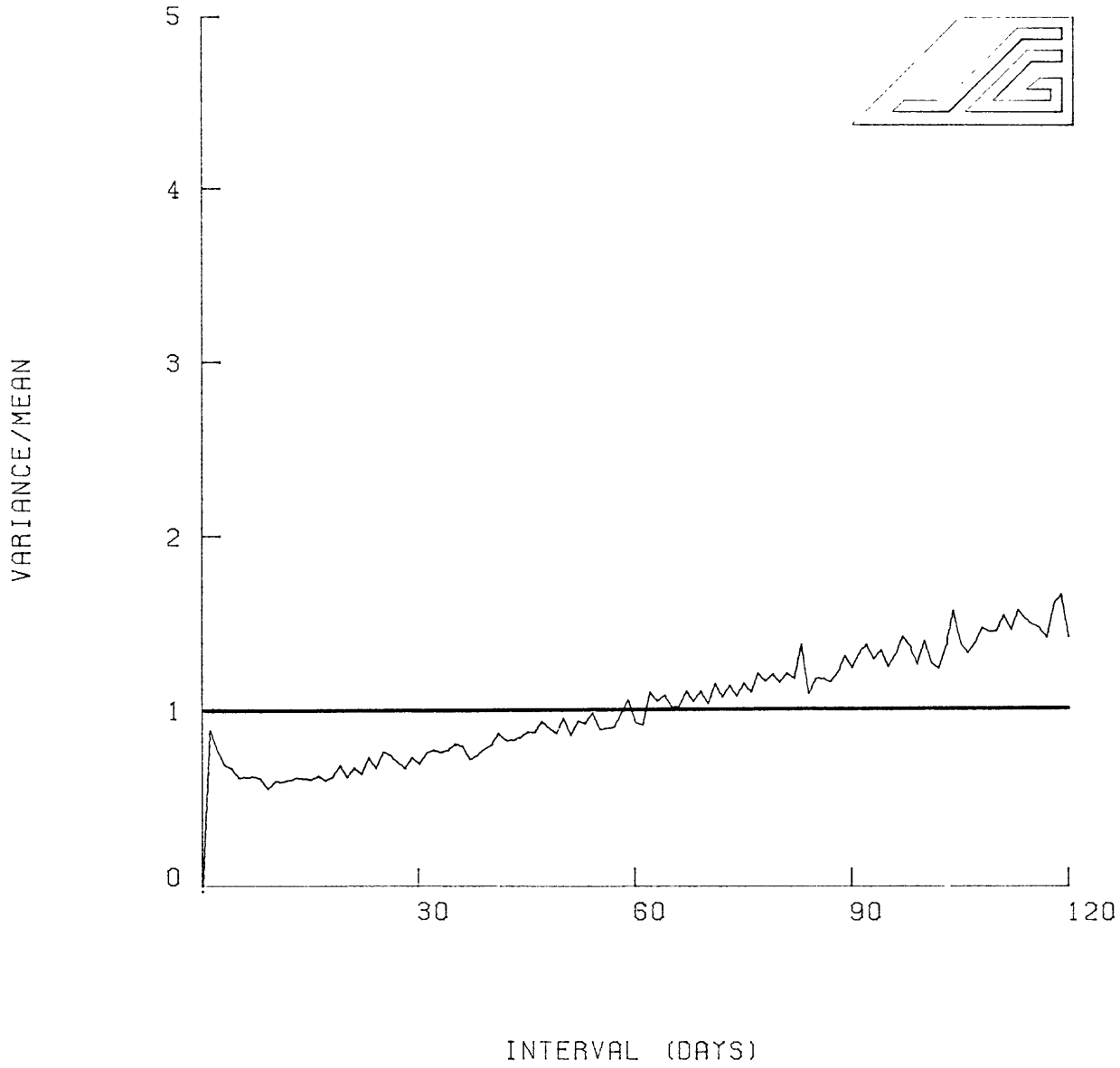

Figure 42. Dispersion coefficients for the San Jacinto catalog, $M_L \geq 2.0$, for the declustering time of 3600 min. (2.5 days).

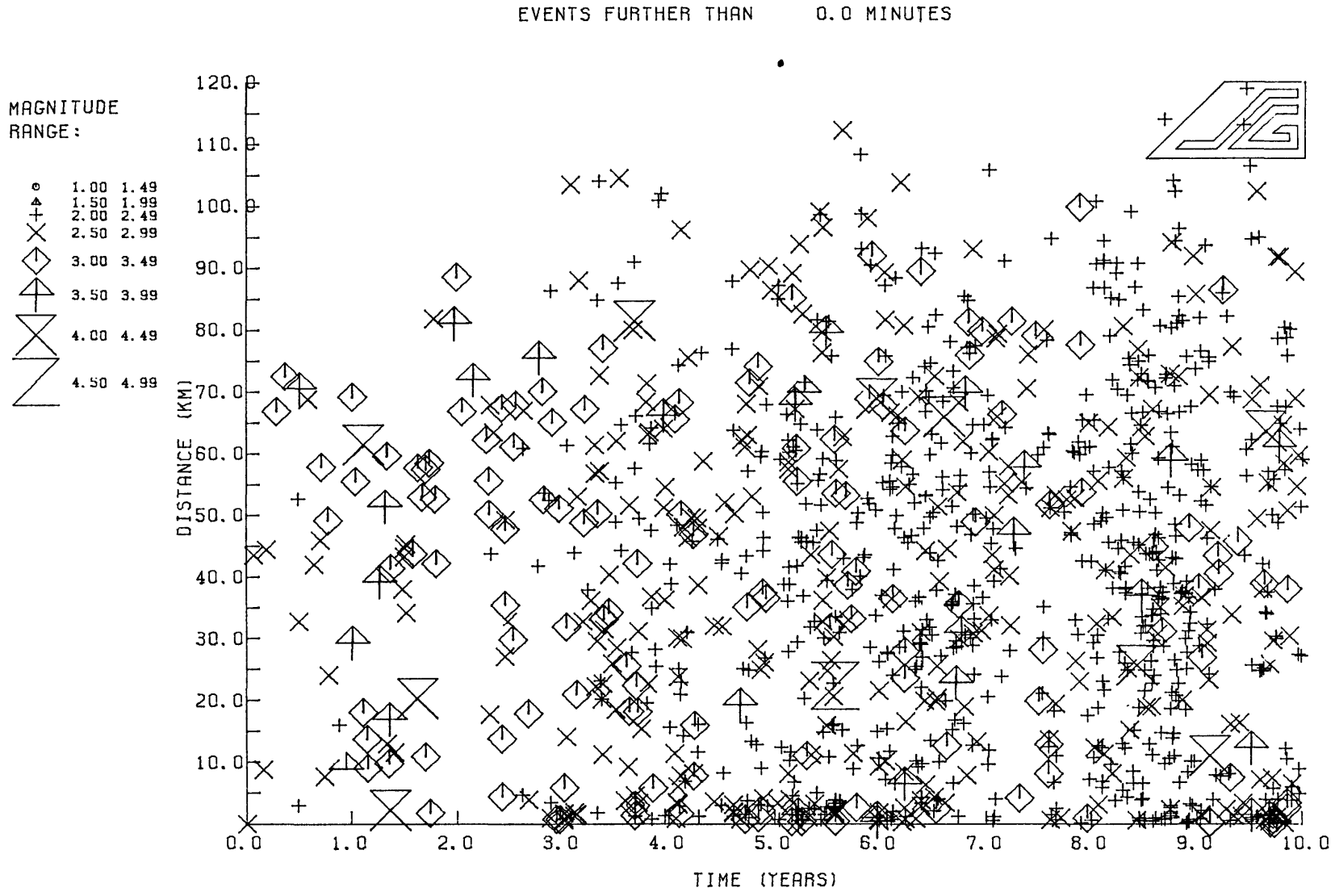

Figure 43. Interoccurrence distance versus time for the raw San Jacinto catalog, $M_L \geq 2.0$.

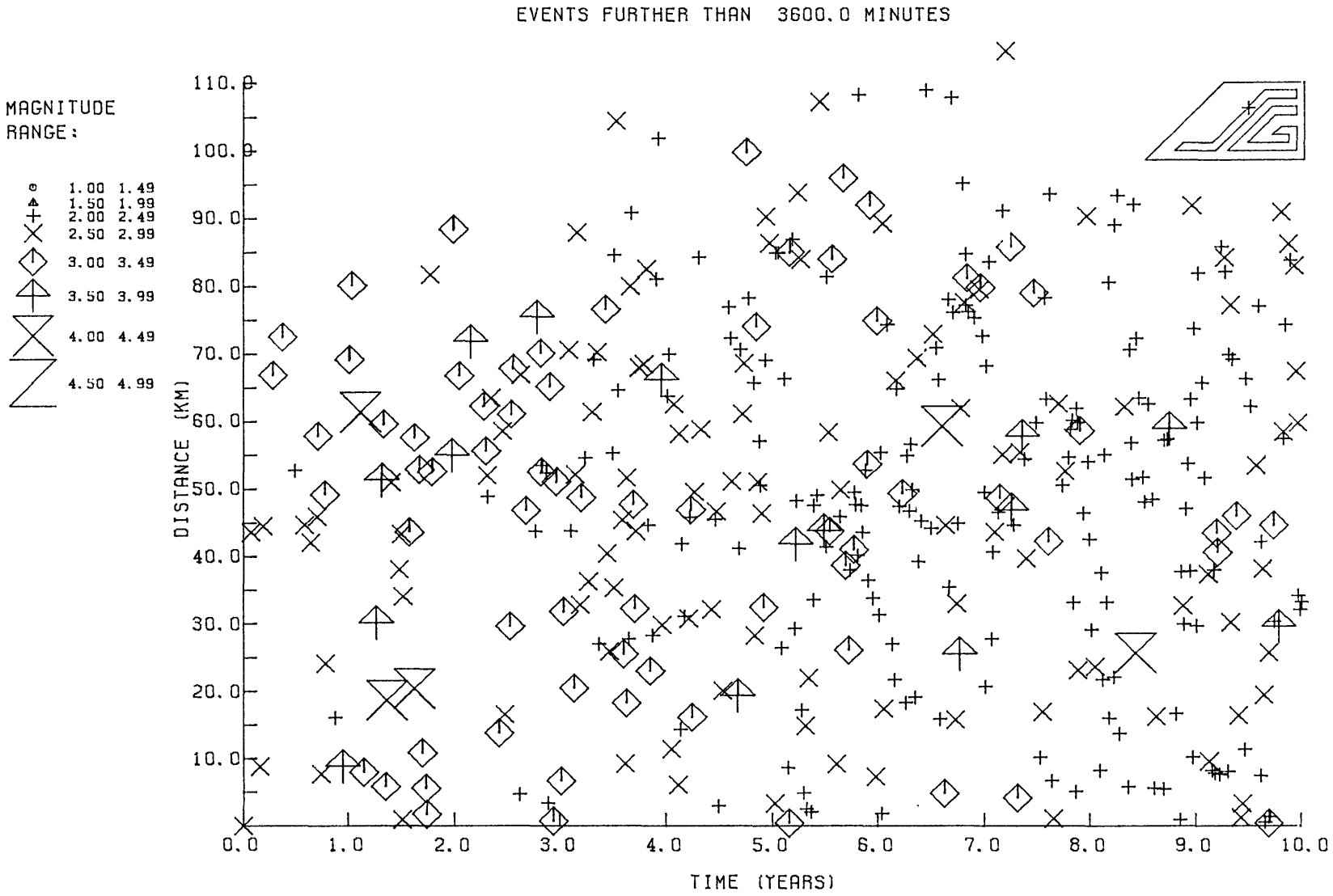

Figure 44. Interoccurrence distance versus time for the declustered San Jacinto catalog, $M_L \geq 2.0$.

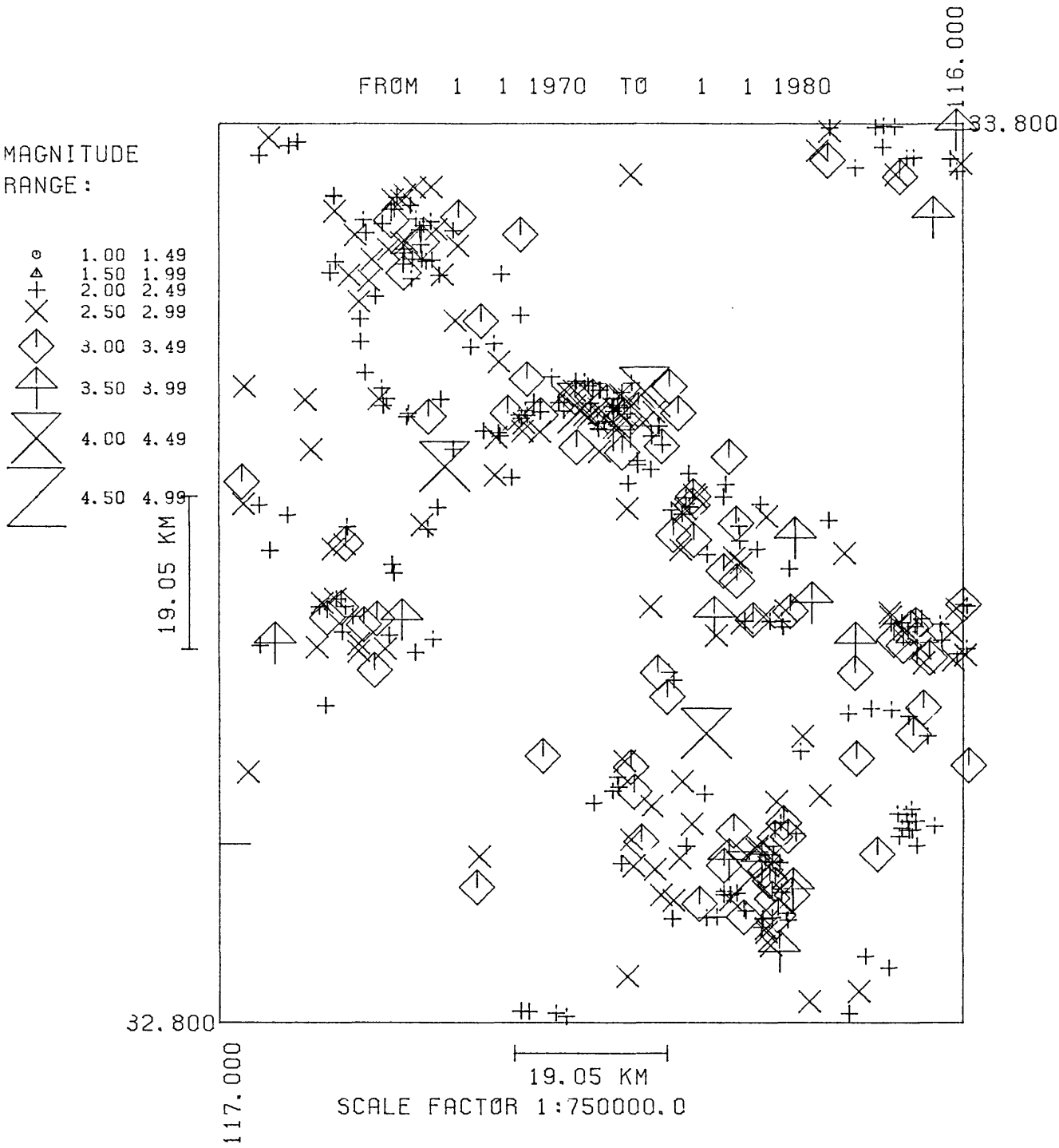

Figure 45. Epicentral locations for the random, independent events from the San Jacinto catalog, $M_L \geq 2.0$.

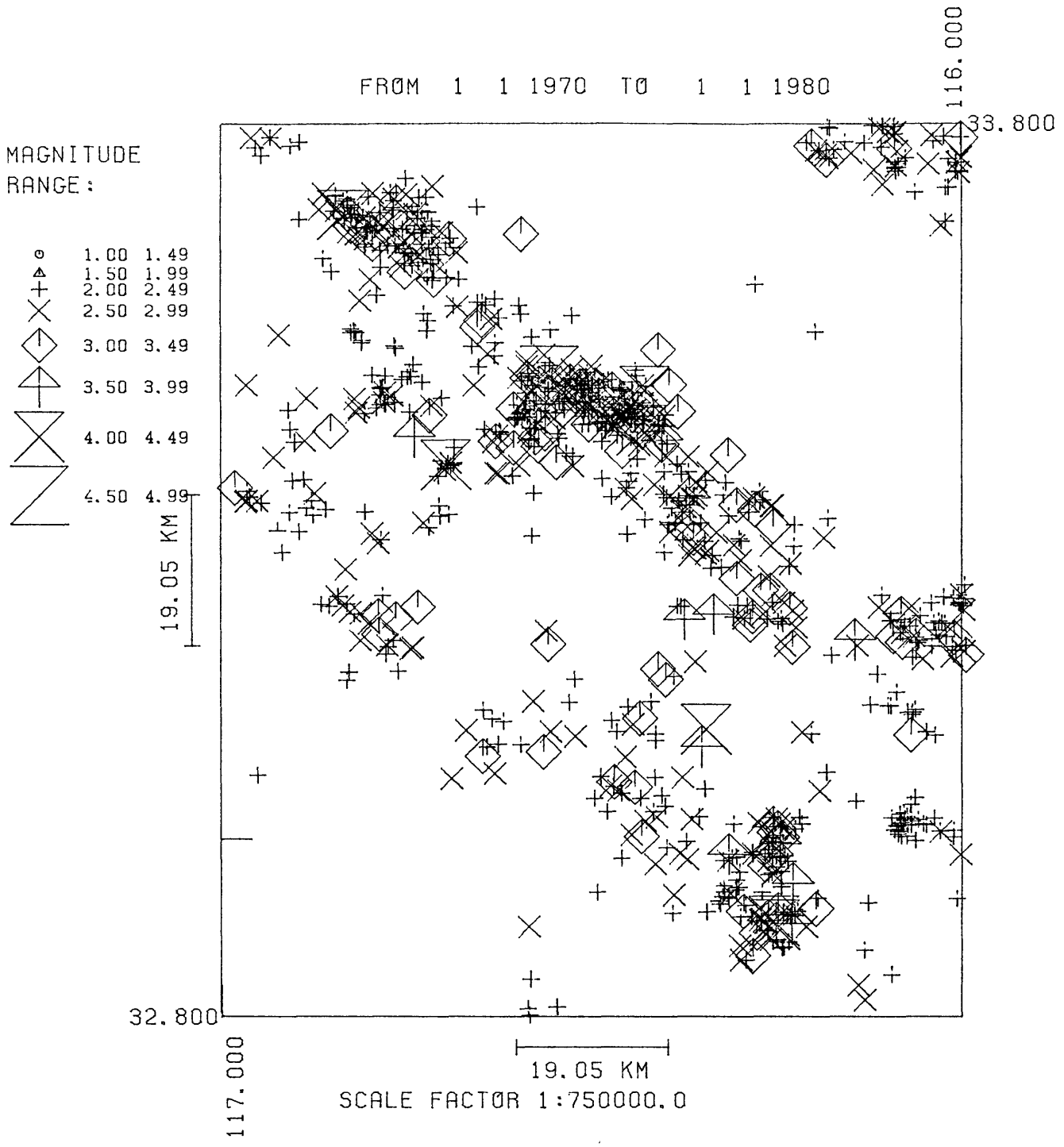

Figure 46. Epicentral locations for the clustered events from the San Jacinto catalog, $M_L \geq 2.0$.

8. DISCUSSION

The goal of this investigation has been to examine the temporal and spatial characteristics of the random and non-random components of seismicity associated with geothermal reservoirs and to quantify those aspects that distinguish or typify "geothermal earthquakes." We have used a Poisson model of random seismicity in time to identify clustered or related events. Using these criteria, the seismic catalogs for each resource have been separated into clustered and random subcatalogs for a range of magnitude thresholds. For each threshold we have computed the best estimate for the declustering time, mean number of events per cluster, b-values, and ratios of number of random to clustered events. A summary of these statistics is listed in Table 1. In addition, epicenter maps for each threshold and each sub-catalog have been prepared and compared with the areal extent of the geothermal resource. Examples of these maps for each area are included in the previous sections.

The original scope of the project was limited to these systems: Imperial Valley, Coso and The Geysers. The anomalous results from The Geysers led us to the examination of a virgin, vapor dominated reservoir (Lassen) in order to characterize pre-production seismicity. Although there seems to be some uncertainty if Lassen is in fact a vapor-dominated system, the seismicity associated with the reservoir is much more similar to that associated with Coso and the Imperial

Table 1. Derived seismic characteristics of the regions studied in this investigation. Column H tabulates a proposed geothermal discriminant. Note that the value for this function is less than 0.1 for geothermal areas and greater than 0.1 for the San Jacinto Control.

	A	B	C	D	E	F	G	H
	Declus. time (d)	# events Total	# random / # cluster	b-values all events	b-random / b-cluster	Mean # Events per cluster	10^E	A*C / G
Imperial								
$M_L \geq 2.0$	0.75	1601	.32	.86	1.44	8.31	27.54	0.009
≥ 2.5	1.50	772	.32	1.11	1.65	7.58	44.67	0.011
Coso								
$M_L \geq 1.25$	0.56	1483	.28	.78	1.03	6.46	10.71	0.015
≥ 1.50	0.62	1136	.33	.97	0.99	5.82	9.77	0.020
≥ 2.0	1.50	385	.37	1.10	1.01	6.28	10.23	0.055
Lassen								
$M_L \geq 1.25$	1.0	185	.64	.68	0.97	3.80	9.33	0.068
San Jacinto								
$M_L \geq 2.0$	2.50	1146	.41	.92	.75	4.53	5.62	0.170
≥ 2.5	1.50	485	2.67	1.11	.87	2.55	7.41	0.54
Geysers								
$M_L \geq 1.25$	0.25	980	3.05	1.26	1.07	2.46	11.75	0.065
≥ 1.50	1.0	491	1.16	1.29	1.19	2.57	15.49	0.075
≥ 2.0	0.5	122	4.28	1.52	1.21	2.25	16.22	0.13

that associated with The
Valley than to Geysers. This observation strengthens the conclusion that production has induced a new component to the local seismicity.

At the conclusion of the study of these four reservoirs, clear similarities among Coso, Lassen and the Imperial Valley could be identified. However, without a control, these characteristics would be rather useless for evaluating the seismicity of a new region. For this reason we have added a fifth region to the study: The San Jacinto
zone
fault. This zone is a very active feature in southern California and is not notably associated with large geothermal resources. All of the same parameters discussed above have been derived for this catalog and are included in Table 1. The following paragraphs discuss our conclusions of the usefulness of the discriminants examined in this study for identifying "geothermal earthquakes."

DECLUSTERING TIME

The most characteristic feature we have found in the catalogs examined is the declustering time. For detection thresholds less than M_L = 2.0, the declustering time for each reservoir is less than ~1.0 day. The corresponding time interval for the San Jacinto fault is 2.5 times longer. A general observation is that the declustering time increases with the magnitude threshold. The trends from the geothermal areas support this observation. However, the seismicity associated with the San Jacinto fault is in

contrast. At a threshold of $M_L \geq 2.5$ the declustering time drops to 1.5 days. This suggests that many of the temporal clusters at a lower threshold are associated with events smaller than $M_L \geq 2.5$. Indeed the ratio of the number of events in the random to the clustered sub-catalog for the San Jacinto changes from less than one to greater than one as the magnitude threshold increases from 2.0 to 2.5.

The declustering time is the most diagnostic indicator derived from the seismic catalogs that can be correlated with geothermal reservoirs. If this correlation is valid, then the declustering time can be used to identify the presence of a geothermal system within the region of study. This detector does not indicate the spatial location of the reservoir and by itself is not self consistent within this limited study.

RANDOM/CLUSTERED EVENT RATIOS

The ratio of the number of events in the random to the clustered sub-catalogs provided an indication of how significant clustering is in the region. Table 1 tabulates this statistic for each area and for each magnitude threshold. For each of the currently non-producing reservoirs, this ratio averages $\sim$0.3 with a maximum of 0.64 for the sparse Lassen catalog. As found in many areas of this study, The Geysers data is anomalous. At the threshold of $M_L \geq 2.5$, the San Jacinto fault has a ratio of 2.67, easily separated from the geothermal ratios. Unfortunately, as with the

declustering time statistic, the random/cluster ratio is not significantly different from to that associated the geothermal regions at the threshold $M_L \geq 2.0$.

b-VALUES

Using a maximum likelihood technique, b values have been computed for each sub-catalog and for each magnitude threshold, Table 1. The magnitude of the b-values varies widely from area to area and from the raw catalog to the sub-catalogs of random and clustered events. We conclude that the raw b-value parameter by itself is not a good discriminant for geothermal resources. A logical normalization is to compare how the b-value changes between the random and clustered sub-catalogs for each region and each magnitude threshold. Table 1 lists this ratio for each area. We note that for all geothermal areas this ratio is approximately one or greater whereas it is less than 0.9 for the San Jacinto fault. This ratio does seem to provide a geothermal discriminant.

MEAN NUMBER OF EVENTS PER CLUSTER

In the process of constructing the clustered sub-catalogs we have calculated the mean number of events per cluster, Table 1. For Coso and the Imperial Valley this statistic is 1.5 to 2.0 times larger than for the San Jacinto fault. However, the results for The Geysers and the sparse Lassen catalog are comparable with the San Jacinto

control. These numbers suggest this measure may be a positive indicator of a geothermal reservoir.

SPATIAL LOCATION OF RANDOM AND CLUSTERED SUB-CATALOGS

Epicenter maps for the random and clustered sub-catalogs, at each magnitude threshold and for each region have been constructed. We have next attempted to correlate the spatial characteristics of events for each map with the areal extent of the known reservoirs. This phase of the study has been largely unsuccessful as we have not found any characteristics that are diagnostic.

9. PROPOSED "GEOTHERMAL" DISCRIMINANT

The above discussed characteristics of seismically active regions suggests several possible discriminants for detecting the presence of a reservoir. If such a discriminant were constructed, seismic catalogs could be easily scanned on a sub-region basis and likely candidates for additional studies flagged. The spatial characteristics of the seismicity seem to be diffuse and unsuitable for defining the areal extent of the reservoir. However, we have combined the three best discriminants discussed above to produce a general, albeit ad hoc, discriminant. The first two discriminants are the declustering time and the ratio of random to clustered events. Although these two do not reliably discriminate by themselves, the points of failure occur in an opposite and compensating manner that is physically related. The last parameter included is the ratio of the b-values for the random and clustered sub-catalogs. The magnitude of the first two discriminants vary over a range of about one decade. The variation of the last parameter is less than a factor of two. To better equalize the weight of this ratio in the construction of a general discriminant, we have used a modified statistic based on the ratio as the exponent of 10, i.e. 10^{ratio}. The results of this weighting scheme are listed in Table 1. Note that the weighted b-values ratio discriminants vary by about a decade. The final discriminant has been constructed by multiplying together the values for the first two discriminants and dividing by the third:

$$\text{Geothermal Discriminant} = \frac{(\text{Declustering time})\ (\#\text{random}/\#\text{Clustered Events})}{\left(10^{\text{b-value ratio}}\right)}$$

We emphasize that this discriminant is very ad hoc. However it does combine several physical parameters into a single number that should be a more robust discriminant than the individual measures. The last column of Table 1 lists the range of numbers computed with this discriminant. Note that the geothermal areas are characterized by values much smaller than 0.1 and the San Jacinto fault zone is greater than 0.1. The results of this discriminant are very promising. However, the validity should be tested with independent data sets from other regions.

REFERENCES CITED

Biehler, S., 1964, Geophysical study of the Salton Trough of southern California, Ph.D. thesis, Calif. Institute of Technology, 139 p.

Brook, C.A., R.M. Mariner, D.R. Mabey, J.R. Swanson, M. Guffanti, and L.J.P. Muffler, 1979, Hydrothermal convection systems with reservoir temperatures 90°C, in Muffler, L.J.P., ed. Assessment of geothermal resources of the United States - 1978, U.S. Geol. Surv. Circ., 790, p. 18-85.

Combs, J., 1980, Heat flow in the Coso geothermal area, Inyo County, California, J. Geophys. Res., 85, p. 2411-2424.

Dronyk, M.P., 1977, Stratigraphy, structure, and a seismic refraction survey of a portion of the San Felipe Hills, Imperial Valley, California, M.S. thesis, Univ. of California, Riverside, 140 p.

Duffield, W.A., C. R. Bacon, and G.B. Dalrymple, 1980, Late Cenozoic volcanism, geochronology and structure of the Coso Range, Inyo County, California, J. Geophys. Res., 85, p. 2381-2404.

Elders, W. A., and S. Biehler, 1975, Gulf of California rift system and its implications for tectonics of western North America, Geology, 3, p.85-87.

Elders, W.A., R. W. Rex, T. Meidav, P.T. Robinson, and S. Biehler, 1972, Crustal spreading in southern California, Science, 178 (4056), p. 15-24.

Francis, T.J.G., 1974, A new interpretation of the 1968 Fernandina Caldera collapse and its implications for the mid-oceanic ridges, R. Astron. Soc., Geophys. J., 39, p. 301-318.

Fuis, G. and M. Schnapp, 1977, The November-December 1976 earthquake swarms in northern Imperial Valley, California: Seismicity of the Brawley fault and related structures (abs.), EOS, 58, p. 1188.

Freckman, J.T., 1978, Fluid inclusion and oxygen isotope geothermometry of rock samples from Sinclair #4 and Elmore #1 boreholes, Salton Sea geothermal field, Imperial Valley, California, U.S.A., Masters Thesis, Univ. of California, Riverside, 66 p.

Garrison, L.E., 1972, Geothermal steam in The Geysers-Clear Lake region, California, Geol. Soc. Am. Bull., 83, p. 1449-1468.

Gilpin, B., and T.C. Lee, 1978, A microearthquake study in the Salton Sea geothermal area, California, Bull. Seis. Soc. Am., V. 68, p. 441-450.

Goldstein, N.E., 1977, Northern Nevada geothermal exploration strategy analysis, Lawrence Berkeley Lab. Publication No. 7012, 55 p.

Gutenberg, Beno, and C.F. Richter, 1949, Seismicity of the Earth and associated phenomena, Princeton, N.J., Princeton Univ. Press, 273 p.

Hamilton, R. M., and L. J. P. Muffler, 1972, Microearthquakes at The Geysers geothermal area, California, J. Geophys. Res., 77, p. 2081-2086.

Hearn, B.C., J. M. Donnelly, and F.E. Goff, 1976, Geology and geochronology of the Clear Lake volcanics, California, in Proceedings, Second United Nations Symposium of the Development and Use of Geothermal Resources, p. 423-428.

Helgeson, H., 1968, Geologic and Thermodynamic Characteristics of the Salton Sea Geothermal System, Am. J. of Science, 266, p. 129-166.

Hill, D., A Model for Earthquake Swarms, J. Geophys. Res. 82, p. 1347-1352, March, 1977.

Hill, D.P., P. Mowinckel and L.G. Peake, 1975, Earthquakes, active faults, and geothermal areas in the Imperial Valley, California, Science, 188, (4195), p. 1306-1308.

Johnson, C.E., 1979, Seismotectonics of the Imperial Valley of Southern California, Part II, Ph.D. thesis, California Institute of Technology, p. 122-332.

Johnson, C.E. and D. M. Hadley, 1976, Tectonic Implications of the Brawley Earthquake Swarm, Imperial Valley, California, January 1975, Bull. Seis. Soc. Am., 66, p. 1133-1144.

Klein, F.W., 1979, Earthquakes in Lassen Volcanic National Park, CA, Bull. Seis. Soc. Am., 69, p. 867-875.

Lee, W.H.K., and J.C. Lahr, 1975, HYPO71 (revised): A computer program for determining hypocenter, magnitude and first motion pattern of local earthquakes, U.S. Geol. Sur. Open-File Report 75-311, 59 p.

Lomnitz, Cinna and Arnoldo Hax, 1966, Clustering in aftershock sequences, in Steinhort, J.S., and T. J. Smith, eds., The Earth Beneath the Continents, Geophys. Monograph 10, Amer. Geophys. Union, p. 502-508.

Ludwin, R.S., and C. G. Bufe, 1980, Continued seismic monitoring of The Geysers, California, Geothermal Area, U.S. Geol. Surv. Open-File Report 80-1060, 53 p.

Mcdonald, G.A., 1966, Geology of the Cascade Range and Modoc Plateau, in: Geology of Northern California, ed: E.H. Bailey, Cal. Div. Mines and Geol., Bull. 190, p. 65-96.

McLaughlin, R.J., 1977, The Franciscan assemblage and Great Valley sequence in The Geysers-Clear Lake region, in Field Trip Guide to The Geysers-Clear Lake area, Cordilleran Section of the Geol. Soc. Am., p. 3-24.

McNally, K.C., 1976, Spatial, temporal, and mechanistic character in earthquake occurrence: A segment of the San Andreas faul in central California, Ph.D. thesis, Univ. of California, Berkeley, 140 p.

Majer, E.L., and T.V. McEvilly, 1979, Seismological investigations at The Geysers geothermal field, Geophysics, 44, p. 246-269.

Mogi, K., 1963, Some discussions on aftershocks, foreshocks, and earthquake swarms - The fracture of a semi-infinite body caused by an inner stress origin and its relation to the earthquake, phenomena, 3, Bull. Earthquake Institute, Tokyo University, 41, p. 615-658.

Shlien, S. and M.N. Toksöz, 1970, A clustering model for earthquake occurrences, Bull. Seis. Soc. Am., 60, p. 1765-1787.

Scholz, C.H., 1968, The Frequency-Magnitude Relation of Microfracturing in Rock and Its Relation to Earthquakes, Bull. Seis. Soc. Am. 58, p. 399-415.

Smith, R.L. and H.R. Shaw, 1975, Igneous-related geothermal systems, U.S. Geol. Surv. Circ., 726, p. 58-83.

Sykes, L.R., 1970, Earthquake swarms and sea floor spreading, J. Geophys. Res., 75, p. 6598-6611.

Van de Kamp, P.C., 1973, Holocene continental sedimentation in the Salton Sea Basin, California, A reconnaissance, Bull. Geol. Soc. Am., 84, p. 827-848.

Vere-Jones, D., and D. Davies, 1966, A statistical survey of earthquakes in the main seismic region of New Zealand, II, time series analysis, New Zealand J. Geol. Geophys., 9, p. 251-284.

Walter, A.W. and C.S. Weaver, 1980, Seismicity of the Coso Range, CA, J. Geophys. Res., 85, p. 2441-2458.

Ward, P.L., G. Palmason, and C. Drake, 1969, Microearthquake Survey and the mid-Atlantic ridge in Iceland, J. Geophys. Res., 74, p. 665-684.

Ward, P.L., and S. Bjornsson, 1971, Microearthquakes, swarms, and the geothermal areas of Iceland, J. Geophys. Res., 76, p. 3953-3982.

Weres, O., K. Tsao, and B. Wood, 1977, Resource technology and environment at The Geysers, Lawrence Berkeley Lab., LBL-5231.

Wyss, M., 1973, Towards a Physical Understanding of the Earthquake Frequency Distribution, R. Astron. Soc. Geophys. J., 31, p. 341-359.